

**GLOBAL OCEAN DATA ANALYSIS PROJECT (GLODAP): RESULTS AND DATA**

Contributed by

Christopher L. Sabine,<sup>1</sup> Richard A. Feely,<sup>1</sup> Robert M. Key,<sup>2</sup> Rik Wanninkhoff,<sup>3</sup> Frank J. Millero,<sup>4</sup>  
Tsung-Hung Peng,<sup>3</sup> John L. Bullister,<sup>1</sup> and Alexander Kozyr<sup>5</sup>

<sup>1</sup>Pacific Marine Environmental Laboratory, NOAA, Seattle, WA, U.S.A.

<sup>2</sup>Department of Geosciences, Princeton University, Princeton, NJ, U.S.A.

<sup>3</sup>Atlantic Oceanographic and Meteorological Laboratory, NOAA, Miami, FL, U.S.A.

<sup>4</sup>Rosenstiel School of Marine and Atmospheric Science, University of Miami, Miami, FL, U.S.A.

<sup>7</sup>Carbon Dioxide Information Analysis Center, Oak Ridge National Laboratory, DOE, Oak Ridge, TN, U.S.A.

Prepared by

Alexander Kozyr

Carbon Dioxide Information Analysis Center  
Oak Ridge National Laboratory  
Oak Ridge, Tennessee, U.S.A.

Date Published: September, 2004

Prepared for the

Climate Change Research Division

Office of Biological and Environmental Research

U.S. Department of Energy

Budget Activity Numbers KP 12 04 01 0 and KP 12 02 03 0

Prepared by the

Carbon Dioxide Information Analysis Center  
OAK RIDGE NATIONAL LABORATORY  
Oak Ridge, Tennessee 37831-6335

managed by

UT-BATTELLE, LLC

for the

U.S. DEPARTMENT OF ENERGY

under contract DE-AC05-00OR22725



# CONTENTS

<b>LIST OF FIGURES</b> .....	<b>v</b>
<b>LIST OF TABLES</b> .....	<b>vii</b>
<b>ACRONYMS</b> .....	<b>ix</b>
<b>ABSTRACT</b> .....	<b>xi</b>
<b>1. BACKGROUND INFORMATION</b> .....	<b>1</b>
<b>2. GLODAP DATA SYNTHESIS TECHNIQUES AND RESULTS</b> .....	<b>3</b>
2.1 Evaluation of Carbon Quality .....	3
2.1.1 Analytical and Calibration Techniques .....	3
2.1.2 Results of Shipboard Analysis of Certified Reference Materials .....	4
2.1.3 Replicate Samples .....	4
2.1.4 Consistency of Deep Carbon Data at the Locations where Cruises Cross or Overlap .....	4
2.1.5 Multiple Linear Regression Analysis .....	5
2.1.6 Isopycnal Analysis .....	5
2.1.7 Internal Consistency of Multiple Carbon measurements .....	5
2.1.8 Final Evaluation of Offsets and determination of Correction to be Applied .....	5
2.2 The Indian Ocean Database Synthesis .....	6
2.2.1 Data Comparison at Crossover Stations: Analytical Procedure .....	6
2.2.2 Internal Consistency of GLODAP Indian Ocean database .....	10
2.2.3 GEOSECS Adjustments .....	17
2.3 The Pacific Ocean Database Synthesis .....	17
2.3.1 Pacific Ocean Total Carbon Dioxide Crossover Analysis .....	23
2.3.1a TCO <sub>2</sub> Isopycnal Analysis .....	31
2.3.2 Pacific Ocean Total Alkalinity Crossover Analysis .....	35
2.3.2a Pacific Ocean TALK Isopycnal Analysis .....	42
2.3.2b TALK Internal Consistency Analysis .....	46
2.3.3 Pacific Ocean <i>f</i> CO <sub>2</sub> Crossover Analysis .....	48
2.3.4 Pacific Ocean pH Crossover Analysis .....	53
2.4 The Atlantic Ocean Database Synthesis .....	55
2.4.1 Atlantic Ocean TCO <sub>2</sub> Crossover Analysis .....	55
2.4.2 Atlantic Ocean TALK Crossover Analysis .....	68
2.4.3 Atlantic Ocean <i>f</i> CO <sub>2</sub> Crossover Analysis .....	69
2.4.4 Atlantic Ocean pH Crossover Analysis .....	70
2.4.5 Summary of Atlantic Ocean Adjustments .....	70

<b>3. DATA SET CONSTRUCTION AND MAPPING PROCEDURE .....</b>	<b>71</b>
<b>4. HOW TO OBTAIN THE DATA AND DOCUMENTATION .....</b>	<b>71</b>
<b>5. REFERENCES .....</b>	<b>72</b>

**APPENDIX A: Reprint of Pertinent Literature ..... A-1**

Lamb, M. F., C. L. Sabine, R. A. Feely, R. Wanninkhof, R. M. Key, G. C. Johnson, F. J. Millero, K. Lee, T.-H. Peng, A. Kozyr, J. L. Bullister, D. Greeley, R. H. Byrne, D.W. Chipman, A. G. Dickson, C. Goyet, P. R. Guenther, M. Ishii, K. M. Johnson, C. D. Keeling, T. Ono, K. Shitashima, B. Tilbrook, T. Takahashi, D. W. R. Wallace, Y. Watanabe, C. Winn, and C. S. Wong. 2001. Consistency and synthesis of Pacific Ocean CO<sub>2</sub> survey data. *Deep-Sea Research II* 49:21–58.

**APPENDIX B: Reprint of Pertinent Literature ..... B-1**

Sabine, C. L., R. M. Key, K. M. Johnson, F. J. Millero, J. L. Sarmiento, D. R. W. Wallace, and C. D. Winn. 1999. Anthropogenic CO<sub>2</sub> inventory of the Indian Ocean. *Global Biogeochemical Cycles* 13:179–98.

**APPENDIX C: Reprint of Pertinent Literature ..... C-1**

Key, R. M., A. Kozyr, C. L. Sabine, K. Lee, R. Wanninkhof, J. Bullister, R. A. Feely, F. Millero, C. Mordy, and T.-H. Peng. 2004. A global ocean carbon climatology: Results from GLODAP. *Global Biogeochemical Cycles*

## LIST OF FIGURES

### Figure

1	The map of the global carbon survey .....	2
2	TCO <sub>2</sub> and TALK distribution along longitude 90° E (I8S + I9N) .....	9
3	Station locations for WOCE (circles), CIVA1/I6S (crosses), INDIGO I (stars), INDIGO II (inverted triangles), INDIGO III (triangles), and GEOSECS (filled squares) Indian Ocean Survey. ....	11
4	Mean difference between deep-water values of TALK (A) and TCO <sub>2</sub> (B) for cruise intersections identified in crossover map (Fig. 3) .....	16
5	Pacific Ocean map of the crossover locations .....	22
6	TCO <sub>2</sub> crossover points comparison in the Pacific Ocean (> 2000 db, 2 <sup>nd</sup> order polynomial fit) .....	23
7	Problematic TCO <sub>2</sub> crossovers in the Pacific Ocean. Multi-parameter analyses approach .....	27
8	Del Poly analyses of TCO <sub>2</sub> adjustments in the Pacific Ocean .....	28
9	Same shape analyses of TCO <sub>2</sub> adjustments in the Pacific Ocean .....	29
10	Results of TCO <sub>2</sub> isopycnal analysis of sections P2 (a) and P16N (b) plotted against $\sigma$ near crossover at 30° N and 152° W .....	32
11	Results of TCO <sub>2</sub> isopycnal analysis of sections P17N (a), CGC91 (b), and P17N(c) plotted against $\sigma_{\theta}$ near crossover at 35° N and 135° W .....	33
12	TALK crossover points comparison in the Pacific Ocean ( $\geq 2000$ db, 2 <sup>nd</sup> polynomial fit) .....	35
13	Multi-parameter analysis approach for TALK crossovers in the Pacific Ocean .....	39
14	Del Poly model for TALK crossover analysis in the Pacific Ocean .....	41
15	Same shape model for TALK crossover analysis in the Pacific Ocean .....	39
16	Plots of measured TALK vs longitude for three isopycnal intervals a) $41.44 < \sigma_3 < 41.47$ , b) $41.48 < \sigma_3 < 41.49$ , and c) $41.49 < \sigma_3 < 41.51$ .....	43
17	Plots of measured TALK vs longitude for three isopycnal intervals a) $41.44 < \sigma_3 < 41.47$ , b) $41.48 < \sigma_3 < 41.49$ , and c) $41.49 < \sigma_3 < 41.51$ .....	44

18	Plot of measured TALK vs latitude for $\sigma_3$ values between 41.44 and 41.51	45
19	Results of TALK isopycnal analysis of P16N (calculated using adjusted $\text{TCO}_2$ values and pH) and P17N (measured) plotted against $\sigma_3$ near crossover at $53^\circ$ N and $152^\circ$ W	45
20	Summary of Internal Consistency calculations	47
21	$\Delta f\text{CO}_2$ values (measured – calculated) vs $f\text{CO}_2$ measurements performed by IR and GC systems	53
22	Atlantic Ocean map of the crossover locations	56
23	$\text{TCO}_2$ crossover comparison in the Atlantic Ocean	60
24	TALK crossover comparison in the Atlantic Ocean	68

## LIST OF TABLES

### Table

1	Indian Ocean data set information . . . . .	7
2	Crossover summary for the carbon measurements in Indian Ocean . . . . .	12
3	Crossover summary for the nutrient measurements in Indian Ocean . . . . .	14
4	Pacific Ocean data set information . . . . .	18
5	Pacific Ocean carbon data adjustments . . . . .	21
6	Summary of TCO <sub>2</sub> crossover results in the Pacific Ocean . . . . .	24
7	Results from the multiple-parameter regression method . . . . .	26
8	Summary of the TCO <sub>2</sub> quality assessment results . . . . .	30
9	The final results of statistical analysis for recommended TCO <sub>2</sub> adjustments in the Pacific Ocean . . . . .	34
10	Summary of TALK crossover results in the Pacific Ocean . . . . .	36
11	Results from the multiple-parameter regression method . . . . .	38
12	Summary of the TALK quality assessment results . . . . .	41
13	Summary of TALK Internal Consistency calculations . . . . .	46
14	The final results of the statistical analysis for recommended TALK adjustments in the Pacific Ocean . . . . .	49
15	Results of the final crossover analysis . . . . .	51
16	Pacific Ocean pH crossover information . . . . .	54
17	Cruises used in the Atlantic Ocean synthesis . . . . .	56
18	Summary of crossover analysis results by location . . . . .	61



## ACRONYMS

AOML	Atlantic Oceanographic and Meteorological Laboratory, NOAA
AMS	accelerator mass spectrometry
AWI	Alfred-Wegener-Institut für Polar und Meeresforschung, Germany
BIO	Bedford Institute of Oceanography, Canada
BSH	Bundesamt für Seeschifffahrt und Hydrographie, Germany
BNL	Brookhaven National Laboratory
<sup>14</sup> C	radiocarbon
CSIRO	Commonwealth Scientific and Industrial Research Organization, Hobart, Tasmania, Australia
CDIAC	Carbon Dioxide Information Analysis Center
CFC	chlorofluorocarbon
CO <sub>2</sub>	carbon dioxide
CTD	conductivity, temperature, and depth sensor
CRM	certified reference material
CRIEPI	Central Research Institute Electric Power Industry, Japan
CSIC	Consejo Superior de Investigaciones Científicas, Spain
DIC	dissolved inorganic carbon
DOE	U.S. Department of Energy
<i>f</i> CO <sub>2</sub>	fugacity of CO <sub>2</sub>
GC	gas chromatograph
GEOSECS	Geochemical Ocean Sections Study
GLODAP	Global Ocean Data Analysis Project
HU	Hokkaido University, Japan
IEO	Instituto Español de Oceanografía
IOC	Institute of Ocean Science, Canada
IR	infrared
JAMSTEC	Japan Marine Science and Technology Center
JGOFS	Joint Global Ocean Flux Study
JMA	Japan Meteorological Agency
LAS	Lave Access Server
LDEO	Lamont-Doherty Earth Observatory
LODYC	Laboratoire d'Océanographie Dynamique et de Climatologie
LPO	Laboratoire de Physique des Océans
MATS	Miami University alkalinity titration systems
MLR	multi-parameter linear regression
NCSU	North Carolina State University
NDIR	non-dispersive infrared analyzer
NDP	numeric data package
NIRE	National Institute for Research and Environment, Japan
NIES	National Institute for Environmental Studies, Japan
NOAA	National Oceanic and Atmospheric Administration
NOSAMS	National Ocean Sciences AMS Facility
NRIFS	National Research Institute of Fisheries Sciences, Japan
OACES	Ocean-Atmosphere Exchange Study
NSF	National Science Foundation
ODV	Ocean data View (software)

OSU	Oregon State University
ORNL	Oak Ridge National Laboratory
ORSTOM	Institut Français de la Recherche Scientifique pour le Développement en Coopération
pCO <sub>2</sub>	partial pressure of CO <sub>2</sub>
PMEL	Pacific Marine Environmental Laboratory
PNL	Pacific National Laboratory
PU	Princeton University
QA	quality assurance
QC	quality control
R/V	research vessel
RSMAS	Rosenstiel School of Marine and Atmospheric Sciences
SIO	Scripps Institution of Oceanography
ShIO	Shirshov Institute of Oceanology, Russia
SOMMA	single-operator multi-parameter metabolic analyzer
SLSQ	simple least-square minimization
SOC	Southampton Oceanography Centre
SMP	Synthesis and Modeling Project
TAMU	Texas A&M University
TALK	total alkalinity
TCO <sub>2</sub>	total carbon dioxide
TU	Tokai University, Japan
UA	University of Alaska
UEA	University of East Anglia
UH	University of Hawaii
UM	University of Miami
UPMC	Université Pierre et Marie Curie, Paris, France
USF	University of South Florida
UW	University of Washington
WHOI	Woods Hole Oceanographic Institution
WOCE	World Ocean Circulation Experiment
WHP	WOCE Hydrographic Program
WLSQ	weighted least-squares
WDLSQ	weighted, damped least-squares

## ABSTRACT

Sabine, C. L., R. A. Feely, R. M. Key, R. Wanninkhof, F. J. Millero, T.-H. Peng, J. L. Bullister, and A. Kozyr. 2003. Global Ocean Data Analysis Project: Results and Data, ed. A. Kozyr, T. Beaty, and G. Morris. ORNL/CDIAC-145, NDP-083. Carbon Dioxide Information Analysis Center, Oak Ridge National Laboratory, U.S. Department of Energy, Oak Ridge, Tennessee, XXX pp.

The Global Ocean Data Analysis Project (GLODAP) is a cooperative effort to coordinate global synthesis projects funded through National Oceanic and Atmospheric Administration (NOAA)/Department of Energy (DOE) and National Science Foundation (NSF) as part of the Joint Global Ocean Flux Study—Synthesis and Modeling Project (JGOFS-SMP). Cruises conducted as part of the World Ocean Circulation Experiment (WOCE), JGOFS, and the NOAA Ocean-Atmosphere Exchange Study (OACES) over the decade of the 1990s have created an oceanographic database of unparalleled quality and quantity. These data provide an important asset to the scientific community investigating carbon cycling in the oceans. The central objective of this project is to generate a unified data set to help determine the global distributions of both natural and anthropogenic inorganic carbon, including radiocarbon. These estimates provide an important benchmark against which future observational studies will be compared. They also provide tools for the direct evaluation of numerical ocean carbon models.

The GLODAP data set is available as a numeric data package (NDP-83) from the Carbon Dioxide Information Analysis Center free of charge through the GLODAP web site ([http://cdiac.ornl.gov/oceans/glodap/Glodap\\_home.htm](http://cdiac.ornl.gov/oceans/glodap/Glodap_home.htm)). The GLODAP bottle data files are available for each ocean in flat ASCII file data format, in Ocean Data View (ODV) format, and through the CDIAC live access server (LAS); the gridded data files are available in flat ASCII data file format and through CDIAC LAS.

**Keywords:** Global CO<sub>2</sub> Survey; carbon cycle; carbon dioxide; radiocarbon; anthropogenic CO<sub>2</sub>; data synthesis; data interpretations; crossover analysis; crossover stations; data adjustments; gridded carbon fields.



## 1. BACKGROUND INFORMATION

Over approximately an 8-year period (1990–1998) the global CO<sub>2</sub> survey produced over 15 times more high-quality carbon measurements than had previous survey efforts. These data were collected on more than 50 individual cruises by more than a dozen different analytical laboratories. For these data to be useful for evaluating global-scale issues (e.g., the oceanic inventory of anthropogenic CO<sub>2</sub>) they must be unified into an internally consistent data set. Wherever possible, we tried to include survey data from parallel international survey programs. The international data were extremely important for filling in ocean regions not covered by the U.S. cruises. The final result is a data set with more than 12,000 oceanographic stations with 353,042 unique samples (Fig. 1). We have put a great deal of effort into evaluating the quality of the survey data and recommending adjustments where necessary. The evaluations were conducted at the basin scale starting with the Indian Ocean, then the Pacific, and finally the Atlantic. The results of this extensive data compilation and evaluation are presented here. Some of the scientific products derived from this data synthesis project are also presented in this publication as appendixes.

Nearly 14,000 samples were collected for <sup>14</sup>C analysis as part of the World Ocean Circulation Experiment (WOCE) Hydrographic Program. Large-volume samples from the deep Pacific were analyzed using the traditional b-counting technique at the University of Miami and the University of Washington (G. Östlund and M. Stuiver, respectively). The majority of samples, however, were analyzed by accelerator mass spectrometry (AMS) at Woods Hole Oceanographic Institution (WHOI), a National Ocean Sciences AMS (NOSAMS) facility. One of the primary reasons for measuring <sup>14</sup>C in the upper ocean during WOCE was to study thermocline ventilation on a decadal time scale. The Geochemical Ocean Sections Study (GEOSECS) program provided the first look at the penetration of bomb-produced <sup>14</sup>C into the thermocline. This data has proven to be extremely useful to classical studies of thermocline processes and to the calibration and verification of numerical global circulation models. The WOCE data set is a second snapshot of the time-integrated result of mixing and ventilation. At the time of GEOSECS the <sup>14</sup>C distribution in the upper ocean was primarily driven by air-sea gas exchange. In the interim between the two programs, the strength of that driving force—i.e. the air-sea gradient in  $\Delta^{14}\text{C}$ —decreased significantly. The distribution at the time of WOCE will show significantly more influence by large-scale mixing and will provide a much greater challenge to modelers. The synthesized results from this project are presented in this document. We also include the results of an improved technique for isolating the bomb component of the <sup>14</sup>C signal.



## 2. GLODAP DATA SYNTHESIS TECHNIQUES AND RESULTS

### 2.1 Evaluation of Inorganic Carbon Quality

The first task of the GLODAP synthesis project has been to assemble a merged data set for each basin. The working data are being assembled at Princeton University (PU) and include all of the U.S. Department of Energy (DOE) survey cruises, all of the NOAA Ocean Atmosphere Carbon Exchange Study (OACES) cruises, and many international WOCE and Joint Global Ocean Flux Study (JGOFS) survey cruises to obtain comprehensive spatial coverage. As the data sets are assembled, consistency is checked by comparing property-property and property vs depth plots for stations that are near (within 50 to 100 km) the intersection of cruise lines (the so-called crossover analysis).

This procedure is the first level of quality control and indicates, but does not eliminate, the possibility of systematic differences between cruises or oceans. The next step is to recommend adjustments to the inorganic carbon data based on a comprehensive check of analytical and data reduction procedures, analysis of crossover, and regional analysis of cruise data. This is necessary to produce a gridded data set of data that is both precise and accurate on a global scale. The quality assurance/quality control (QA/QC) procedure involved a careful examination using the techniques discussed below.

#### 2.1.1 Analytical and Calibration Techniques

- **Total carbon dioxide (TCO<sub>2</sub>) analysis and calibration**

All TCO<sub>2</sub> samples that were retained in this synthesis work were analyzed by coulometric titration. The primary differences between the various groups were the sample volume use, the level of automation, and the primary calibration method. On many cruises the coulometer (UIC, Inc.) was coupled to a semi-automated sample analyzer (Johnson and Wallace 1992; Johnson et al. 1985, 1987, 1993, 1998). The most common system, a single-operator multiparameter metabolic analyzer (SOMMA), was typically outfitted with a 20- to 30-mL pipette and was calibrated by filling a gas loop with a known volume of pure CO<sub>2</sub> gas, then introducing the gas into the carrier gas stream and performing subsequent coulometric titration (Johnson and Wallace 1992; Johnson et al. 1987, 1993, 1998). Some systems were calibrated by analyzing sodium carbonate standards. In TCO<sub>2</sub> systems that were not coupled with a semi-automated sample analyzer, the sample was typically introduced manually by a pipette or a syringe.

- **Total alkalinity (TALK) analysis and calibration**

All shipboard TALK measurements were made by potentiometric titration using a titrator and a potentiometer. TALK was determined either by characterizing a full titration curve (Brewer et al. 1986; Millero et al. 1993; DOE 1994; Ono et al. 1998) or by a single-point titration (Perez and Fraga 1987). Analytical differences were in the volume of sample analyzed, the use of either an open or closed titration cell, and the calibration methods. Results were obtained from different curve-fitting techniques such as Gran plots, nonlinear fitting, or single-point analysis.

- **Fugacity CO<sub>2</sub> (fCO<sub>2</sub>) analysis and calibration**

Two different types of instruments were used to measure discrete fCO<sub>2</sub> samples. With each, an aliquot of seawater was equilibrated at a constant temperature of either 4 or 20°C with a head space of known initial CO<sub>2</sub> content. Subsequently, the head space CO<sub>2</sub> concentration was

determined by a nondispersive infrared analyzer (NDIR) or by quantitatively converting the  $\text{CO}_2$  to  $\text{CH}_4$  and then analyzing the concentration using a gas chromatograph (GC) with a flame ionization detector. The initial  $f\text{CO}_2$  in the water was determined after correcting for loss (or gain) of  $\text{CO}_2$  during the equilibration process. This correction can be significant for large initial  $f\text{CO}_2$  differences between the head space and the water, and for systems with a large head-space-to-water volume ratio (Chen et al. 1995).

- **pH analysis and calibration**

The pH measurements were determined by a spectrophotometric method (Clayton and Byrne 1993), with m-cresol purple as the indicator and either scanning or diode array spectrophotometers, or by using pH electrodes.

### **2.1.2 Results of Shipboard Analysis of Certified Reference Materials**

Certified reference materials (CRMs) were used on many of the cruises as secondary standards for  $\text{TCO}_2$ , with some exceptions during the Pacific Ocean and Atlantic survey. (See Table 2 in Lamb et al. 2002, reprinted in Appendix A.) Routine analysis of shipboard CRMs helped verify the accuracy of sample measurements. Certification of CRMs for  $\text{TCO}_2$  is based on vacuum extraction/manometric analysis of samples in the laboratory of C. D. Keeling at Scripps Institution of Oceanography (SIO). A complete discussion of the technique developed for CRMs can be found at [http://www-mpl.ucsd.edu/people/adickson/CO2\\_QC/](http://www-mpl.ucsd.edu/people/adickson/CO2_QC/). Most groups which routinely ran CRM samples for  $\text{TCO}_2$  also analyzed the samples for TALK. The CRMs were certified for TALK in July 1996. However, archived CRMs produced prior to 1996 were calibrated as well so that post-cruise adjustments of TALK could be made. (See Table 3 in Lamb et al. 2002, Appendix A.) CRMs are not currently available for the other carbon parameters.

### **2.1.3 Replicate Samples**

Replicate samples were routinely collected and analyzed at sea, thus allowing the analyst to determine the overall precision of the measurement. The imprecision of replication includes the errors associated with the collection and handling of the carbon sample, as well as the analytical precision. In addition, replicate samples for  $\text{TCO}_2$  were collected and stored for analysis ashore at SIO by laboratory of C. D. Keeling (Guenther et al. 1994).

### **2.1.4 Consistency of Deep Carbon Data at the Locations Where Cruises Cross or Overlap**

One approach for evaluating the consistency of the cruises was to compare data where cruises crossed or overlapped. A location was considered a crossover if stations from two cruises were within  $1^\circ$  ( $\sim 100$  km) of each other. If more than one station from a particular cruise fell within that limit, the data were combined for the comparison. For this analysis, only deep-water measurements ( $>2000$  m for the Pacific Ocean,  $>2500$  m for the Indian Ocean, and  $>3000$  m for the Atlantic Ocean) were considered, because  $\text{CO}_2$  concentrations in shallow water can be variable, and the penetration of anthropogenic  $\text{CO}_2$  can change relationships between the carbon parameters measured at different times. Once the stations were chosen, the data were plotted against potential density referenced to 3000 dB (or 4000 dB in the Atlantic), since water moves primarily along isopycnal surfaces. In order to quantitatively estimate the mean difference between legs, each of the two fitted curves for a restricted deep water density range was evaluated at evenly spaced

intervals covering the range of space common to the selected stations from both legs. A mean was taken of the differences, and standard deviation was calculated.

### **2.1.5 Multiple Linear Regression Analysis**

Another approach used to evaluate the data at the crossover locations was a multiparameter linear regression analyses (MLR). Brewer et al. (1995) and subsequently others (Wallace 1995; Slansky et al. 1997; Goyet and Davis 1997; Sabine et al. 1999), have shown that both  $\text{TCO}_2$  and TALK concentrations in deep and bottom waters can be fit well with MLR functions using commonly measured hydrographic quantities for the independent parameters. The geographic extent over which any such function is applicable depends on the number of water masses present, and the uniformity of chemical and biological processes which have affected the carbon species concentration in each water mass.

### **2.1.6 Isopycnal Analysis**

At a few locations in the North Pacific the estimated offsets at the crossovers were not consistent with the offsets from the basinwide MLR analysis. In an attempt to determine whether the limited number of stations analyzed biased on the crossovers, we expanded the crossover analysis to include additional stations along each cruise and/or stations from neighboring cruises. The deep (>2200 m) station data were averaged at specific potential density ( $\sigma\text{-3}$ ) values and fitted with a 2nd-order polynomial function. The average differences and standards deviations were determined from evenly spaced differences along the curves. The range of values observed for a particular cruise at each isopycnal level indicated whether the stations initially used in the crossover analysis were offset from the surrounding stations. Although more assumptions about oceanographic consistency are necessary, the additional stations used in the isopycnal analysis can provide a better estimate of the difference between cruises because more data points are included in the analysis.

### **2.1.7 Internal Consistency of Multiple Carbon Measurements**

An additional independent approach for evaluating the accuracy of data is the examination of the internal consistency of the  $\text{CO}_2$  system parameters. The  $\text{CO}_2$  system parameters in seawater can be characterized by temperature, salinity, phosphate and silicate, and two of the four measured inorganic carbon parameters:  $\text{TCO}_2$ , TALK,  $f\text{CO}_2$ , or pH. Thus, the carbon system is overdetermined on cruises where three or more carbon parameters were measured. By comparing estimates using different pairs of carbon measurements, one can evaluate potential offsets. In addition, examination of internal consistency over several cruises lends confidence to the reliability of the equilibrium constants. The constants of Mehrbach et al. (1973) as well as a refit by Dickson and Millero (1987) were used for this analysis, along with equilibrium constants for other components (e.g., boric acid dissociation, solubility of  $\text{CO}_2$ , water hydrolysis, and phosphoric and silicic acid dissociation) necessary to characterize the carbonate system in seawater as recommended in Millero (1995). This choice was made based on the analysis of a large data set (15,300 samples) obtained from all the ocean basins (Lee et al. 2000; Millero et al. 2002). For this analysis, TALK was calculated using a combination of either  $\text{TCO}_2$  and  $f\text{CO}_2$ , or  $\text{TCO}_2$  and pH [adjusted upward by 0.0047 (DeValls and Dickson 1998) for the Pacific and Indian Ocean but not for the Atlantic analysis].

### **2.1.8 Final Evaluation of Offsets and Determination of Correction To Be Applied**

Based on the available information, an assessment was made of the offsets necessary to make the data sets in a basin mutually consistent. Any cruises that showed consistent offsets are adjusted, and the data are combined into a unified data set that is consistent between cruises. Two important points must be considered when evaluating the various approaches used to examine the data quality of the cruises.

First, most of the approaches assume that the deep ocean does not change over the time-period of the various cruises. Thus, very little variability would be expected in the deep waters (pressure > 2000 dbar) at the crossover points. Second, the various approaches have different strengths and weaknesses and may be more or less reliable in different oceanographic regions. Furthermore, the calculated offsets and associated errors may not be directly comparable. As a result, some level of subjectivity is necessarily a part of the adjustments proposed in this section. We have made every attempt to consider all of the various lines of evidence available. Adjustments were based on a preponderance of evidence and implemented only when we felt an adjustment was clearly necessary.

## **2.2 The Indian Ocean Database Synthesis**

The Indian Ocean database consists primarily of all the U.S. WOCE and NOAA cruises. Carbon measurements were made as part of the JGOFS Global Survey funded through DOE. Details of the WOCE/JGOFS Indian Ocean CO<sub>2</sub> measurement program—including personnel, sampling and measurement protocols, and data quality assurance/quality control checks—are provided in Johnson et al. 1998, Millero et al. 1998, and Johnson et al. 2002 (ORNL/CDIAC-138, NDP-080).

We have also included the data from the French INDIGO and CIVA1 cruises (contributed by A. Poisson). A summary of the combined data set can be found in Sabine et al. 1999 (Appendix B of this document). Table 1 gives some details about the individual cruises in Indian Ocean compiled for this project.

The WOCE/DOE and CIVA TCO<sub>2</sub> data have an estimated accuracy of ±2 μmol/kg. Proposed adjustments for the INDIGO I, II, and III CO<sub>2</sub> data to bring them in line with the WOCE/DOE data are +10.7, - 9.4, and +6.4 μmol/kg, respectively. The WOCE/DOE and CIVA alkalinity data have an estimated accuracy of ±3 μmol/kg. Proposed adjustments for the INDIGO I and II alkalinity data to bring them in line with the WOCE/DOE data are +6.5 and +6.8 μmol/kg, respectively. These results have been published in Sabine et al. 1999 (Appendix B of this document). As part of this work we also evaluated the quality of the GEOSECS carbon data. Our study indicates that the GEOSECS TCO<sub>2</sub> values are 22.6 μmol/kg—high relative to the WOCE/DOE data in the deep Indian Ocean. No adjustment was proposed for the GEOSECS alkalinity data.

### **2.2.1 Data Comparison at Crossover Stations: Analytical Procedure**

The purpose of this analysis was to determine if any significant systematic offset existed between the various legs of the WOCE/JGOFS Indian Ocean survey of carbon measurements. Once the technique was developed, it was also applied to the salinity and silicate measurements from the same stations that were used for the carbon comparison. For reference and to obtain a general idea of the property distribution with depth, see Fig. 2, which shows both TCO<sub>2</sub> and TALK distribution along longitude 90° E (I8S + I9N).

**Table 1. Indian Ocean data set information<< List will generate here**

<b>Cruise/ Dates (Mon./Year)</b>	<b>Chief Sci. Inst.</b>	<b>Hydro Inst.</b>	<b>Nutrients Inst.</b>	<b>TCO<sub>2</sub> PI/Inst.</b>	<b>TALK PI/Inst.</b>	<b>fCO<sub>2</sub> PI/Inst.</b>	<b>pH PI/Inst.</b>	<b>CRM TCO<sub>2</sub>/TALK/ fCO<sub>2</sub>/pH</b>	<b>CFC PI/Inst.</b>	<b><sup>14</sup>C PI/Inst.</b>
GEOSECS 12/77-04/78		M	M	M	M	N	N	N/N/N/N	N	M
INDIGO 2-3/85, 4/86, 1-2/87	Poisson UPMC	M UPMC	M UPMC	M/Poisson/U PMC	M/Poisson/UP MC	N	N	N/N/N/N	M/Poisson/ UPMC	M/Ostlan d/?
I08A 1-3/94	Tillbrook CSIRO	M CSIRO	M CSIRO	M/Tillbrook CSIRO	M/Tillbrook CSIRO	N	N	M/M/N/N	N	N
I8SI9S 12/94-01/95	McCartney WHOI	M WHOI	M OSU	M/Wallace BNL	M/Wallace BNL	N	N	M/MC/N/N	M/Smethie LDEO	M/Quay UW
I9N 1-3/95	A.Gordon LDEO	M SIO	M SIO	M/Sabine PU	M/Sabine PU	N	N	M/MC/N/N	M/Fine RSMAS	M/Key PU
I8NI5E 3-4/95	Talley SIO	M SIO	M SIO	M/Winn UH	M/Winn UH	N	N	M/MC/N/N	M/Smethie LDEO	M/Key PU
I3 4-6/95	Nowlin TAMU	M SIO	M SIO	M/Millero RSMAS	M/Millero RSMAS	N	N	M/MC/N/N	M/Weiss SIO	M/Key PU
I5WI4 6-7/95	Toole WHOI	M SIO	M SIO	M/Wallace BNL	M/Wallace BNL	N	N	M/MC/N/N	M/Fine RSMAS	M/Key PU
I7N 7-8/95	Olson RSMAS	M SIO	M SIO	M/Winn UH	M/Winn UH	N	N	M/MC/N/N	M/Fine RSMAS	M/Key PU
I1 8-10/95	Morrison NCSU	M WHOI	M OSU	M/Goyet WHOI	M/Goyet WHOI	N	N	M/MC/N/N	M/Warner UW	M/Key PU
I10 11/95	Bray SIO	M SIO	M SIO	M/Sabine PU	M/Sabine PU	N	N	M/MC/N/N	M/Fine RSMAS	M/Key PU

**Table 1 (continued)**

<b>Cruise/ Dates (Mon./Year)</b>	<b>Chief Sci. Inst.</b>	<b>Hydro Inst.</b>	<b>Nutrients Inst.</b>	<b>TCO<sub>2</sub> PI/Inst.</b>	<b>TALK PI/Inst.</b>	<b>fCO<sub>2</sub> PI/Inst.</b>	<b>pH PI/Inst.</b>	<b>CRM TCO<sub>2</sub>/TALK/ fCO<sub>2</sub>/pH</b>	<b>CFC PI/Inst.</b>	<b><sup>14</sup>C PI/Inst.</b>
I2 12/95	Johnson PMEL	M WHOI	M OSU	M/Winn UH	M/Winn UH	N	N	M/MC/N/N	M/Bullister PMEL	M/Key PU
I8R 9–10/95	Molinari PMEL	M PMEL	M PMEL	M/Millero RSMAS	M/Wanninkhof AOML	M/Wanninkhof AOML	M/Millero RSMAS	MC/MC/M/M	M/Bullister PMEL	N
S4I 5–6/96	Whitworth TAMU	M SIO	M SIO	M/Takahashi LDEO	M/Millero RSMAS	M/Takahashi LDEO	N	M/MC/M/N	M/Smethie LDEO	M/Key PU
I6S (CIVA-1) 1–3/93	Poisson UPMC	M UPMC	M UPMC	M/Poisson UPMC	M/Poisson UPMC	N	N	M/N/N/N	M/Poisson UPMC	M/Arnold CNRS

Abbreviations: M — Measured; N — Not measured; MC — CRM used and data corrected.

Affiliated institutions:

UPMC	Université Pierre et Marie Curie, Paris, France
CSIRO	Commonwealth Scientific and Industrial Research Organization, Hobart, Tasmania, Australia
WHOI	Woods Hole Oceanographic Institution
OSU	Oregon State University
BNL	Brookhaven National Laboratory
LDEO	Lamont-Doherty Earth Observatory
UW	University of Washington
SIO	Scripps Institution of Oceanography
PU	Princeton University
RSMAS	Rosenstiel School of Marine and Atmospheric Science, University of Miami
UH	University of Hawaii
TAMU	Texas A&M University
NCSU	North Carolina State University
PMEL	Pacific Marine Environmental Laboratory, NOAA
AOML	Atlantic Oceanographic and Meteorological Laboratory, NOAA

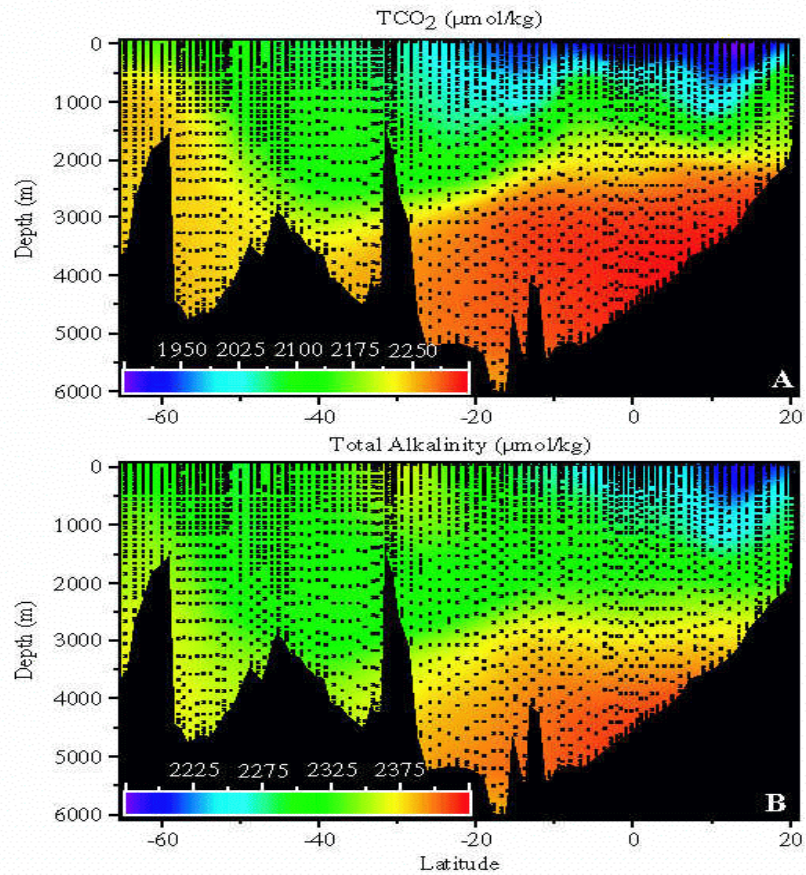


**Fig. 2. TCO<sub>2</sub> and TALK distribution along longitude 90°E (I8S + I9N).**

The stations selected for each crossover are those which are close to the crossover point and on which carbon measurements were made. Fig. 3 shows the locations of the 35 crossovers. The number of stations selected was somewhat subjective, but was such that sufficient measurements were present for the analysis without getting too far away from the crossover location. In all cases the stations were within approximately 1° of latitude or longitude of the crossover point. Table 2 lists the stations used for each crossover. In two cases the legs did not actually cross (crossover 7 and 14). The analysis here was done using the last station from one leg and the first from the next leg which had carbon data.

Once the stations were chosen, the data from the appropriate stations were plotted against potential density referenced to 3000 dB. Only data from pressures greater than 2500 dB was included. The data set used was the preliminary data prepared by either the SIO or WHOI conductivity, temperature, and depth (CTD) groups at the end of each leg. For each crossover, a smooth curve was fitted to the combined station data from each leg so long as there were seven or

more data points which could be used for the fit. The fitting curve chosen was a “robust loess” function designed to minimize the influence of outliers. In cases having fewer than seven points, linear segments were used to “connect the dots.” Only data which had been marked with a quality control flag of 2 (good) or 6 (replicate) were included in the analyses, and the salinity flags were applied to the calculated values.

In order to quantitatively estimate the mean difference between legs, each of the two fitted curves was evaluated at 50 evenly spaced intervals covering the range of space common to the selected stations from both legs. The 50 differences were then averaged. In each case the difference was taken as later cruise minus earlier cruise (or higher station number minus lower). Table 2 summarizes the mean differences and standard deviations for all of the crossovers and indicates the sense of the differences in terms of the cruise leg designations ( $\Delta$ ).

In addition to the WOCE/JGOFS survey, NOAA carried out one cruise which repeated a portion of WOCE leg I8NI5E between 20° S and 5° N. For the overlap region, a somewhat more detailed comparison can be made. The data in the overlap region from each cruise were individually gridded as a section vs space. The two gridded sections were then subtracted, the results contoured, and a mean difference calculated. This procedure was repeated for each of the four parameters used in the crossover comparisons. Only “good” data from pressures >2500db were used in the comparisons.

The crossover summary for nutrients is presented in Table 3.

### **2.2.2 Internal Consistency of GLODAP Indian Ocean Database**

The internal consistency of the Indian Ocean cruises (Table 1) was examined by comparing carbon values in the deep waters (pressure > 2500 dbar) at the intersections of different legs following the procedures described in the crossover study (see Sec. 2.2.1). The mean and standard deviation of the difference in TALK and TCO<sub>2</sub> at the 35 intersections identified in Figure 3 are shown in Figure 4. The long-term stability of the WOCE/JGOFS measurements can be estimated from the first 17 crossover results. The mean of the absolute values for the leg-to-leg differences was less than the estimated accuracy for both TCO<sub>2</sub> ( $1.8 \pm 0.8 \mu\text{mol/kg}$ ) and TALK ( $2.4 \pm 1.6 \mu\text{mol/kg}$ ). Although there is only one reliable crossover point between the WOCE/JGOFS cruises and the CIVA1 (I6S) cruise, the differences for both parameters is within the estimated accuracy of the measurements. Results from the analysis of CRMs on the CIVA1 cruise also support the quality of the measurements. Some of the older INDIGO cruises, however, did appear to have offsets relative to the WOCE/JGOFS and CIVA1 data. INDIGO I and II TALK values averaged 6.5  $\mu\text{mol/kg}$  high and 6.8  $\mu\text{mol/kg}$  low, respectively, while the INDIGO III TALK values showed no clear offset. The INDIGO TCO<sub>2</sub> values were all consistently high relative to WOCE/JGOFS and CIVA1, with differences of 10.7, 9.4 and 6.4  $\mu\text{mol/kg}$ , respectively. These offsets are consistent with differences observed between at-sea values and replicate samples run at C. D. Keeling’s shore-based TCO<sub>2</sub> facility. Since the INDIGO cruises were run prior to the introduction of CRMs, these offsets were presumed to be calibration differences and each leg was adjusted to bring the values in line with the remaining cruises. The dotted boxes in Figure 4 show the original offsets at the crossovers. The solid boxes show the final offsets for the GLODAP database. The mean of the absolute values for the leg-to-leg differences for all 35 crossover analyses suggest that the final data set is internally consistent to 2.2 and 3.0  $\mu\text{mol/kg}$  for TCO<sub>2</sub> and TALK, respectively.

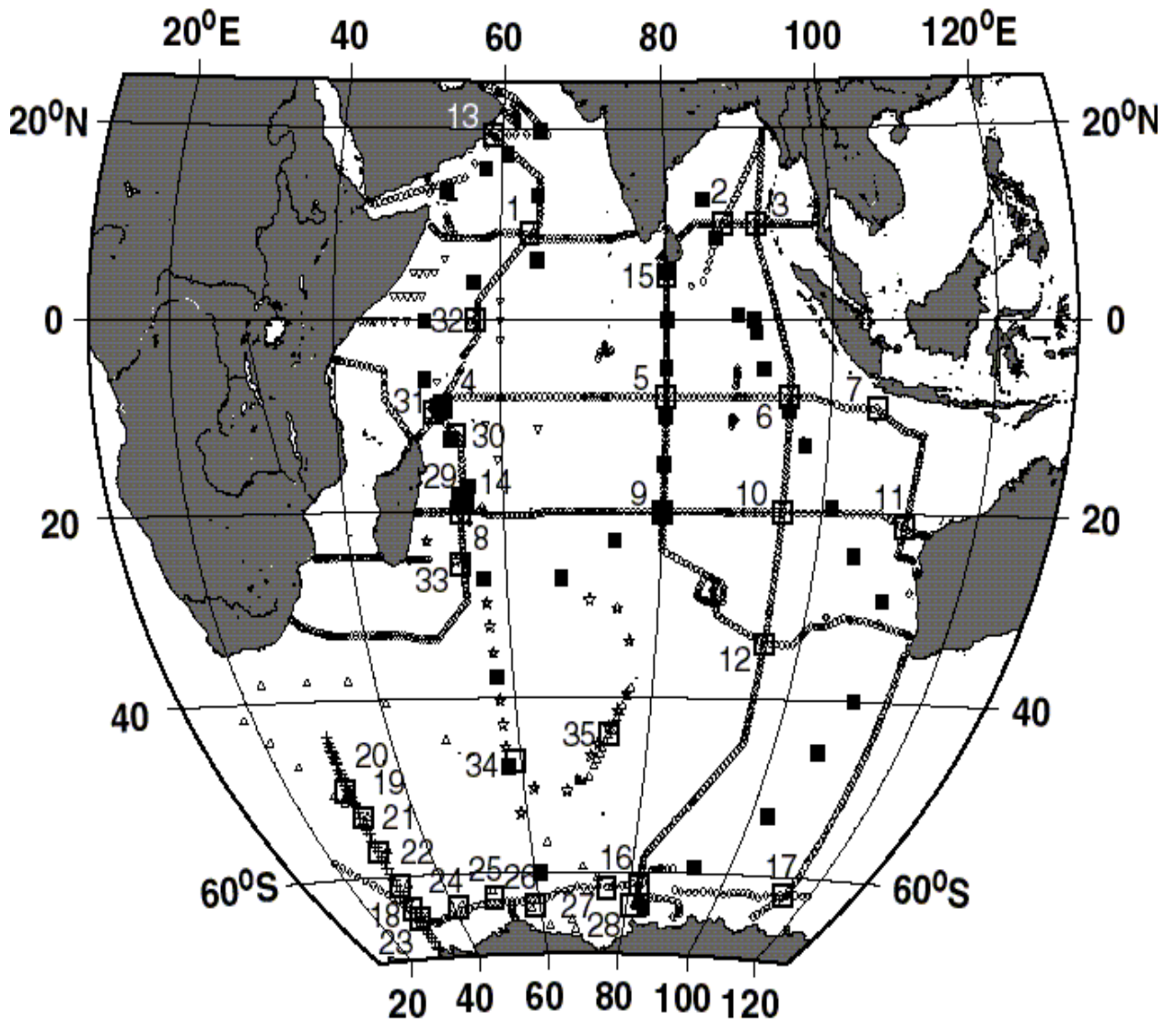


**Fig. 3.** Station locations for WOCE (circles), CIVA1/I6S (crosses), INDIGO I (stars), INDIGO II (inverted triangles), INDIGO III (triangles), and GEOSECS (filled squares) Indian Ocean Survey. Numbered boxes indicate location of crossovers discussed in the text.

**Table 2. Crossover summary for the carbon measurements in Indian Ocean**

Crossover no.	Stations: cruise 1 cruise 2	Cruise 1 – Cruise 2	$\Delta$ Salinity	$\Delta$ TCO <sub>2</sub> $\mu\text{mol/kg}$	$\Delta$ TALK $\mu\text{mol/kg}$
1	927, 929, 931 780, 782, 784	I1-I7N	-0.0003±0.0002	-2.5±0.5	1.7±1.0
2	987;990 <sup>a</sup> 266, 268, 270	I1-I9N	0.0013±0.0001	-2.7±6.3 <sup>b</sup>	-2.1±5.9 <sup>b</sup>
3	996;998 <sup>a</sup> 233, 235	I1-I9N	-0.0005±0.0003	-0.9±1.7	1.2±0.8
4	1205 728, 730	I2-I7N	0.0028±0.0001	-0.4±1.1	5.6±2.4
5	1137, 1139 320, 324	I2-I8NI5E	0.0015±0.0003	1.5±1.5	3.4±2.2
6	1094, 1096 191, 193	I2-I9N	-0.0008±0.0004	-3.0±0.7	-3.4±1.4
7	1078 1075	I2-I10	0.0000±0.0019	-1.5±1.5	1.8±2.4
8	705 547, 549	I5WI4-I3	0.0002±0.0003	1.6±0.5	0.7±1.7
9	498, 499, 501 346, 348	I3-I8NI5E	-0.0005±0.0005	-2.6±0.7	-0.8±2.3
10	472 169	I3-I9N	-0.0010±0.0003	1.1±1.2	-0.8±0.6
11	1039 452, 454	I10-I3	-0.0003±0.0001	1.1±0.3	-1.0±0.7
12	404, 406, 408 9, 11, 13	I8NI5E-I8SI9S	-0.0008±0.0012	-1.1±1.0	-2.7±3.8
13 <sup>b</sup>	861 808	I1-I7N	0.0011±0.0007	1.3±0.4	0.3±0.6
14	709 707	I7N-I5WI4	-0.0004±0.0005	-2.9±0.6	2.4±1.7
15	966, 968, 969 283, 287	I1-I8NI5E	0.0018±0.0003	-3.1±0.8	-4.2±4.5 <sup>d</sup>
16	62 75, 77	S4I-I8SI9S	-0.005±0.0022	1.7±0.8	-5.8±1.6
17	104 92	S4I-I8SI9S	-0.0005±0.0015	1.6±0.3	2.7±2.9
18	13, 14 10, 13	I6S-S4I	0.0007±0.0004	1.5±0.6	3.3±0.8
19	30 90	I6S-INDIGO	-0.0062±0.0065	-15.7±2.0	2.4±0.7

**Table 2 (continued)**

Crossover no.	Stations: cruise 1 cruise 2	Cruise 1 – Cruise 2	$\Delta$ Salinity	$\Delta$ TCO <sub>2</sub> $\mu\text{mol/kg}$	$\Delta$ TALK $\mu\text{mol/kg}$
20	34, 36 91, 93	I6S- INDIGO	-0.0028±0.0006	-7.8±1.9	3.9±1.9
21	22, 24, 26 89	I6S- INDIGO	-0.0017±0.0014	-5.6±1.3	-0.7±0.7
22	16, 18, 20 88	I6S- INDIGO	0.0005±0.001	-3.5±1.9	0.3±1.0
23	10, 12, 13 87	I6S- INDIGO	0.0019±0.0012	-4.2±1.3	-5.8±0.5
24	26 86	S4I- INDIGO	-0.0016±0.0003	-6.5±0.5	-4.5±1.0
25	32 85	S4I- INDIGO	-0.0052±0.0008	-8.2±0.9	-5.0±0.8
26	46 84	S4I- INDIGO	0.0041±0.0013	-6.9±2.6	-2.1±1.2
27	58 78	S4I- INDIGO	-0.003±0.0057	-3.5±0.7	-9.2±0.5
28	79 82, 84	INDIGO- S4I	-0.003±0.0015	11.3±1.3	1.4±0.2
29	27, 28 705,707,709,711	INDIGO- WOCE	-0.0013±0.0003	5.3±0.9	-0.8±1.3
30	32 720, 722	INDIGO- I7N	0.0009±0.0006	12.5±1.0	-8.7±2.1
31	34, 35 732,736,1196, 1200,1202	INDIGO- WOCE	0.0008±0.0012	10.9±0.7	-12.0±1.2
32	44 758, 760	INDIGO- I7N	0.0018±0.0015	6.2±1.7	-4.3±2.3
33	2 691, 694	INDIGO- I5WI4	0.0016±0.0009	10.8±0.3	8.7±1.8
34	103 11	INDIGO III- INDIGO I	0.006±0.0013	-2.3±2.4	-5.5±2.1
35	111, 112 19	INDIGO III- INDIGO I	-0.001±0.0048	3.4±4.3	-1.2±3.5

<sup>a</sup> Colons indicate an inclusive range of stations.<sup>1</sup>

<sup>b</sup> This difference is considered an upper limit due to the unusual curve fit to the I1 data.

<sup>c</sup> Not considered reliable due to insufficient data.

<sup>d</sup> Not considered reliable due to strong north-south gradient in deep water and poor alkalinity precision.

**Table 3. Crossover summary for nutrient measurements in Indian Ocean**

Crossover no.	Stations: <sup>a</sup> cruise 1 cruise 2	Cruise 1 – Cruise 2	Oxygen $\mu\text{mol/kg}$	$\Delta$ Nitrate $\mu\text{mol/kg}$	$\Delta$ Silicate $\mu\text{mol/kg}$	$\Delta$ Phosphate $\mu\text{mol/kg}$
1	928:929 781:782	I1-I7N	-0.9 $\pm$ 2.2	0.5 $\pm$ 0.1	2.7 $\pm$ 1.1	-0.04 $\pm$ 0.01
2	987:990 267:269	I1-I9N	2.1 $\pm$ 0.9	0.17 $\pm$ 0.05	-0.6 $\pm$ 1.0	-0.022 $\pm$ 0.005
3	996:998 <sup>b</sup> 233:235	I1-I9N	2.0 $\pm$ 0.5	-0.25 $\pm$ 0.03	1.6 $\pm$ 0.6	-0.0007 $\pm$ 0.0048
4	1205:1206 729:730	I2-I7N	-1.4 $\pm$ 0.4		-0.2 $\pm$ 0.6	
5	1137:1139 321:323	I2-I8NI5E	-2.0 $\pm$ 0.8	-0.001 $\pm$ 0.078	0.5 $\pm$ 0.8	-0.006 $\pm$ 0.006
6	1094:1095 191:193	I2-I9N	0.3 $\pm$ 0.3	-0.27 $\pm$ 0.05	0.2 $\pm$ 0.4	-0.042 $\pm$ 0.006
7	1078 1075	I2-I10	0.9 $\pm$ 2.1	-0.15 $\pm$ 0.03	-1.6 $\pm$ 0.6	-0.011 $\pm$ 0.006
8	704:706 547:549	I5WI4-I3	-0.2 $\pm$ 0.2	0.03 $\pm$ 0.04		0.011 $\pm$ 0.006
9	498:499 346:347	I3-I8NI5E	-0.8 $\pm$ 0.8	-0.26 $\pm$ 0.03	1.2 $\pm$ 0.6	-0.002 $\pm$ 0.010
10	471:473 168:170	I3-I9N	-0.5 $\pm$ 0.6	-0.24 $\pm$ 0.06	-1.1 $\pm$ 0.3	-0.014 $\pm$ 0.002
11	1038:1039 452:453	I10-I3	-0.6 $\pm$ 0.4	0.11 $\pm$ 0.02	0.2 $\pm$ 0.1	0.001 $\pm$ 0.004
12	405:407 10:12	I8NI5E-I8SI9S	0.5 $\pm$ 0.3	-0.79 $\pm$ 0.09	-2.6 $\pm$ 0.5	-0.041 $\pm$ 0.003
13	861 807:808	I1-I7N	-0.2 $\pm$ 0.4	-0.48 $\pm$ 0.04	3.1 $\pm$ 0.4	-0.154 $\pm$ 0.006
14	709 707	I7N-I5WI4	0.4 $\pm$ 0.3	-0.30 $\pm$ 0.03	-1.5 $\pm$ 0.2	-0.027 $\pm$ 0.003
15	967:969 286:287	I1-I8NI5E	2.7 $\pm$ 0.4	-0.08 $\pm$ 0.03	-0.7 $\pm$ 0.4	-0.034 $\pm$ 0.009
16	62:64 <sup>c</sup> 75:77	S4I-I8SI9S	1.7 $\pm$ 0.7	-0.79 $\pm$ 0.05	-1.2 $\pm$ 2.2	-0.082 $\pm$ 0.004
17	104:106 91:93	S4I-I8SI9S	1.0 $\pm$ 0.1		0.01 $\pm$ 1.43 <sup>d</sup>	-0.018 $\pm$ 0.006 <sup>d</sup>
18	12:14 14	S4I-I6S	1.0 $\pm$ 1.3	0.52 $\pm$ 0.04	-9.2 $\pm$ 1.5	-0.236 $\pm$ 0.009
19	30 90	I6S-INDIGO III <sup>e</sup>	-4.1 $\pm$ 1.8	1.0 $\pm$ 0.1	-2.7 $\pm$ 2.2	-0.006 $\pm$ 0.017

Table 3 (continued)

Crossover no.	Stations: <sup>a</sup> cruise 1 cruise 2	Cruise 1 - Cruise 2	Oxygen $\mu\text{mol/kg}$	$\Delta$ Nitrate $\mu\text{mol/kg}$	$\Delta$ Silicate $\mu\text{mol/kg}$	$\Delta$ Phosphate $\mu\text{mol/kg}$
20	34, 36 90, 91, 93	I6S-INDIGO III	0.1 $\pm$ 0.9	0.8 $\pm$ 0.2 <sup>f</sup>	-4.2 $\pm$ 2.1	-0.02 $\pm$ 0.02 <sup>f</sup>
21	24 89	I6S-INDIGO III <sup>e</sup>	1.3 $\pm$ 0.4		-2.1 $\pm$ 1.7	-0.3 $\pm$ 0.01
22	18, 20 88	I6S-INDIGO III	1.0 $\pm$ 0.3	2.2 $\pm$ 0.3	-4.4 $\pm$ 0.2	0.006 $\pm$ 0.009
23	12, 13 87	I6S-INDIGO III	-2.5 $\pm$ 1.7	0.7 $\pm$ 0.5 <sup>g</sup>	6.3 $\pm$ 1.2	-0.01 $\pm$ 0.03 <sup>g</sup>
24	26 86	S4I-INDIGO III	3.9 $\pm$ 0.6	1.5 $\pm$ 0.3	-6.7 $\pm$ 1.9	
25	31:32 85	S4I-INDIGO III <sup>e</sup>	3.9 $\pm$ 2.0		-8.2 $\pm$ 1.2	-0.10 $\pm$ 0.03
26	46 84	S4I-INDIGO III <sup>e</sup>	-3.6 $\pm$ 1.1	0.8 $\pm$ 0.2	9.5 $\pm$ 3.8	-0.087 $\pm$ 0.003
27	58:59 78	S4I-INDIGO III <sup>e</sup>	4.7 $\pm$ 1.6	-0.02 $\pm$ 0.13	-2.7 $\pm$ 1.9	-0.082 $\pm$ 0.006
28	85 79	S4I-INDIGO		1.5 $\pm$ 0.1	4.3 $\pm$ 2.9	-0.13 $\pm$ 0.01
29		INDIGO- WOCE				
30	720 32	I7N-INDIGO II	-1.0 $\pm$ 0.3	-0.3 $\pm$ 0.1	-0.8 $\pm$ 0.3	-0.0009 $\pm$ 0.0073
31		INDIGO- WOCE				
32	760 44	I7N-INDIGO II	-1.5 $\pm$ 0.4	0.48 $\pm$ 0.08	-0.02 $\pm$ 0.31	-0.08 $\pm$ 0.02
33	692:694 2	I5W14-INDIGO I	-4.6 $\pm$ 1.3			
34	11 103	INDIGO III- INDIGO I	-3.8 $\pm$ 0.2	0.09 $\pm$ 0.04	1.8 $\pm$ 0.9	0.116 $\pm$ 0.006
35	110 19	INDIGO III- INDIGO I	1.8 $\pm$ 2.8			
36	616:653 3:5,13:15, 20:27	I5W14-C. Darwin 29	-3.6 $\pm$ 1.2	-0.3 $\pm$ 0.2	2.6 $\pm$ 1.3	-0.06 $\pm$ 0.02
37	379:380 67:68	I8NI5E-C. Darwin 29	-1.9 $\pm$ 0.9	-0.02 $\pm$ 0.08	0.2 $\pm$ 0.6	-0.008 $\pm$ 0.011
38	337:339 68:69	I8NI5E-C. Darwin 29	-2.3 $\pm$ 1.3	-0.6 $\pm$ 0.1	1.5 $\pm$ 1.7	-0.016 $\pm$ 0.003

<sup>a</sup> Colons indicate an inclusive range of stations.

<sup>b</sup> Station 996 silicate anomalously high relative to stations 994:998.



### 2.2.3 GEOSECS Adjustments

Since CRMs were not available at the time of GEOSECS, the only way to infer consistency with the WOCE data set is to assume that the deep water carbon distributions have not changed since the GEOSECS survey. The most reliable way to compare the two data sets is to examine the difference between the predicted  $\text{TCO}_2$  and the measured  $\text{TCO}_2$  (excess  $\text{CO}_2$ ) in deep waters. The basic assumption with this technique is that the correlation between the different hydrographic parameters in the deep waters does not change with time. Given the long residence time of the deep and bottom waters in the ocean, this should be a reasonable assumption. This technique has the advantage that it implicitly accounts for the possibility of real variability in hydrographic properties between the two expeditions which would not be taken into account by simply comparing carbon profiles.

Examination of the excess  $\text{CO}_2$  values in waters that should be free of anthropogenic  $\text{CO}_2$  [pressures > 2000 dbar, containing no detectable chlorofluorocarbons (CFCs)] revealed that the GEOSECS values were  $22.5 \pm 3 \mu\text{mol/kg}$  higher than the comparable WOCE measurements. This difference is comparable to the correction of  $-18 \pm 7 \mu\text{mol/kg}$  noted by Weiss et al. (1983) to make the  $\text{TCO}_2$  measurements consistent with the TALK and discrete  $\text{pCO}_2$  measurements based on the Merbach et al. (1973) dissociation constants. Additional support for an adjustment of the original GEOSECS data comes from C. D. Keeling's shore-based analysis of  $\text{TCO}_2$  samples collected on both the GEOSECS and the WOCE/JGOFS expeditions. Weiss et al. (1983) point out that the shore-based analyses were systematically smaller than the at-sea measurements by  $16.5 \pm 5 \mu\text{mol/kg}$  during GEOSECS. Comparable comparisons between the WOCE/JGOFS at-sea measurements and Keeling's shore-based analyses indicate that the shore-based samples are approximately  $5 \mu\text{mol/kg}$  higher than the at-sea values. Together, the GEOSECS-Keeling-WOCE/JGOFS combination suggests an offset of  $21.5 \mu\text{mol/kg}$  between GEOSECS and WOCE/JGOFS at-sea measurements. It is also important to note that there is no indication of a depth- or concentration-dependent correction for the GEOSECS data. The shore-based comparison, based only on samples collected at the surface, is within  $1 \mu\text{mol/kg}$  of the deep comparison described above. Based on these results, a constant correction of the  $22\text{--}22.5 \mu\text{mol/kg}$  should be applied to the original reported GEOSECS  $\text{TCO}_2$  values to improve the consistency with the WOCE/JGOFS data sets.

### 2.3 The Pacific Ocean Database Synthesis

Between 1991 and 1999, investigators from 15 different laboratories and 4 countries analyzed carbon measurements on 25 WOCE/JGOFS/OACES cruises in the Pacific Ocean. The Pacific Ocean database compiled from these measurements consists of over 136,000 unique sample locations from these cruises. Carbon measurements were made as part of the DOE-funded JGOFS Global Survey. Details of the WOCE/JGOFS Pacific Ocean  $\text{CO}_2$  measurement program—including personnel, sampling and measurement protocols, and data quality assurance/quality control checks—are described in Lamb et al. 2002, which is reprinted as Appendix A in this document. Table 4 gives some details about the individual cruises in the Pacific Ocean compiled for this project.

The Pacific Ocean quality assessment required a much greater effort than did the Indian Ocean assessment. In the Indian Ocean the same parameters were measured with exactly the same equipment, the cruises were carried out as one expedition over a 2-year period, and CRMs were used on all WOCE and NOAA legs. The Pacific measurements involved many of the same principal investigators as the Indian Ocean expedition, but each group used different equipment, different parameter combinations were measured, and the measurements were spread over 8 years. During this synthesis work, we compiled data from 26 cruises in the Pacific Ocean, including data from Canadian,

**Table 4. Pacific Ocean data set information**

<b>Cruise/ Dates (Mon./Year)</b>	<b>Chief Sci. Inst.</b>	<b>Hydro Inst.</b>	<b>Nutrients Inst.</b>	<b>TCO<sub>2</sub> PI/Inst.</b>	<b>TALK PI/Inst.</b>	<b>fCO<sub>2</sub> PI/Inst.</b>	<b>pH PI/Inst.</b>	<b>CRM TCO<sub>2</sub>/TALK/ fCO<sub>2</sub>/pH</b>	<b>CFC PI/Inst.</b>	<b><sup>14</sup>C PI/Inst.</b>
CGC-91/1 2/91	Wisegarver PMEL	M PMEL	M SIO	M/Feely PMEL	N	N	M/Byrne USF	MC/N/N/N	M/Bullister PMEL	M/Key PU
P16N 2-4/91	Bullister PMEL	M PMEL	M SIO	M/Feely PMEL	N	N	M/Byrne USF	MC/N/N/N	M/Bullister PMEL	M/Key PU
P17C 5-7/91	Tsuchiya SIO	M SIO	M SIO	M/Goyet WHOI	M/Goyet WHOI	N	N	N/N/N/N	M/Fine RSMAS	M/Key PU
P16S17S 7-8/91	Swift SIO	M SIO	M SIO	M/Takahashi LDEO	M/Goyet WHOI	M/Takahashi LDEO	N	M/N/N/N	M/Fine RSMAS	M/Key PU
P16C 8-10/91	Talley SIO	M SIO	M OSU	M/Goyet WHOI	M/Guenther SIO	N	N	M/N/N/N	M/Bullister PMEL	M/Quay UW
S4P 2-4/92	Koshlyakov ShIO	M ShIO	M SIO	M/Takahashi LDEO	N	M/Takahashi LDEO	N	M/N/N/N	M/Bullister PMEL	M/Schlosser LDEO
P6 5-7/92	Bryden, McCartney, Toole WHOI	M WHOI	M OSU	M/Wallace BNL	M/Wallace BNL	N	N	M/N/N/N	M/Fine RSMAS Warner/UW Weiss/SIO	M/Key PU
P14C 8-9/92	Roemmich SIO	M SIO	M SIO	M/Bingler PNL	M/Bingler PNL	N	N	M/N/N/N	M/Warner UW	M/Key PU
P13N 8-10/92	Bullister PMEL	M PMEL	M USF	M/Dickson SIO	M/Keeling SIO	N	N	M/MC/N/N	M/Bullister PMEL	M/Quay UW
EQPAC-Fall 9-12/92	Feely PMEL Wanninkhof AOML	M PMEL	M PMEL	M/Feely PMEL Wanninkhof AOML	M/Millero RSMAS	M/Feely PMEL Wanninkhof AOML	M/Byrne USF	MC/MC/N/N	N	M/ Togweiller UW
EQPAC- Spring 4-5/92	Feely PMEL	M PMEL	M PMEL	M/Feely PMEL	M/Millero RSMAS	M/Wanninkhof AOML	M/Byrne USF	MC/MC/N/N	N	N
P17E19S 12/92-1/93	Swift SIO	M SIO	M SIO	M/Takahashi LDEO	N	M/Takahashi LDEO	N	M/N/M/N	M/Weiss SIO	M/Key PU
P16A17A 10-11/92	Reid SIO	M SIO	M OSU	M/Takahashi LDEO	N	M/Takahashi LDEO	N	M/N/N/N	M/Weiss SIO	M/Key PU

Table 4 (continued)

Cruise/ Dates (Mon./Year)	Chief Sci. Inst.	Hydro Inst.	Nutrients Inst.	TCO <sub>2</sub> PI/Inst.	TALK PI/Inst.	fCO <sub>2</sub> PI/Inst.	pH PI/Inst.	CRM TCO <sub>2</sub> /TALK/ fCO <sub>2</sub> /pH	CFC PI/Inst.	<sup>14</sup> C PI/Inst.
P19C 2-4/93	Talley SIO	M SIO	M SIO	M/Takahashi LDEO	N	M/Takahashi LDEO	N	M/N/M/N	M/Fine RSMAS	M/Key PU
P17N 5-6/93	Musgrave UA	M SIO	M SIO	M/Goyet WHOI	M/Goyet WHOI	N	N	M/N/N/N	M/Fine RSMAS	M/Key PU
P2 1-2/94	Okuda NRIFS	M TU	M NIES	M/Ono HU	M/Ono HU	N	M/Ono HU	M/N/N/N	M/Watanab e NIRE	N
P10 10-11/93	Hall WHOI	M WHOI	M OSU	M/Sabine PU	M/Sabine PU	N	N	MC/MC/N/N	M/Warner UW	M/Key PU
P14N 7-8/93	Roden UW	M UW	M SIO	M/Winn UH	M/Millero RSMAS	N	M/Winn UH	M/M/N/N	M/Warner UW	M/Schlosser LDEO
P31 1-2/94	Roemmich SIO	M SIO	M SIO	M/Winn UH	M/Winn UH	N	M/Winn UH	M/M/N/N	M/Warner UW	N
P18 CGC-94 1-4/94	Johnson PMEL	M PMEL	M UW	M/Feely PMEL	M/Millero RSMAS	M/Wanninkhof AOML	M/Byrne USF	MC/MC/N/N	M/Bullister PMEL	M/Quay UW
P21 3-5/94	McCartney WHOI	M WHOI	M OSU	M/Winn/UH Goyet/WHOI	M/Goyet/WHOI Millero RSMAS	N	M/Millero RSMAS	MC/MC/N/M	M/Bullister PMEL	N
P9 7/94	Kaneko Kawae JMA	M JMA	M JMA	M/Ishii JMA	N	N	N	MC/MC/N/N	M/Tamak Kaneko JMA	M/Ishii JMA
P15N 9-11/94	Freeland IOC	M IOC	M IOC	M/Wong IOC	M/Wong IOC	N	N	M/M/N/N	M/Wong IOC	M/Wong IOC
SR4S4 12/94-1/95	Rintoul CSIRO	M CSIRO	M CSIRO	M/Tilbrook CSIRO	M/Tilbrook CSIRO	N	N	MC/MC/N/N	M/Bullister PMEL	N
P14S15S CGC-96 1-3/96	Bullister Feely/PME L	M PMEL	M PMEL	M/Feely PMEL	M/Millero RSMAS	M/Feely PMEL	M/Byrne USF	MC/MC/N/N	M/Bullister PMEL	M/Quay UW
P8S 6-7/96	Yoshioka JAMSTEC	M JAMSTEC	M JAMSTEC	M/Shitashima CRIEPI	M/Shitashima CRIEPI	N	M/Shitashima CRIEPI	M/N/N/N	N	M/Saito JAMSTEC

*Notes to Table 4:*

Abbreviations: M — Measured; N — Not measured; MC — CRM used and data corrected.

Affiliated institutions:

PMEL	Pacific Marine Environmental Laboratory, NOAA
SIO	Scripps Institution of Oceanography
USF	University of South Florida
PU	Princeton University
WHOI	Woods Hole Oceanographic Institution
RSMAS	Rosenstiel School of Marine and Atmospheric Science, University of Miami
LDEO	Lamont-Doherty Earth Observatory
OSU	Oregon State University
UW	University of Washington
ShIO	Shirshov Institute of Oceanology, Russia
BNL	Brookhaven National laboratory
PNL	Pacific National Laboratory
AOML	Atlantic Oceanographic and Meteorological Laboratory, NOAA
UA	University of Alaska
NRIFS	National Research Institute of Fisheries Science, Japan
TU	Tokai University, Japan
NIES	National Institute for Environmental Studies, Japan
HU	Hokkaido University, Japan
NIRE	National Institute for Research and Environment, Japan
UH	University of Hawaii
JMA	Japan Meteorological Agency, Japan
IOC	Institute of Ocean Sciences, Canada
CSIRO	Commonwealth Scientific and Industrial Research Organization, Australia
JAMSTEC	Japan Marine Science and Technology Center
CRIEPI	Central Research Institute Electric Power Industry, Japan

Japanese, and Australian cruises. Our assessment of the Pacific TCO<sub>2</sub> data indicates that the reported values are accurate to  $\pm 3$   $\mu\text{mol/kg}$  after recommended adjustments of +4, -7, and -4  $\mu\text{mol/kg}$  for legs P16N, P17N, and P2, respectively. The TALK data are generally good to  $\pm 5$   $\mu\text{mol/kg}$  after adjustments of +6, -9, -12, +14, and -6  $\mu\text{mol/kg}$  for legs P8S, P17C, P17N, P2, and P31, respectively. We also adjusted all reported spectrophotometric pH values by +0.0047 to improve the internal consistency with the other carbon measurements.

Table 5 lists the proposed adjustments for some sections.

**Table 5. Pacific Ocean carbon data adjustments<sup>2</sup>**

Section	TCO <sub>2</sub> ( $\mu\text{mol/kg}$ )	TALK ( $\mu\text{mol/kg}$ )	pH	Section	TCO <sub>2</sub> ( $\mu\text{mol/kg}$ )	TALK ( $\mu\text{mol/kg}$ )	pH
P8S	NA <sup>b</sup>	+6	NA	P16S, 17S	NA	CAL <sup>d</sup>	ND
P16N	+4	ND <sup>c</sup>	+0.0047	P14N	NA	NA	+0.0047
P17C	NA	-9	ND	P14S, 15S	NA	NA	+0.0047
P17N	-7	-12	ND	EQS92	NA	NA	+0.0047
P2	-4	+14	NA	P18	NA	NA	+0.0047
P31	NA	-6	+0.0047	P21	NA	NA	+0.0047 <sup>a</sup>

Abbreviations: NA — no adjustments recommended; ND — no data reported; CAL — parameter was calculated.

<sup>a</sup> Western section only.

This paragraph<sup>3</sup> contains detailed information on the QA/QC procedures used to examine the quality of the Pacific data. These procedures can be used to infer the internal consistency of the basinwide data set and may be used to infer an offset with a given parameter on a particular cruise (see Table 5). The primary means of evaluating the internal consistency of the data was to compare deep- water concentrations in locations where two or more cruises intersect or overlap. Crossover locations are given in Fig. 5.

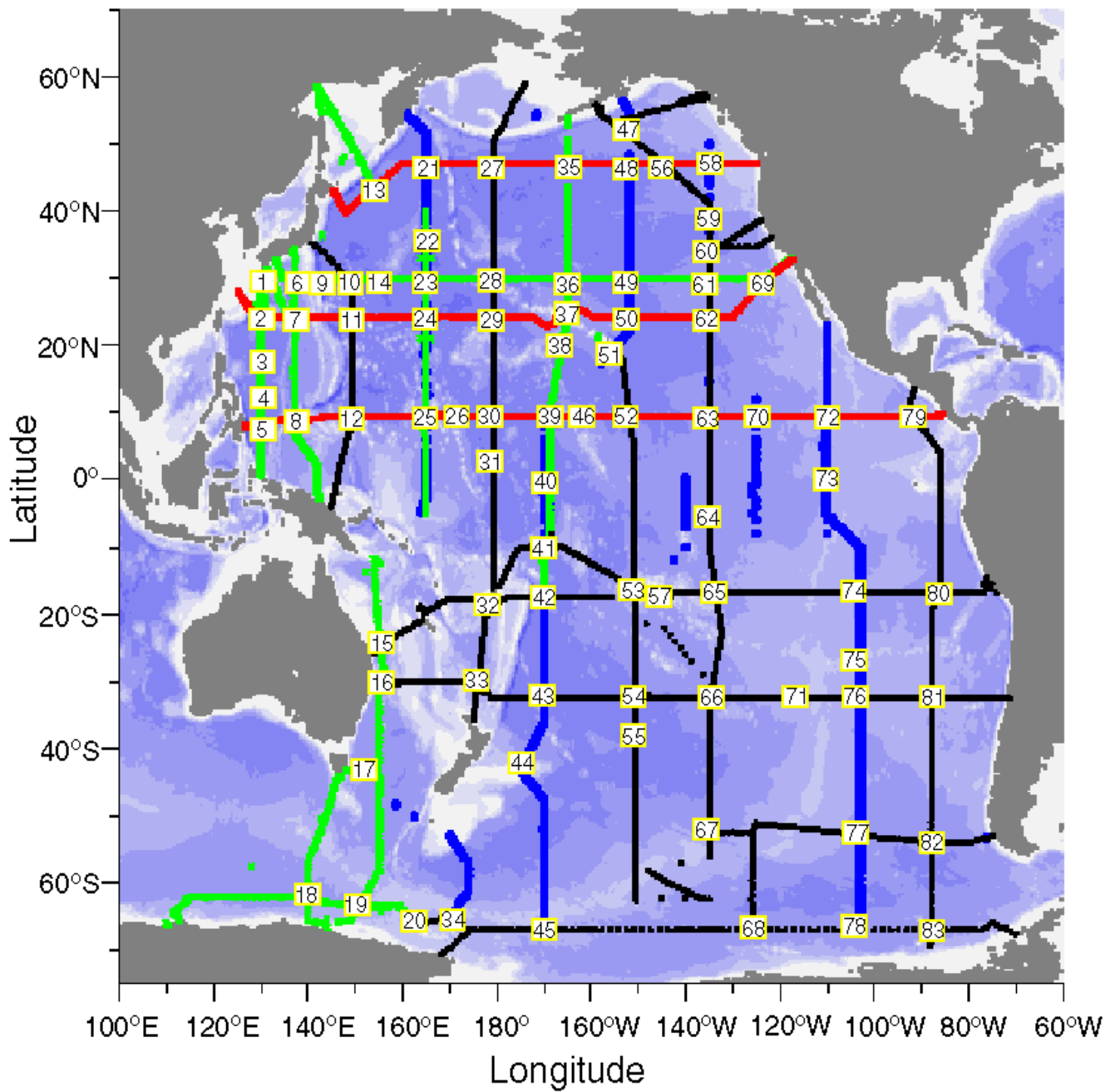


**Fig. 5. Pacific Ocean map of the crossover locations.**

### 2.3.1 Pacific Ocean Total Carbon Dioxide Crossover Analysis

The purpose of this analysis was to determine if any significant systematic offset existed between the various legs of the WOCE/NOAA/JGOFS Pacific Ocean TCO<sub>2</sub> measurements. The stations selected for each crossover were those with carbon data which were close to the crossover point. The number of stations selected was somewhat subjective, but was such that sufficient measurements were present for the analysis without getting too far away from the crossover location. In all cases the stations were within approximately 1° of latitude or longitude of the crossover point. Data from deep water (>2000 m) at each of the crossover locations were plotted against the density anomaly referenced to 3000 dbar ( $\sigma$ -3) and fit with a second-order polynomial. The difference and standard deviation between the two curves was then calculated from 10 evenly spaced intervals over the density range common to both sets of crossover (Fig. 6 and Table 6).

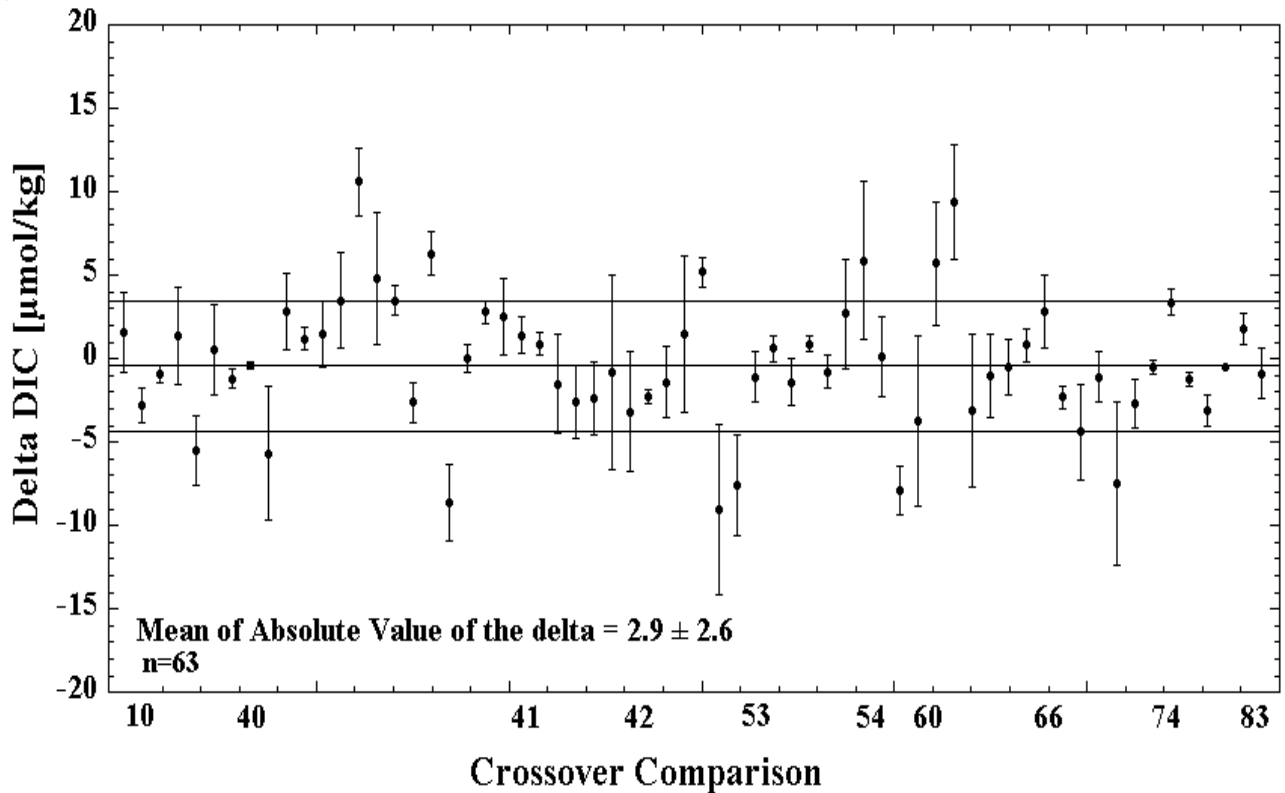


Fig. 6. TCO<sub>2</sub> crossover points comparison in the Pacific Ocean (>2000 db, 2nd-order polynomial fit).

**Table 6. Summary of TCO<sub>2</sub> crossover results in the Pacific Ocean**

Crossing no.	Latitude	Longitude	Section 1	Section 1 station	Section 2	Section 2 station	ΔTCO <sub>2</sub> st. dev. (μmol/kg)
6	30° N	135° E	P9	21	P2	19, 21	1.6±2.4
10	30° N	148° E	P10	74, 77	P2	37	-2.8±1.0
18	63° S	140° E	SR3S4	33	SR3S4	65	-0.9±0.5
20	66° S	164° E	SR3S4	51	S4P	791	1.4±2.9
23	30° N	165° E	P13	54, 55	P2	48	-5.5±2.1
28	30° N	178° E	P14N	63	P2	58	0.5±2.7
33	31° N	177° E	P6C	188	P6E	191	-1.2±0.6
34	66° S	171° E	P14S15S	32	S4P	783, 787	0.4±0.2
36	30° N	165° W	P15N	52, 54	P2	65	-5.7±4.0
40a	0°	170° W	P14S15S	174	EQS92	56	2.8±2.3
40b	0°	170° W	P14S15S	174	P15N	112	1.2±0.7
40c	0°	170° W	P15N	112	EQS92	56	1.5±2.0
40d	1° S	170° W	P14S15S	173	P15N	114	3.5±2.9
40e	2° S	170° W	P14S15S	172	P15N	116	10.6±2.0
40f	3° S	170° W	P14S15S	171	P15N	118	4.8±4.0
40h	4° S	170° W	P14S15S	170	P15N	120	3.5±0.9
40i	5° S	170° W	P14S15S	169	EQS92	63	-2.6±1.2
40j	5° S	170° W	P14S15S	169	P15N	122	6.3±1.3
40k	5° S	170° W	P15N	122	EQS92	63	-8.6±2.3
40l	6° S	170° W	P14S15S	167	P15N	124	0.0±0.8
40m	7° S	170° W	P14S15S	165	P15N	126	2.8±0.7
40n	8° S	170° W	P14S15S	163	P15N	128	2.5±2.3
40o	12° S	170° W	P14S15S	155	P15N	134, 136	1.4±1.1
41a	10° S	170° W	P14S15S	157, 159, 161	P15N	130, 132	0.9±0.7
41b	10° S	170° W	P14S15S	157, 159, 161	EQS92	66	-1.5±3.0
41c	10° S	170° W	P14S15S	157, 159, 161	P31	54, 57, 61	-2.6±2.2
41d	10° S	170° W	P15N	130, 132	EQS92	66	-2.4±2.2
41e	10° S	170° W	EQS92	66	P31	54, 57, 61	-0.8±5.8

**Table 6 (continued)**

Crossing no.	Latitude	Longitude	Section 1	Section 1 station	Section 2	Section 2 station	$\Delta\text{TCO}_2$ st. dev. ( $\mu\text{mol/kg}$ )
41f	10° S	170° W	P15N	130, 132	P31	54, 57, 61	-3.2±3.6
42	17° S	170° W	P14S15S	141, 142, 144	P21	193, 195, 197	-2.3±0.4
43	32° S	170° W	P14S15S	110, 112, 114	P6	153, 165	-1.4±2.1
44	40° S	173° W	P14S15S/1	93	P14S15S/2	94	1.5±4.7
45	67° S	169° W	P14S15S	33	S4P	755	5.2±0.9
47	53° N	152° W	P16N	58, 59, 66	P17N	78	-9.0±5.1
49	30° N	152° W	P16N	30, 31, 32	P2	70	-7.6±3.0
53a	17° S	150° W	P16C	222	P16S17S	220	-1.1±1.5
53b	17° S	150° W	P16C	222	P31	2, 5	0.6±0.8
53c	17° S	150° W	P16C	222	P21	157, 160	-1.4±1.4
53d	17° S	150° W	P16S17S	220	P31	2, 5	0.9±0.5
53e	17° S	150° W	P16S17S	220	P21	157, 160	-0.8±1.0
53f	17° S	150° W	P21	157, 160	P31	2, 5	2.7±3.3
54	32° S	150° W	P16S17S	190	P6	127, 129	5.9±4.7
55	37° S	150° W	P16S17S	180	P16A17A	3	0.1±2.4
59	40° N	135° W	CGC91/1	10	P17N	37, 38, 45	-7.9±1.5
60a	35° N	135° W	CGC91/1	12	P17N	28	-3.7±5.1
60b	35° N	135° W	CGC91/1	12	P17C	17	5.7±3.7
60c	35° N	135° W	P17N	28	P17C	17	9.4±3.4
61	30° N	135° W	P17C	26	P2	78	-3.1±4.6
64	6° S	135° W	P17C	121	P16S17S	124	-1.0±2.5
65	16° S	133° W	P16S17S	148	P21	131	-0.5±1.7
66a	33° S	135° W	P16S17S	179	P6	108	0.8±1.0
66b	33° S	135° W	P16S17S	179	P16A17A	119	2.8±2.2
66c	33° S	135° W	P16A17A	119	P6	108	-2.3±0.7
67	53° S	135° W	P16A17A	77	P17E19S	128	-4.4±2.9
68	66° S	126° W	P17E19S	163	S4P	723, 727	-1.1±1.5
73	5° N	110° W	P18	155, 159	EQS92	6	-7.5±4.9
74	17° S	103° W	P18	105, 106	P21	77	-2.7±1.5

**Table 6 (continued)**

Crossing no.	Latitude	Longitude	Section 1	Section 1 station	Section 2	Section 2 station	$\Delta\text{TCO}_2$ st. dev. ( $\mu\text{mol/kg}$ )
76	32° S	103° W	P18	73	P6	56, 58	-0.5±0.4
77	52° S	103° W	P18	37	P17E19S	194	3.4±0.8
78	67° S	103° W	P18	10, 11	S4P	711, 712, 713	-1.2±0.4
80	16° S	86° W	P19	333	P21	49	-3.1±0.9
81	32° S	88° W	P19	299	P6	32, 34, 36	-0.5±0.1
82	53° S	88° W	P19	256	P17E19S	206	1.8±0.9
83	67° S	88° W	S4P	703	P17E19S	229	-0.9±1.5
<b>Average: -0.3±3.9</b>							

A secondary check was performed on crossover with large deltas or large standard deviations from the crossover analysis. A multi-parameter liner least square regression method is used to examine the offsets at selected crossover locations. Data in Cruise 1 are used as a reference to derive a best-fit equation:

$$\text{TCO}_2 = a + b \times \text{Sal} + c \times \text{T} + d \times \text{Oxy} , \quad (1)$$

where  $a$ ,  $b$ ,  $c$ , and  $d$  are constants; Sal is salinity; T is temperature; and Oxy is oxygen concentration. Once the equation is derived,  $\text{TCO}_2$  is calculated from the Cruise 2 Sal, T, and Oxy data. The difference between this predicted  $\text{TCO}_2$  and the observed  $\text{TCO}_2$  at the Cruise 2 stations is defined as  $\Delta\text{TCO}_2$ . Results from the multiple-parameter regression method are listed in Table 7.

**Table 7. Results from the multiple-parameter regression method**

Crossing no.	Cruise 1- station	Cruise 2- station	$\Delta\text{TALK}$ ( $\mu\text{mol/kg}$ )	St. dev.
23	P13-54, 55	P2-48	6.2	8.8
36	P15N-52, 54	P2-65	-2.9	3.4
40d	P14S15S-173	P15N-114	-3.3	4.3
40e	P14S15S-172	P15N-116	2.2	1.5
40f	P14S15S-171	P15N-118	-1.3	2.7
40h	P14S15S-170	P15N-120	-1.5	3.2
40j	P14S15S-169	P15N-122	-0.5	3.1
40k	P15N-122	EQS92-63	-0.6	1.7
41b	P14S15S-157	EQS92-66	-3.5	3.2
41f	P15N-130, 132	P31-54, 57, 61	-1.2	4.4
44	P14S15S/1-93	P14S15S/2-94	-0.1	2.1

Table 7 (continued)

Crossing no.	Cruise 1- station	Cruise 2- station	$\Delta$ TALK ( $\mu\text{mol/kg}$ )	St. dev.
45	P14S15S-33	S4P-755	6.6 <sup>a</sup>	3.4
47	P16N-58, 59, 66	P17N-78	-10.0	3.4
49	P16N-30, 31, 32	P2-70	-1.9	1.9
53f	P21-157, 160	P31-2, 5	3.4 <sup>a</sup>	4.3
54	P16S17S-190	P6-127, 129	3.7	1.6
60a	CGC91-12	P17N-28	-7.7	5.3
60b	CGC91-12	P17C-17	-3.5	5.3
60c	P17N-28	P17C-17	11.3	5.5
61	P17C-26	P2-78	2.2	4.6
67	P16A17A-77	P17E19S-128	4.7 <sup>a</sup>	13.6
73	P18-155, 159	EQS92-6	-0.6	1.2
77	P18-37	P17E19S-194	2.9 <sup>a</sup>	1.6
80	P19-333	P21-49	-2.2 <sup>a</sup>	2.3

<sup>a</sup>  $\Delta$ TALK deemed unreliable because of poor fits.

These results are compared with the deltas derived from curve-fitting method in Fig. 7.

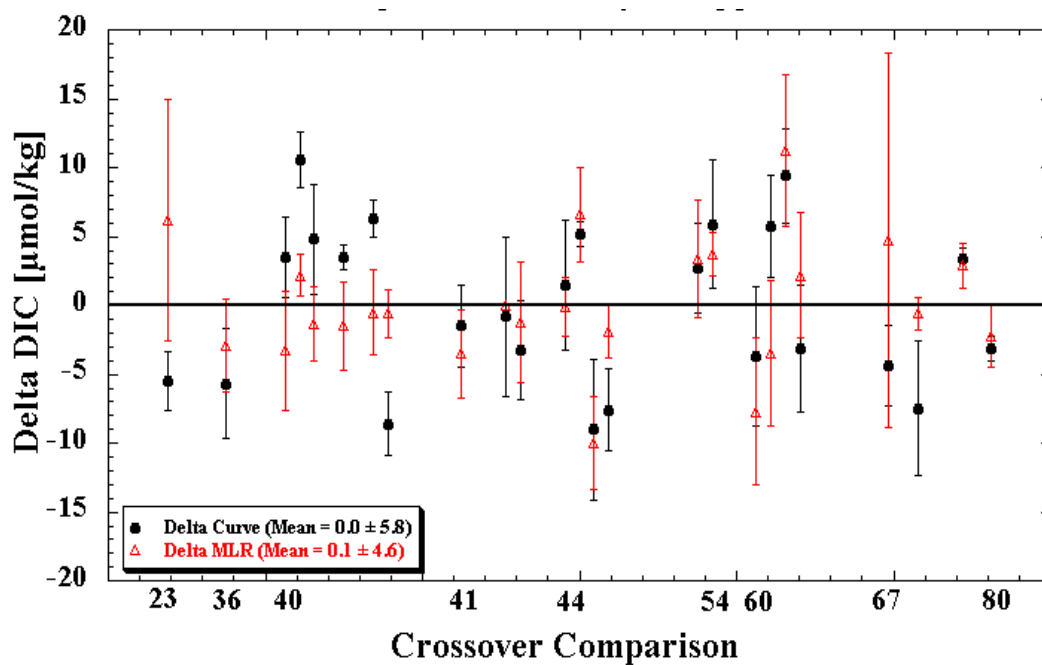


Fig. 7. Problematic  $\text{TCO}_2$  crossovers in the Pacific Ocean (multi-parameter analyses approach).

The multi-parameter method generally had smaller delta values, suggesting that some of the differences in the crossovers with large deltas could actually be due to real changes in the water mass properties.

Optimum cruise adjustments, based on the crossover results, were evaluated using several approaches. The first approach was a simple least-squares minimization (SLSQ). The optimized cruise adjustments based on an equal weighting of the crossover data are shown in the Figs 8 and 9. The second approach for calculating the adjustments was weighted least-squares (WLSQ); the weighting used the error estimates from the polynomial fits, and focused on making adjustments to minimize offsets at crossover, where they were better determined. The more crossovers used to determine the adjustments, and the smaller the offset uncertainties at those crossovers, the smaller the adjustment uncertainties. The third approach was weighted, damped least-squares (WDLSQ), formally equivalent to a Gauss-Markov model (Wunsch, 1996). The damping used was a prior guess of the variance at crossover, estimated to be a constant  $32 \mu\text{mol/kg}$  for  $\text{TCO}_2$ —hopefully, what one might have guessed this RMS value of crossover differences to be before the survey was started. One could also choose to vary the damping on a cruise-by-cruise basis to reflect prior information on the accuracy of individual cruises (e.g., whether or not CRMs were used when determining  $\text{TCO}_2$  concentrations, or when the measurements were made, or even who made the measurements); for this study, a constant damping was used. A summary of the proposed adjustments based on the three different approaches using a Del Poly model is given in Fig. 8.

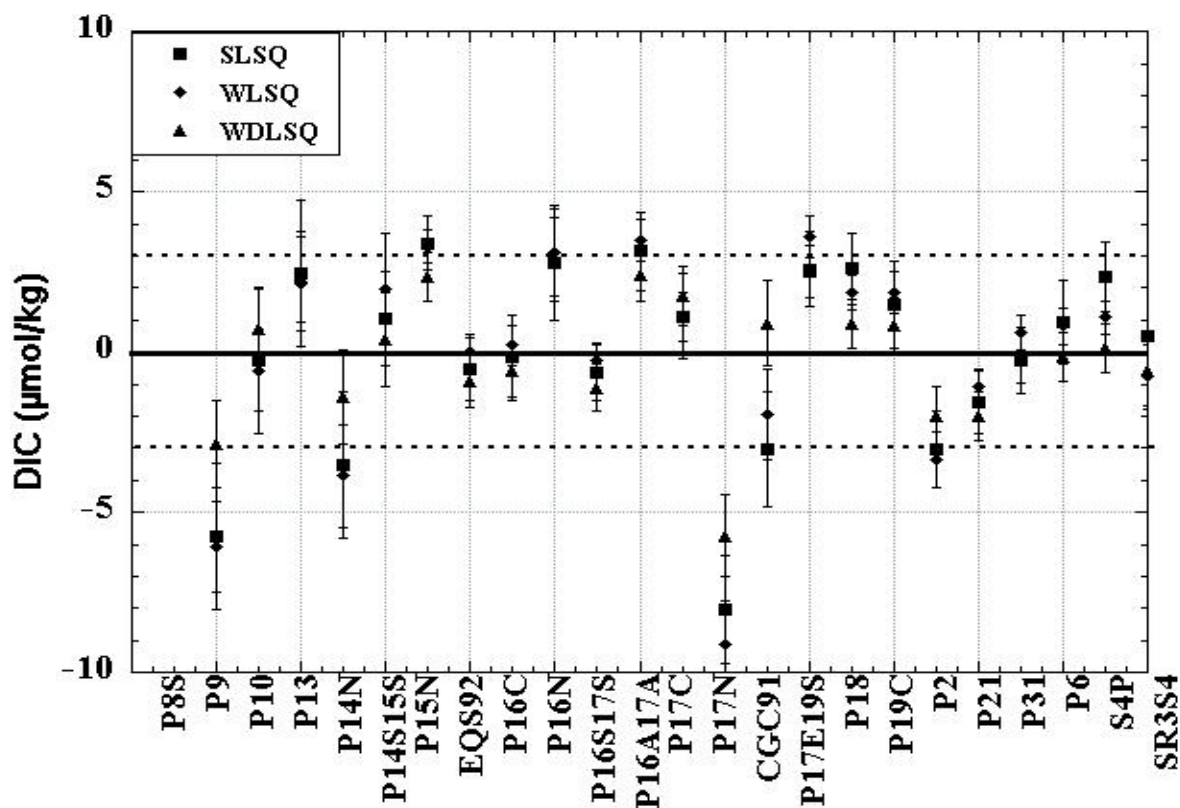


Fig. 8. Del Poly analyses of  $\text{TCO}_2$  adjustments in the Pacific Ocean.

In an effort to ensure that sparse sampling combined with either noisy data or variability resulting from water mass variations was not significantly biasing the estimates of the offsets, we examined a second approach to the polynomial fit. We will call this approach the Del Poly model.<sup>4</sup> For the second approach (termed the same shape model) we fitted a second-order polynomial function to data from both Cruise 1 and Cruise 2 in a way that allowed a constant offset for the two cruises but identical slope and curvature

terms. The assumption was made that for any given crossover, the differences between the data from the two cruises could be expressed in the same shape model as a constant offset for  $\text{TCO}_2$  and TALK. The assumption of a constant offset was made partly because an offset was the simplest adjustment; however, with the relatively uniform oceanic values for  $\text{TCO}_2$  and TALK, additive or multiplicative adjustments would give similar results. Fig. 9 provides a summary of the proposed adjustments based on the three different approaches using the same shape model. The proposed adjustments from the three different least-squares models were similar to the adjustments from the Del Poly analysis.

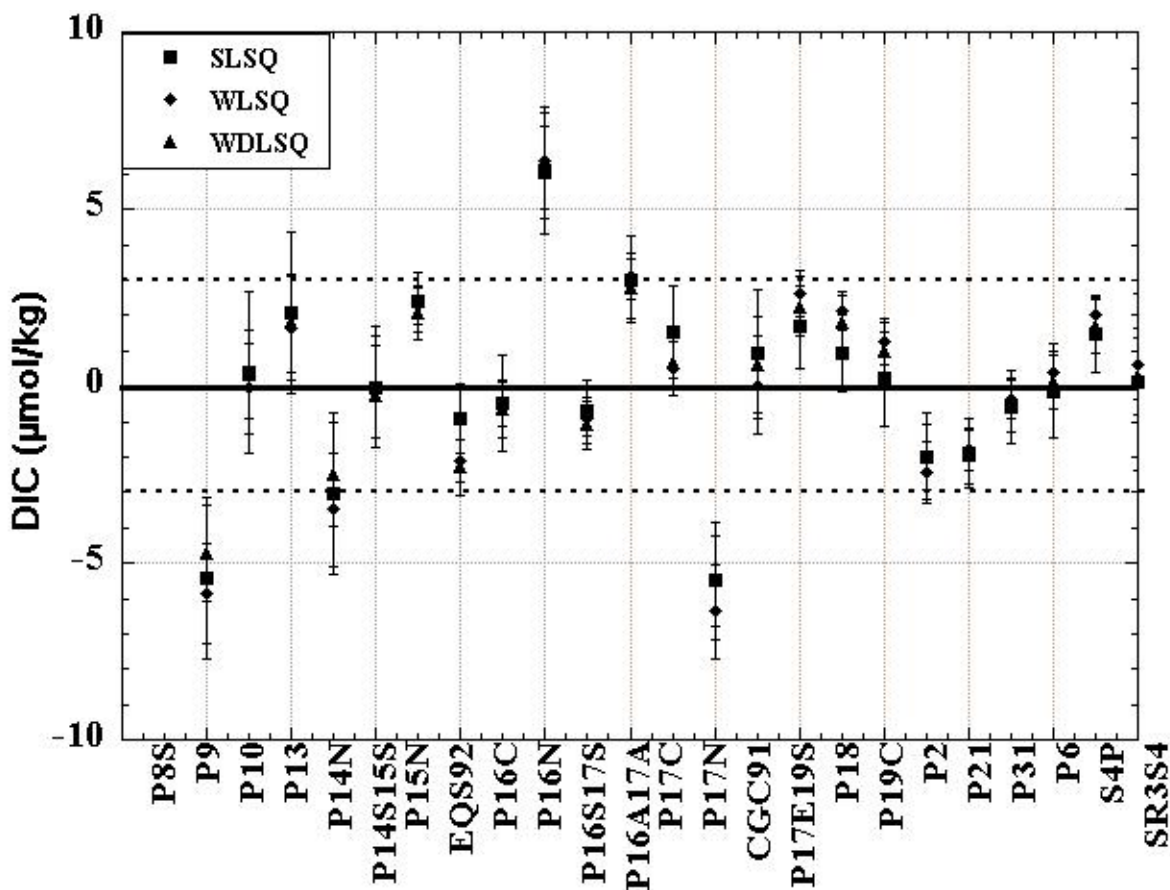


Fig. 9. Same-shape analyses of  $\text{TCO}_2$  adjustments in the Pacific Ocean.

Using the crossover differences estimated from the polynomial fits, the 64 crossovers for  $\text{TCO}_2$  had an average and standard deviation of  $0.3 \pm 4.0 \mu\text{mol/kg}$ . The average of the absolute values of the differences was  $2.9 \pm 2.6 \mu\text{mol/kg}$ . Twenty-four  $\text{TCO}_2$  crossover with differences from the polynomial fits  $>3 \mu\text{mol/kg}$  were further examined using the MLR crossover approach. Unlike the polynomial fit crossover approach, the MLR method does not assume that the waters are identical, only that the relationships between  $\text{TCO}_2$  and the other properties do not change, and that the effects of measurement errors in the independent variables can be neglected. In the South Pacific, most of the crossovers with large differences were from the P14S15S-P15N crossover comparisons near the equatorial region [a series of zonal crossover comparisons between the equator and  $12^\circ \text{S}$  along  $170^\circ \text{W}$  (crossover 40)]. In general, the use of the crossover MLR analysis resulted in smaller differences, suggesting that the assumption of identical waters may not be valid for this area. The MLR analysis did show, however, that P13 and P17N should be decreased by  $6 \mu\text{mol/kg}$  and  $10 \mu\text{mol/kg}$ , respectively, and that P16N, CGC91, and S4P should all be increased by  $6 \mu\text{mol/kg}$  (see Table 5).

Both the Del Poly and same shape models give very similar differences, but the uncertainties are generally smaller for the same shape model. It is difficult to say which approach is more appropriate for

these data, since the answer depends somewhat on the nature of the errors. If we assume a priori that the primary difference between the data sets results from a constant offset, then the same shape model is most appropriate. Of the three least squares models examined, the WDL SQ adjustments and errors make use of the most information (error estimates and prior guesses on crossover differences) to determine adjustments and their uncertainties. The results from WDL SQ show that almost all cruises during the Pacific Ocean TCO<sub>2</sub> survey are within ~3 μmol/kg for TCO<sub>2</sub>. A few cruises lie outside this cutoff. These results indicate that P9 should be decreased by 3–5 μmol/kg, P17N should be decreased by 5–6 μmol/kg, and P16N should be increased by 3–6 μmol/kg.

All of these results must be considered in conjunction with the other lines of evidence on the quality of the TCO<sub>2</sub> measurements from the various cruises. The TCO<sub>2</sub> data were also examined using a basinwide MLR approach (see Appendix A) and using an isopycnal analysis [see Sec. 2.3.1(a) below]. Table 8 presents a summary of the TCO<sub>2</sub> quality assessment results.

**Table 8. Summary of the TCO<sub>2</sub> quality assessment results**

Cruise	TCO <sub>2</sub> analysis technique	TCO <sub>2</sub> P.I.	Standardization technique	Sample vol. (mL)	CRM correction SIO-cruise	Field replicate analyses Average Difference	SIO shorebase replicate analyses		
							Average difference shore-ship (μmol/kg)	Std. Dev. of difference (μmol/kg)	N
P8S	Coulorimeter	Shitashima	Liquid Standards	30	2.0±2.8	1.8	ND	ND	ND
P9	Coulorimeter	Ishii	Liquid Standards	23	1.1±1.3	2.0	ND	ND	ND
P10	Coulorimeter/SOMMA	Sabine	Gas Loops	22	±1.9	1.7	0.6	1.8	9
P13	Coulorimeter/SOMMA	Dickson	Gas Loops <sup>a</sup>	30	±2.4	0.9	-1.4	3.1	138
P14N	Coulorimeter/SOMMA	Winn/Millero	Gas Loops	20	ND	ND	0.7	2.3	27
P14S15S	Coulorimeter/SOMMA	Feely	Gas Loops	26	-1.1±0.9	1.9	ND	ND	ND
P15N	Coulorimeter/SOMMA	Wong	Liquid Standards	29	-0.1±2.7	ND	ND	ND	ND
EQS92	Coulorimeter/SOMMA	Feely	Gas Loops	26	-0.8±1.2	ND	ND	ND	ND
P16C	Coulorimeter/SOMMA	Goyet	Liquid Standards <sup>a</sup>	30	ND	ND	-2.1	2.4	66
P16N	Coulorimeter	Feely	Liquid Standards	50	3.0±2.5	2.8	ND	ND	ND

**Table 8 (continued)**

Cruise	TCO <sub>2</sub> analysis technique	TCO <sub>2</sub> P.I.	Standardization technique	Sample vol. (mL)	CRM correction SIO-cruise	Field replicate analyses average difference	SIO shorebase replicate analyses		
							Average difference shore-ship (μmol/kg)	Std. dev. of difference (μmol/kg)	N
P16S17S	Coulorimeter	Takahashi	Gas Loops	20	1.3±1.5	0.03%	-3.5	2.0	11
P16A17A	Coulorimeter	Takahashi	Gas Loops	20	1.0±1.7	0.03%	-3.4	1.8	14
P17C	Coulorimeter/ SOMMA	Goyet	Liquid Standards <sup>a</sup>	30	0 <sup>b</sup>	ND	-3.4	-4.0	40
P17N	Coulorimeter/ SOMMA	Goyet	Liquid Standards	30	0 <sup>b</sup>	ND	-1.0	4.1	9
CGC91	Coulorimeter	Feely	Liquid Standards	50	3.0±2.5	2.8	ND	ND	ND
P17E19S	Coulorimeter	Takahashi	Gas Loops	20	1.4±2.1	0.03%	ND	ND	ND
P18	Coulorimeter/ SOMMA	Feely	Gas Loops	26	-1.3±1.4	2.0	-0.4	2.0	28
P19C	Coulorimeter	Takahashi	Gas Loops	20	-0.2±2.1	0.03%	-1.0	1.9	15
P2	Coulorimeter	Ono	Gas Loops	32	6.8±3.1	ND	ND	ND	ND
P21	Coulorimeter/ SOMMA	Millero	Gas Loops	20	0.9±1.1	ND	-2.3	1.5	15
P31	Coulorimeter/ SOMMA	Winn	Gas Loops	21	-0.9±2.7	2.0	0.2	3.4	8
P6	Coulorimeter/ SOMMA	Wallace	Gas Loops	28	-0.6±1.9	ND	-2.6	1.9	21
S4P	Coulorimeter	Takahashi	Gas Loops	20	-0.9±1.8	0.03%	ND	ND	ND
SR3S4	Coulorimeter/ SOMMA	Tilbrook	Gas Loops	22	10.0±0.95	2.0	ND	ND	ND

Abbreviations: ND — no data; SOMMA — single-operator multiparameter analyzer

<sup>a</sup> CRM used as a primary standard.

<sup>b</sup> CRMs were not available.

### 2.3.1(a) TCO<sub>2</sub> Isopycnal Analysis

At a few locations in the North Pacific Ocean the estimated carbon offsets at the crossovers were not consistent with the offsets from the basinwide MLR analysis. In an attempt to determine whether the crossovers were biased by the limited number of stations analyzed, we expanded the crossover analysis to include additional stations along each cruise and/or stations from neighboring cruises. The deep (>2200 m) station data were averaged at specific potential density values ( $\sigma_\theta$  or  $\sigma_3$ ), and the mean values were compared at several isopycnal intervals for each cruise. The range of values observed for a particular cruise at each isopycnal level indicated whether the initial stations used in the crossover analysis were offset from the surrounding stations. The additional stations also provided more robust estimates of the difference between cruises, since more data points were included in the analysis.

*Analysis of P2 - P16N - P14 TCO<sub>2</sub>*

Results of isopycnal analysis of P2 and P16N TCO<sub>2</sub> near 30° N, 152° W indicates consistently higher TCO<sub>2</sub> values (8–10 μmol/kg) in deep water on the P2 line as compared with P16N (Fig. 10). The P14 data along 179° W also show slightly higher deep-water values (mean = 4 μmol/kg) than the P16N results. In the previous crossover and MLR analyses P14 showed no obvious offsets, whereas the P2 data were generally found to be high and the P16N were consistently low. The results of the isopycnal analysis can be reconciled with the findings of the other methods if the P16N data are increased by ~4 μmol/kg and the P2 data are decreased by 4–6 μmol/kg.

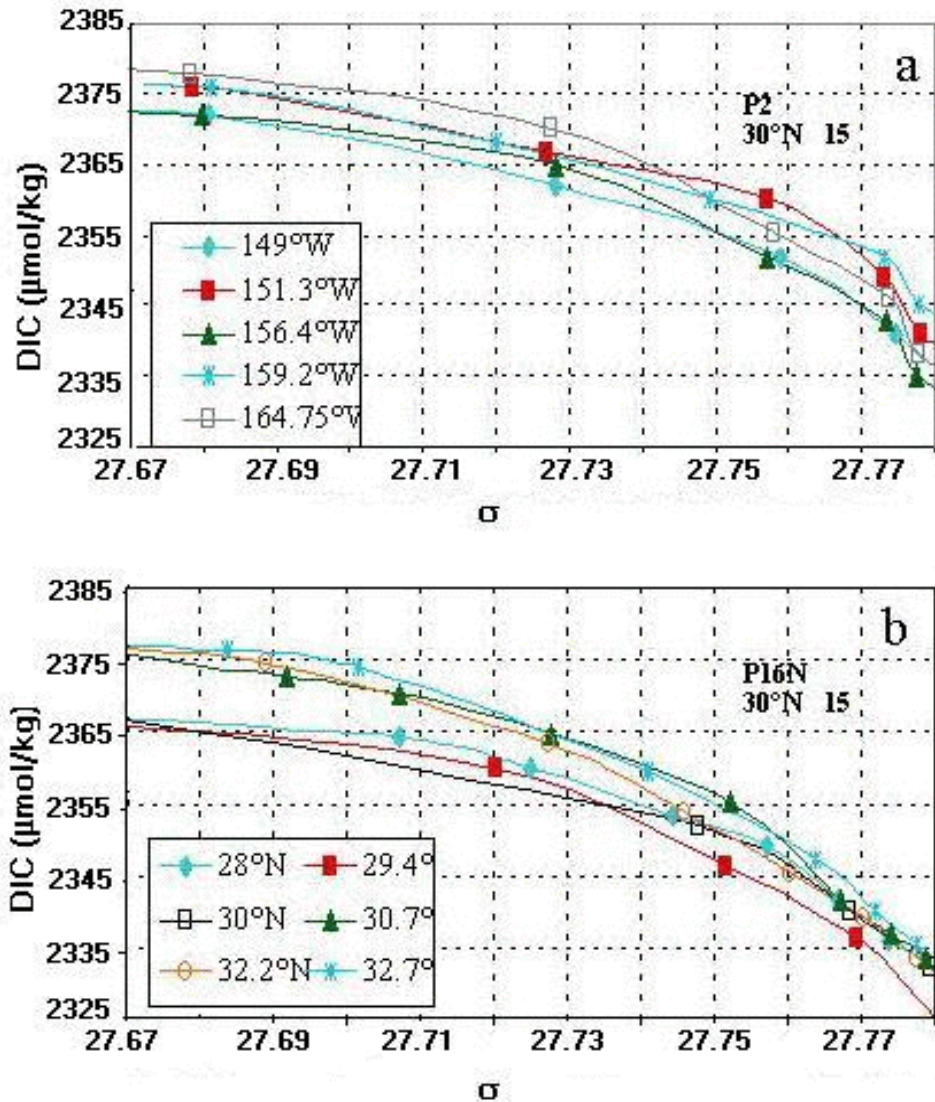


**Fig. 10. Results of TCO<sub>2</sub> isopycnal analysis of sections P2 (a) and P16N (b) plotted against σ near crossover at 30° N and 152° W.**

*Analysis of P17N - P17C - CGC91 TCO<sub>2</sub>*

In the region near 37° N, 135° W, the isopycnal analysis indicated that the P17N data are consistently higher (range: 6–16  $\mu\text{mol/kg}$ ) than the P17C and CGC91 data (Fig. 11). The CGC91 data agree reasonably well with the P17C results at higher densities, but are somewhat higher at the lowest densities. The crossover and MLR analyses of P17N indicate that the P17N data need to be decreased by 3–10  $\mu\text{mol/kg}$ . An average decrease of  $\sim 6$   $\mu\text{mol/kg}$  in P17N will account for most of the observed differences with P17C and CGC91, but not all of the observed 6–16  $\mu\text{mol/kg}$  range. The MLR techniques suggest that CGC91 should be increased by 4–5  $\mu\text{mol/kg}$ , but the crossover results are much smaller and none of the techniques indicate a large correction is necessary for P17C. All of these results cannot be reconciled, but a small increase of  $\sim 2$   $\mu\text{mol/kg}$  in both CGC91 and P17C would minimize all of the observed offsets from the various approaches.

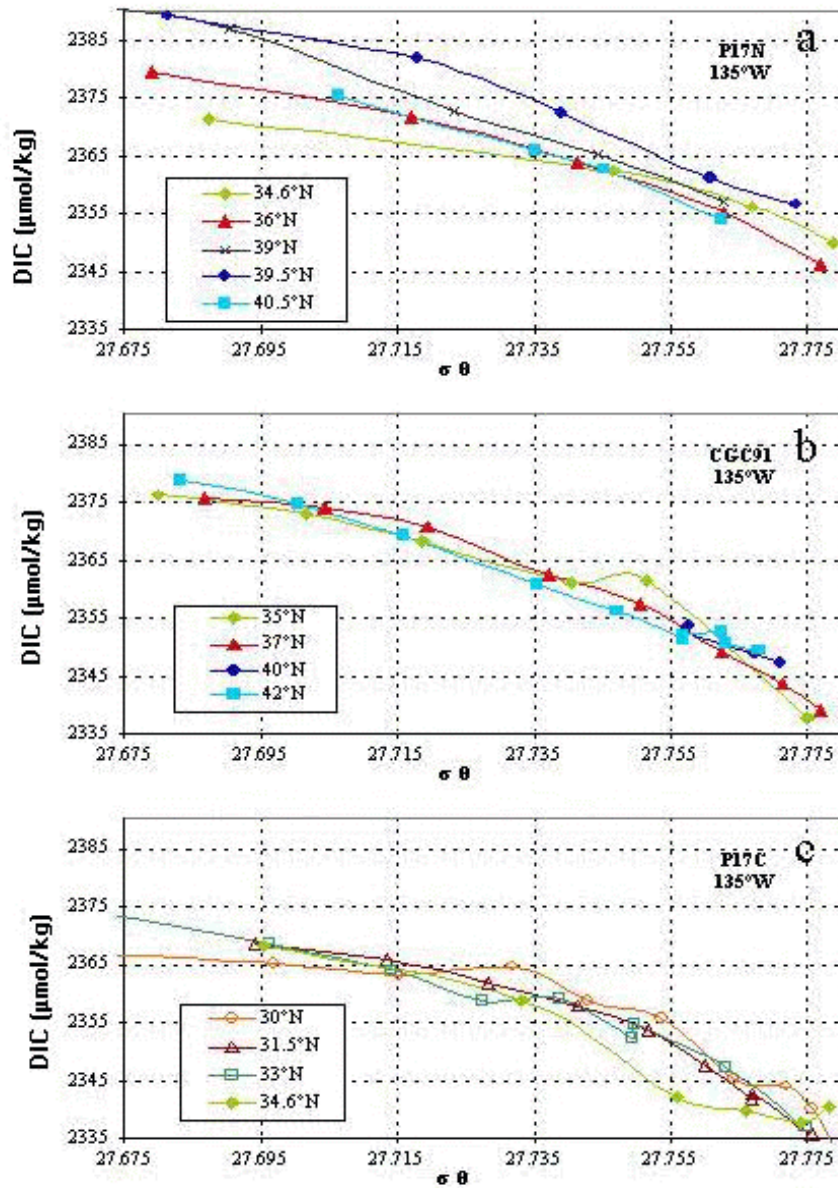


**Fig. 11. Results of TCO<sub>2</sub> isopycnal analysis of sections P17N (a), CGC91 (b), and P17C (c) plotted against  $\sigma_\theta$  near crossover at 35° N and 135° W.**

Results of statistical analysis for recommended adjustments of TCO<sub>2</sub> during the Global CO<sub>2</sub> Survey cruises in the Pacific Ocean are presented in Table 9.

**Table 9. Final results of statistical analysis for recommended TCO<sub>2</sub> adjustments in the Pacific Ocean.**

Cruise name	$\Delta$ WDL SQ (Del Poly)	Std. dev.	$\Delta$ WDL SQ (same shape)	Std. dev.	MLR Analyses			$\Delta$ Isopycnal analysis	
					Crossover (residual average)	Std. dev.	NP basin-wide (residual average)		
P8S	ND	ND	ND	ND	ND	ND	8.4	2.2	ND
P9	-4.7	1.3	-2.9	2.0	ND	ND	-1.9	3.7	ND
P10	0.3	1.3	0.7	1.5	ND	ND	0.7	2.8	ND
P13	1.8	1.4	2.3	1.9	-6.2	8.8	1.7	2.9	ND
P14N	-2.5	1.5	-1.4	2.1	ND	ND	0.0	3.7	ND
P14S15S	-0.3	1.4	0.4	1.7	0.2	3.3	ND	ND	ND
P15N	2.1	0.7	2.3	0.8	-0.3	2.1	2.3	3.6	ND
EQS92	-2.3	0.8	0.9	1.0	-1.6	1.7	ND	ND	ND
P16C	-0.6	0.8	-0.6	1.0	ND	ND	-2.5	2.8	ND
P16N	6.0	1.3	2.9	2.1	6.0	5.7	3.1	4.1	4.0
P16S17S	-1.1	0.7	-1.1	0.9	-3.7	1.6	ND	ND	ND
P16A17A	2.8	0.8	2.4	1.0	-4.7	13.6	ND	ND	ND
P17C	0.7	0.9	1.7	1.6	1.9	8.2	-0.5	4.1	2.0
P17N	-5.5	1.3	-5.7	1.8	-9.7	1.8	-2.6	6.7	-6.0
CGC91	0.6	1.3	0.9	1.8	5.6	3.0	4.3	3.6	2.0
P17E19S	2.3	0.8	2.5	0.9	3.8	1.3	ND	ND	ND
P18	1.8	0.7	0.9	0.8	-1.2	2.5	-2.8	2.6	ND
P19C	1.0	0.8	0.8	0.8	2.2	2.3	-3.1	3.4	ND
P2	-2.0	0.9	-2.0	1.3	0.9	4.2	-4.3	5.4	-5.0
P21	-2.0	0.8	-2.0	0.8	-2.8	0.8	ND	ND	ND
P31	-0.5	0.8	-0.2	0.9	1.1	3.3	ND	ND	ND
P6	0.1	0.8	-0.2	0.9	3.7	1.6	ND	ND	ND
S4P	1.7	0.7	0.1	0.8	6.6	3.4	ND	ND	ND
SR3S4	0.3	1.1	-0.6	1.8	ND	ND	ND	ND	ND

ND — No data

### 2.3.2 Pacific Ocean Total Alkalinity Crossover Analysis

The purpose of this analysis was to determine if any significant systematic offset existed between the various legs of the WOCE/NOAA/JGOFS Pacific Ocean TALK measurements. The stations selected for each crossover were those with carbon data which were close to the crossover point. The number of stations selected was somewhat subjective, but was such that sufficient measurements were present for the analysis without getting too far away from the crossover location. In all cases the stations were within approximately 1° of latitude or longitude of the crossover point. Data from deep water (>2000 m) at each of the crossover locations were plotted against the density anomaly referenced to 3000 dbar ( $\sigma\text{-3}$ ) and fit with a second-order polynomial. The difference and standard deviation between the two curves was then calculated from 10 evenly spaced intervals over the density range common to both sets of crossovers (Fig. 12, Table 10).

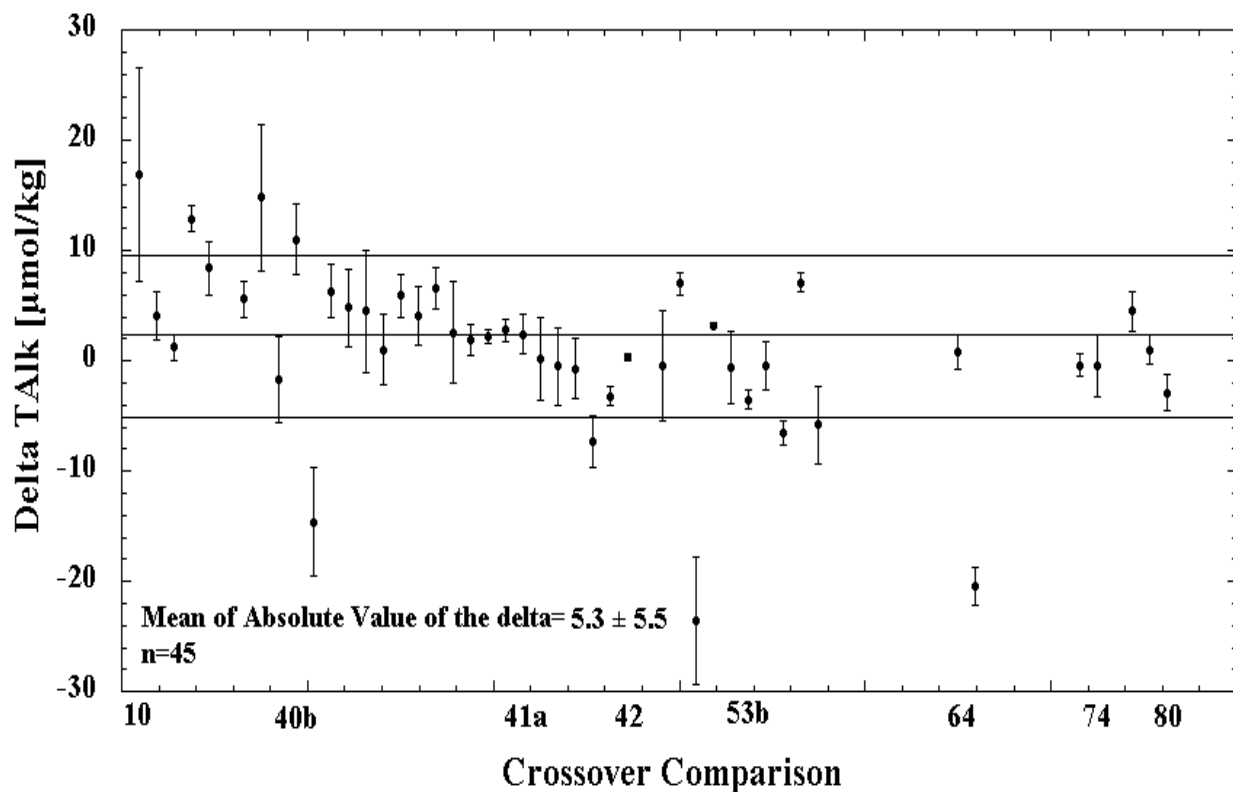


**Fig. 12. TALK crossover points comparison in the Pacific Ocean ( $\geq 2000$  dbar, 2nd-order polynomial fit).**

**Table 10. Summary of TALK crossover results in the Pacific Ocean**

Crossing no.	Latitude	Longitude	Section 1	Section 1 station	Section 2	Section 2 station	$\Delta$ TALK st. dev. ( $\mu$ mol/kg)
10	30° N	148° E	P10	74, 77	P2	37	16.9±9.7
18	63° S	140° E	SR3S4	33	SR3S4	65	4.1±2.2
20	66° S	164° E	SR3S4	51	S4P	791	1.2±1.1
23	30° N	165° E	P13	54, 55	P2	48	12.9±1.2
28	30° N	178° E	P14N	63	P2	58	8.4±2.4
34	66° S	171° E	P14S15S	32	S4P	783, 787	5.6±1.6
36	30° N	165° W	P15N	52, 54	P2	65	14.8±6.7
40a	0°	170° W	P14S15S	174	EQS92	56	-1.7±3.9
40b	0°	170° W	P14S15S	174	P15N	112	11.0±3.2
40c	0°	170° W	P15N	112	EQS92	56	-14.6±4.9
40d	1° S	170° W	P14S15S	173	P15N	114	6.3±2.4
40e	2° S	170° W	P14S15S	172	P15N	116	4.8±3.5
40f	3° S	170° W	P14S15S	171	P15N	118	4.5±5.6
40h	4° S	170° W	P14S15S	170	P15N	120	1.0±3.2
40i	5° S	170° W	P14S15S	169	EQS92	63	5.9±2.0
40j	5° S	170° W	P14S15S	169	P15N	122	4.1±2.7
40k	5° S	170° W	P15N	122	EQS92	63	6.6±1.9
40l	6° S	170° W	P14S15S	167	P15N	124	2.6±4.6
40m	7° S	170° W	P14S15S	165	P15N	126	1.9±1.4
40n	8° S	170° W	P14S15S	163	P15N	128	2.2±0.6
40o	12° S	170° W	P14S15S	155	P15N	134, 136	2.8±1.0
41a	10° S	170° W	P14S15S	157, 159, 161	P15N	130, 132	2.4±1.8
41b	10° S	170° W	P14S15S	157, 159, 161	EQS92	66	0.2±3.8
41c	10° S	170° W	P14S15S	157, 159, 161	P31	54, 57, 61	-0.5±3.5
41d	10° S	170° W	P15N	130, 132	EQS92	66	-0.7±2.7
41e	10° S	170° W	EQS92	66	P31	54, 57, 61	-7.3±2.3
41f	10° S	170° W	P15N	130, 132	P31	54, 57, 61	-3.2±0.9
42	17° S	170° W	P14S15S	141, 142, 144	P21	193, 195, 197	0.34±0.35

**Table 10 (continued)**

Crossing no.	Latitude	Longitude	Section 1	Section 1 station	Section 2	Section 2 station	$\Delta\text{TCO}_2$ st. dev. ( $\mu\text{mol/kg}$ )
44	40° S	173° W	P14S15S/1	93	P14S15S/2	94	-0.4±5.0
45	67° S	169° W	P14S15S	33	S4P	755	7.0±1.0
47	53° N	152° W	P16N	58, 59, 66	P17N	78	-23.6±5.8
49	30° N	152° W	P16N	30, 31, 32	P2	70	3.2±0.2
53a	17° S	150° W	P16C	222	P16S17S	220	-0.6±3.3
53b	17° S	150° W	P16C	222	P31	2, 5	-3.5±0.9
53c	17° S	150° W	P16C	222	P21	157, 160	-0.4±2.2
53d	17° S	150° W	P16S17S	220	P31	2, 5	-6.5±1.1
53e	17° S	150° W	P16S17S	220	P21	157, 160	7.1±0.9
53f	17° S	150° W	P21	157, 160	P31	2, 5	-5.8±3.5
64	6° S	135° W	P17C	121	P16S17S	124	0.8±1.5
65	16° S	133° W	P16S17S	148	P21	131	-20.5±1.7
73	5° N	110° W	P18	155, 159	EQS92	6	-0.4±1.0
74	17° S	103° W	P18	105, 106	P21	77	-0.5±2.8
77	52° S	103° W	P18	37	P17E19S	194	4.5±1.8
78	67° S	103° W	P18	10, 11	S4P	711, 712, 713	1.0±1.3
80	16° S	86° W	P19	333	P21	49	-2.9±1.6
<b>Average: 1.1±7.6</b>							

A secondary check was performed on crossovers with large deltas or large standard deviations from the crossover analysis. A multiparameter liner least square regression method is used to examine the offsets at selected crossover locations. Data from Cruise 1 are used as a reference to derive a best fit equation:

$$\text{TALK} = a + b \times \text{Sal} + c \times \text{T} + d \times \text{Oxy}, \quad (2)$$

where  $a$ ,  $b$ ,  $c$ , and  $d$  are constants; Sal is salinity; T is temperature; and Oxy is oxygen concentration. Once the equation is derived, TALK is calculated from the Cruise 2 Sal, T, and Oxy. The difference between this predicted TALK and the observed TALK at the Cruise 2 stations is defined as  $\Delta\text{TALK}$ . Results from the multiple-parameter regression method are listed in Table 11.

**Table 11. Results from the multiple-parameter regression method**

Crossing no.	Cruise 1- sta.	Cruise 2- sta.	$\Delta$ TALK ( $\mu\text{mol/kg}$ )	St. dev.
10	P10-74,77	P2-37	27.0	3.5
23	P13-54, 55	P2-48	28.5	5.7
28	P14N-63	P2-58	9.3	2.8
34	P14S15S-32	S4P-783,787	6.0	1.9
36	P15N-52, 54	P2-65	10.4	2.1
40b	P14S15S-174	P15N-112	6.6	4.2
40c	P15N-112	EQS92-56	-8.2	7.8
40d	P14S15S-173	P15N-114	3.4	5.3
40f	P14S15S-171	P15N-118	5.0	4.7
40i	P14S15S-169	EQS92-63	12.2	8.0
40k	P15N-122	EQS92-63	14.0	7.9
44	P14S15S/1-93	P14S15S/2-94	-7.5	6.6
45	P14S15S-33	S4P-755	6.6*	3.4
47	P16N-58, 59, 66	P17N-78	-10.0	3.4
53d	P16S17S-220	P31-2, 5	-11.3	7.1
53e	P16S17S-220	P21-157, 160	2.3	7.4
53f	P21-157, 160	P31-2, 5	-11.8	4.0
65	P16S17S-148	P21-131	-18.5	3.1

These results are compared with the deltas derived from curve-fitting method in Fig. 13. The multiparameter method generally had smaller delta values, suggesting that some of the differences in the crossovers with large deltas could actually be due to real changes in the water mass properties.

Optimum cruise adjustments, based on the crossover results, were evaluated using the three approaches discussed beginning on page 30, above.<sup>5</sup> The optimized cruise adjustments based on an equal weighting of the crossover data (SLSQ approach) are shown in the Figs. 14 and 15. The second and third approaches were a set of adjustments calculated using WLSQ and WDLSQ. The damping used for the WDLSQ approach was a prior guess of the variance at crossovers, estimated to be a constant  $5^2 \mu\text{mol/kg}$  for TALK. A summary of the proposed adjustments based on the three different approaches is given in Fig. 14. A summary of the proposed adjustments based on the three different least squares models is given in Fig. 15. The proposed adjustments from the three different least squares models were similar to the adjustments from the Del Poly analysis.

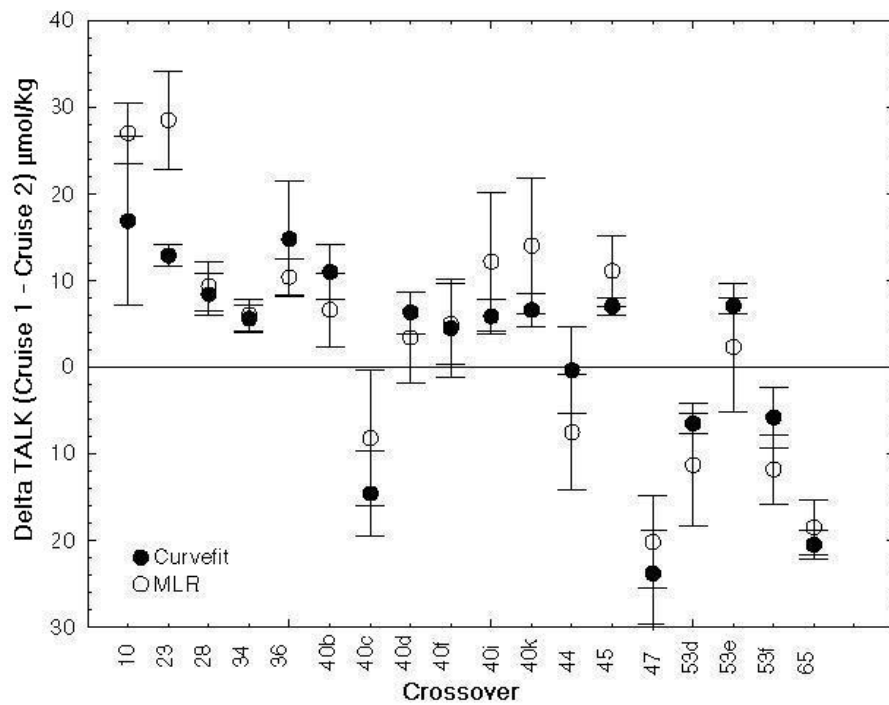


Fig. 13. Multiparameter analysis approach for TALK crossovers in the Pacific Ocean.

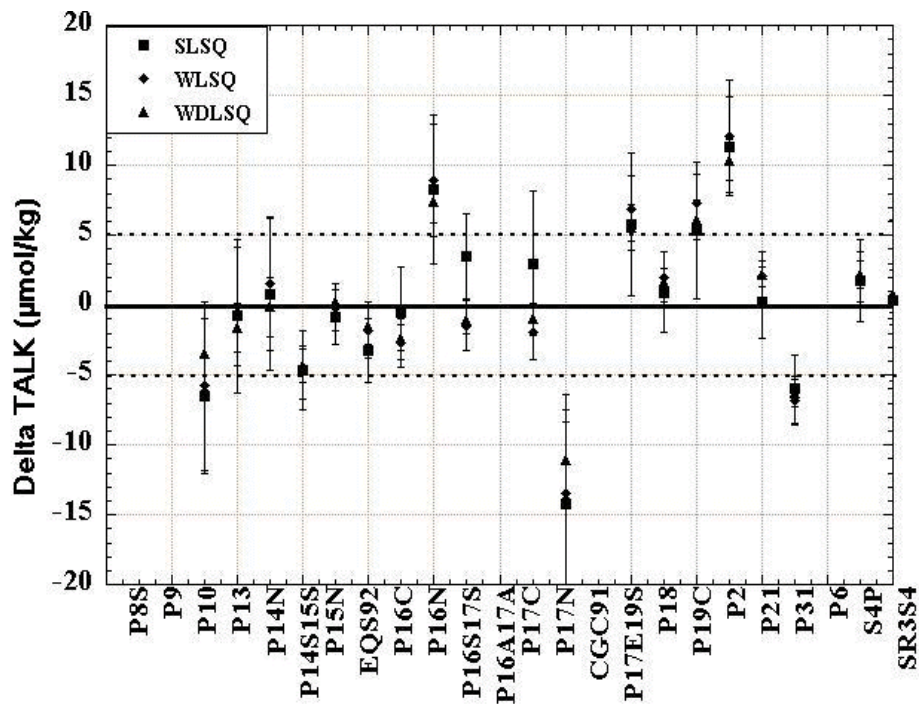


Fig. 14. Del Poly model for TALK crossover analysis in the Pacific Ocean.

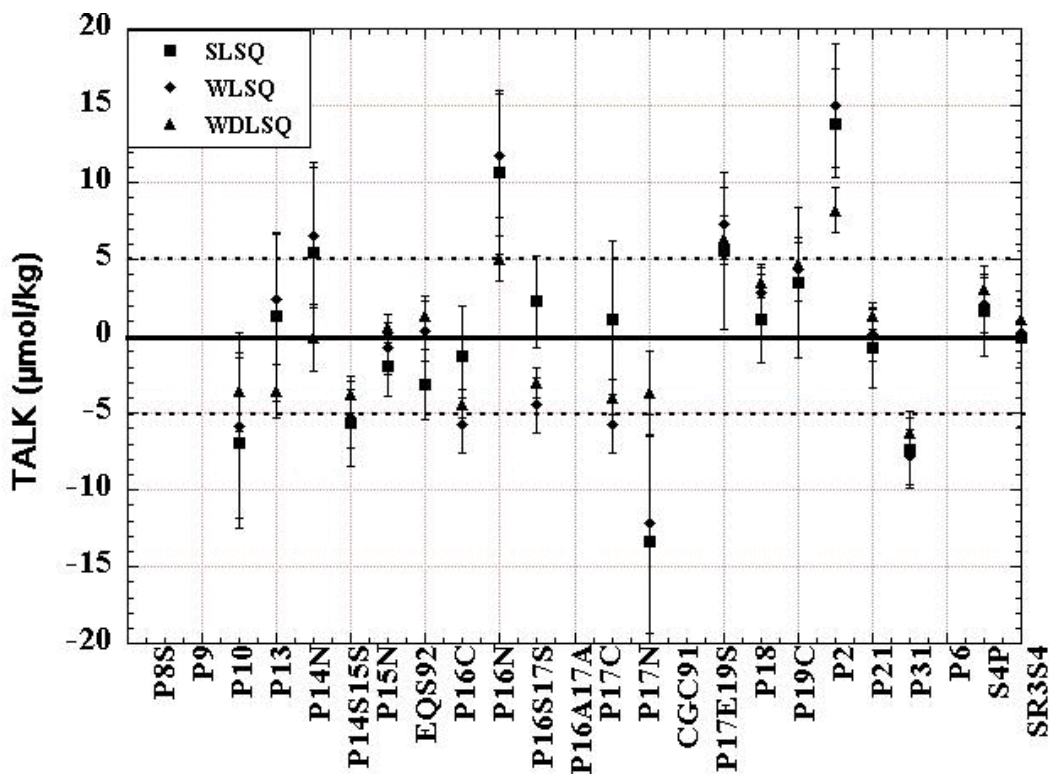


Fig. 15. Same shape model for TALK crossover analysis in the Pacific Ocean.

Using the crossover differences estimated from the polynomial fits, the 45 crossovers for TALK had an average and standard deviation of  $2.2 \pm 7.4 \mu\text{mol/kg}$ . The average and of the absolute values of the differences was  $5.1 \pm 5.7 \mu\text{mol/kg}$ . Eighteen TALK crossovers with differences from the polynomial fits of  $>5 \mu\text{mol/kg}$  were further examined using the MLR crossover analysis. Unlike the polynomial fit approach, the MLR method does not assume that the waters are identical, only that the relationships between TALK and the other properties do not change, and that the effects of measurement errors in the independent variables can be neglected. In most cases, the offsets implied from the original crossover analysis were the same or larger with the MLR analysis. This suggests that the differences observed in the initial polynomial fits cannot be explained by changes in the distribution of water masses.

Both the Del Poly and same shape models give very similar differences, but the uncertainties are generally larger for the same shape model. It is difficult to say which approach is more appropriate for these data, since the answer depends somewhat on the nature of the errors. If we assume a priori that the primary difference between the data sets results from a constant offset, then the same shape model is most appropriate. Of the three least squares models examined, the WDLSQ adjustments and errors make use of the most information (error estimates and prior guesses on crossover differences) to determine adjustments and their uncertainties. The results from the WDLSQ show that most of the cruises during the Pacific Ocean  $\text{CO}_2$  survey are within  $\sim 5 \mu\text{mol/kg}$  for TALK. A few cruises lie outside this cutoff. The crossovers suggest that P17N and P31 should be lowered by 4–11 and 6  $\mu\text{mol/kg}$ , respectively, and that P2 should be increased by 8–10  $\mu\text{mol/kg}$  (see Table 5).

All of these results must be considered in concert with the other lines of evidence on the quality of the TALK measurements from the various cruises. Table 12 is a summary of the TALK quality assessment results. The TALK data were also examined using a basinwide MLR approach (Appendix A), using an isopycnal analysis [see Sec. 2.3.2(a), below], and with internal consistency calculations [see Sec. 2.3.2(b) below].

**Table 12. Summary of the TALK quality assessment results**

Cruise name	TALK analysis technique	P.I. name	Sample volume (~mL)	Shore-based st. dev. ( $\mu\text{mol/kg}$ )	No. of shore-based observations
P8S	Potentiometric	Shitashima	50	4.3	17
P9	ND	ND	ND	ND	ND
P10	Potentiometric	Sabine	100	ND	ND
P13	Potentiometric	Guenther/Keeling	91	ND	ND
P14N	Potentiometric	Millero	200	ND	ND
P14S15S	Potentiometric	Millero	200	ND	ND
P15N	Potentiometric	Wong	203	ND	ND
EQS92	Potentiometric	Millero	200	ND	ND
P15C	Potentiometric	Guenther/Keeling	91	ND	ND
P16N	ND	ND	ND	ND	ND
P16S17S	Potentiometric	Goyet	100	3.2	12
P16A17A	ND	ND	ND	ND	ND
P17C	Potentiometric	Goyet	100	9.0	24
P17N	Potentiometric <sup>a</sup>	Goyet	100	ND	ND
CGC91	ND	ND	ND	ND	ND
P17E19S	ND	ND	ND	ND	ND
P18	Potentiometric	Millero	200	ND	ND
P19C	ND	ND	ND	ND	ND
P2	Potentiometric	Ono	150	ND	ND
P21	Potentiometric	Millero	200	ND	ND
P31	Potentiometric	Winn	200	ND	ND
P6	ND	ND	ND	ND	ND
S4P	ND	ND	ND	ND	ND
SR3S4	Potentiometric	Tilbrook	210	ND	ND

ND — No data

<sup>a</sup> CRMs not analyzed.

### 2.3.2(a) Pacific Ocean TALK Isopycnal Analysis

At a few locations in the North Pacific the estimated TALK offsets at the crossovers were not consistent with the offsets from the basinwide MLR analysis. In an attempt to determine whether the crossovers were biased by the limited number of stations analyzed, we expanded the crossover analysis to include additional stations along each cruise and/or stations from neighboring cruises. The deep (>2200 m) station data were averaged at specific potential density values ( $\sigma_\theta$  or  $\sigma_{-3}$ ), and the mean values were compared at several isopycnal intervals for each cruise. The range of values observed for a particular cruise at each isopycnal level indicated whether the initial stations used in the crossover analysis were offset from the surrounding stations. The additional stations also provided more robust estimates of the difference between cruises since more data points were included in the analysis.

An isopycnal analysis for P2 TALK was used to evaluate the P2 data relative to the meridional cruises that this cruise crosses. The P2 data were plotted as a function of longitude for three isopycnal intervals representing data between 3000 and 4000 m (Fig. 16). Values from P10, P13N, P14N, and P15N, with latitudes between 25 and 35° N, were consistently higher than the P2 data, indicating that a significant positive correction is necessary for this cruise.

TALK for section P31 was compared with a nearly parallel section, P21, that was run along 20° S and the intersecting meridional cruises P15N, P15S, and P16C (Fig. 17). The P31 data at either end of the section, where the meridional lines intersect, are only slightly higher than the data for the other lines. In the middle of the section, however, the P31 data are much higher than the P21 values, suggesting that a correction is in order.

TALK for P17C and neighboring cruises were examined as a function of latitude for  $\sigma_{-3}$  values between 41.44 and 41.51 (Fig. 18). The larger density range was necessary to encompass enough data for comparison. The P17C data appear to be slightly higher than those for P16C or P15N. The low P2 data relative to P15N are also seen in the Fig. 18.

The data for P17N - P16N TALK was reexamined at the intersection of P17N with P16N to include data from a larger region and a wider depth range than initially considered with the crossover analysis (Fig. 19). The calculated TALK values for P16N also include a +4  $\mu\text{mol/kg}$  adjustment in the  $\text{TCO}_2$  values that is proposed from this study. The resulting extended crossover has an average offset of 12  $\mu\text{mol/kg}$ .

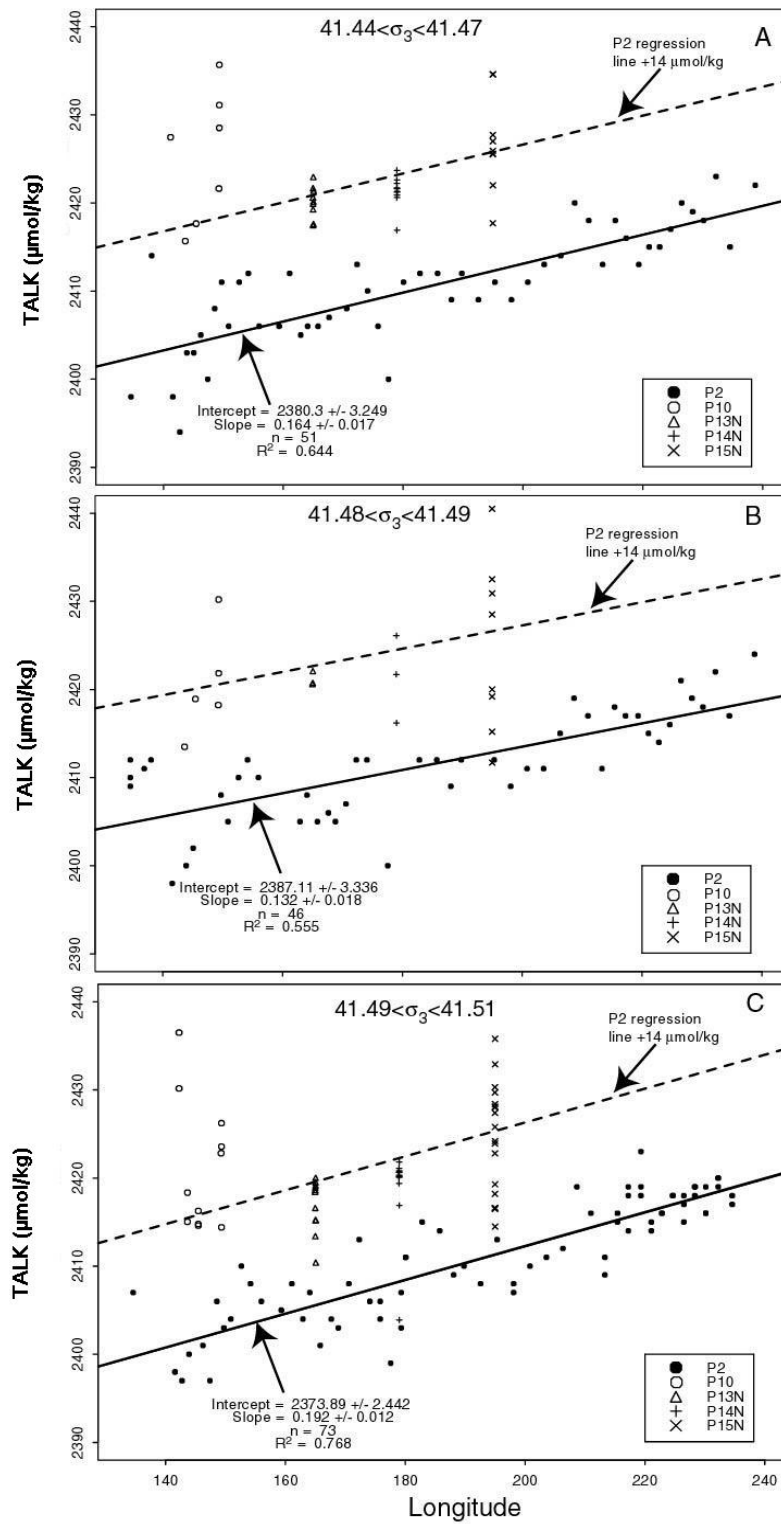


**Fig. 16.** Plots of measured TALK vs longitude for three isopycnal intervals: (a)  $41.44 < \sigma_3 < 41.47$ , (b)  $41.48 < \sigma_3 < 41.49$ , and (c)  $41.49 < \sigma_3 < 41.51$ . The solid line is a linear regression through the P6 data. The dashed line is the P2 fit plus  $11 \mu\text{mol/kg}$ . Data for P10, P13N, P14N, and P15N are limited to latitude range  $25\text{--}35^\circ \text{N}$ .

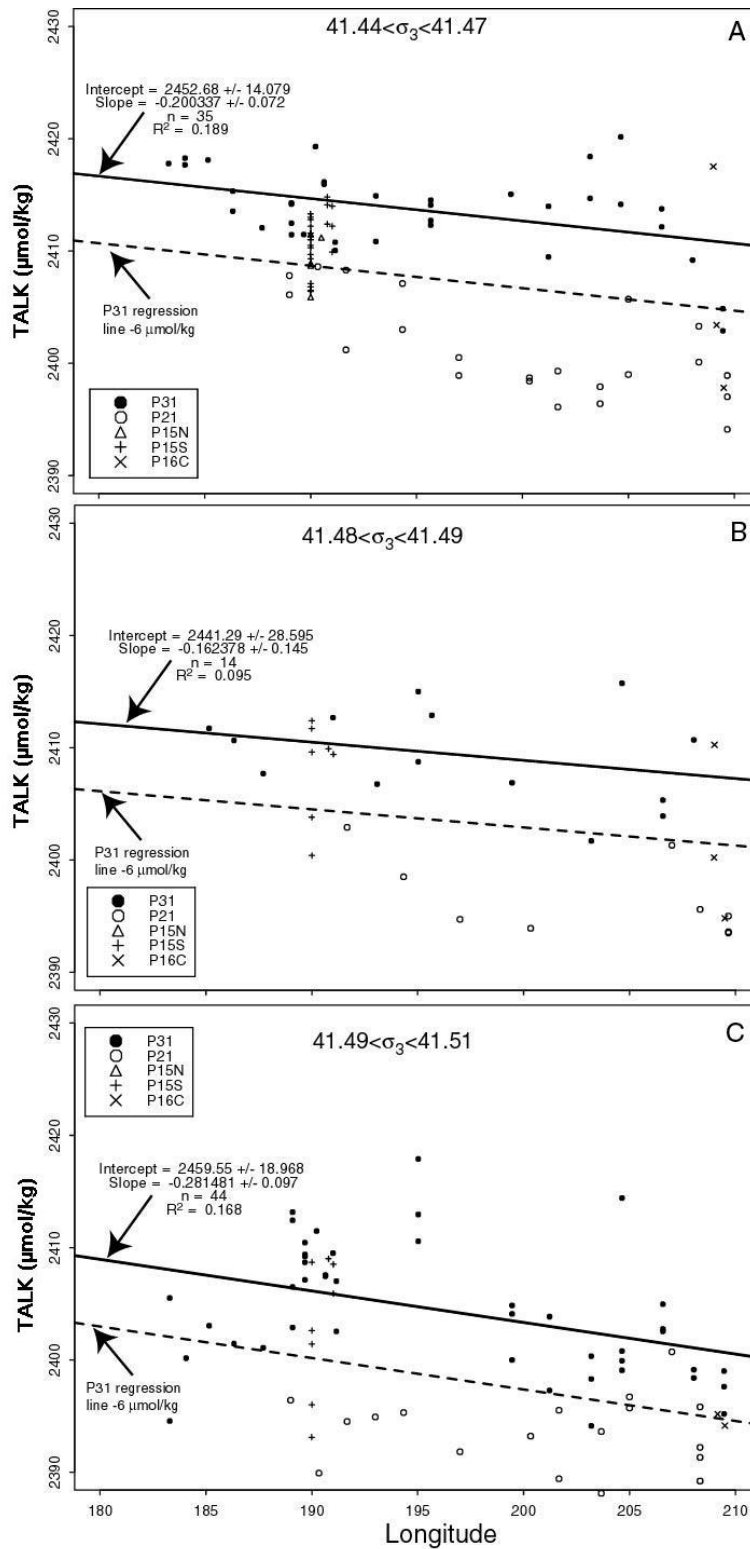


**Fig. 17. Plots of measured TALK vs longitude for three isopycnal intervals: (a)  $41.44 < \sigma_3 < 41.47$ , (b)  $41.48 < \sigma_3 < 41.49$ , and (c)  $41.49 < \sigma_3 < 41.51$ . The solid line is a linear regression through the P31 data. The dashed line is the P31 fit minus  $6 \mu\text{mol/kg}$ . Data for P15N, P15S, and P16C are limited to latitude range  $15\text{--}25^\circ \text{S}$ .**

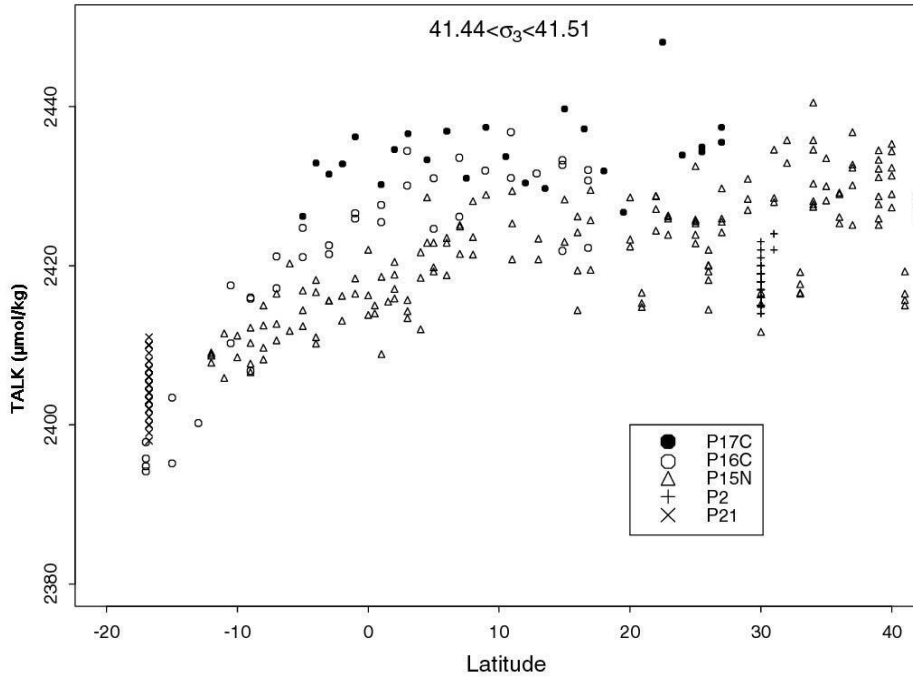


**Fig. 18.** Plot of measured TALK vs latitude for  $\sigma_3$  values between 41.44 and 41.51. P2 and P21 data are restricted to longitudes between 120 and 140° W.

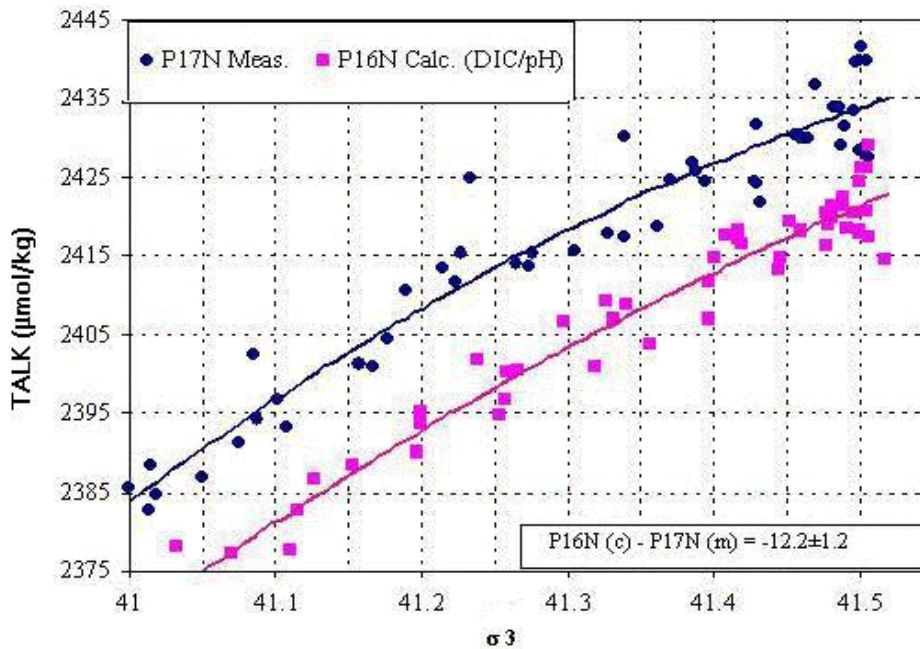


**Fig. 19.** Results of TALK isopycnal analysis of P16N (calculated using adjusted  $\text{TCO}_2$  values and pH) and P17N (measured) plotted against  $\sigma_3$  near crossover at 53° N and 152° W.

### 2.3.2(b) TALK Internal Consistency Analysis

An independent approach for evaluating the accuracy of data is examination of the internal consistency of the CO<sub>2</sub> system parameters. The CO<sub>2</sub> system in seawater can be defined by knowing T, S, nutrient and boron concentrations, and two of the four measurable carbon parameters: TCO<sub>2</sub>, TALK, *f*CO<sub>2</sub>, and pH. Thus, cruises on which three or more carbon parameters were measured were overdetermined. By comparing the carbon system distributions estimated from different pairs of carbon measurements on a cruise, one can evaluate potential offsets in one of the measured parameters. By examining the internal consistency over several cruises, one can gain confidence in the reliability of the constants being used and evaluate the implied offsets.

The constants of Mehrbach et al. (1973) as refit by Dickson and Millero (1987) were used for this analysis, along with equilibrium constants for other components (e.g., boric acid dissociation, solubility of CO<sub>2</sub>, water hydrolysis, and phosphoric and silicic acid dissociation) necessary to characterize the carbonate system in seawater as recommended in Millero (1995). The selection of the constants of Mehrbach et al. (1973) was based on the analysis of a large field data set (15,300 samples) obtained from all the ocean basins (Lee et al. 2000).

This approach relied heavily on two basic premises. The first was that all of the pH measurements needed to be adjusted upward by 0.0047 (see Table 5). The second premise was that offsets in the internal consistency checks were attributed to errors in the TALK measurements. This premise is supported by the crossover analysis and other approaches which suggested that the other carbon parameters were within acceptable ranges for the cruises in question.

We compared measured alkalinity vs alkalinity calculated from two different input combinations: pH + TCO<sub>2</sub> or *f*CO<sub>2</sub> + TCO<sub>2</sub>. The results of these comparisons are presented in Table 13 and Fig. 20.

**Table 13. Summary of TALK Internal Consistency calculations**

Cruise name	$\Delta$ TALK <sup>a</sup> (Input: pH+TCO <sub>2</sub> )	$\Delta$ TALK <sup>b</sup> (Input: <i>f</i> CO <sub>2</sub> +TCO <sub>2</sub> )	Number
Pacific Ocean			
P8S	-1.9±6.9	N/A	70
P14N	-5.5±6.1	N/A	550
P14S15S	4.2±3.2	6.4±4.5	2530
P18	-2.5±4.6	-1.7±4.9	1980
P21	5.4±4.8	N/A	905
P31	1.3±5.8	N/A	470
EQPAC 92 - Fall	1.0±4.9	1.8±5.1	1970
Atlantic Ocean			
A20R (20° W)	2.6±3.5	1.8±4.2	1600
Indian Ocean			
I8R	3.8±3.5	3.4±4.3	1660

<sup>a</sup>  $\Delta$ TALK (μmol/kg) = (measured - calculated). pH data adjusted upward by 0.0047 pH units were used in these calculations. Without pH adjustment, +5 μmol/kg should be added to  $\Delta$ TALK.

<sup>b</sup>  $\Delta$ TALK (μmol/kg) = (measured - calculated).

### Summary of Internal Consistency

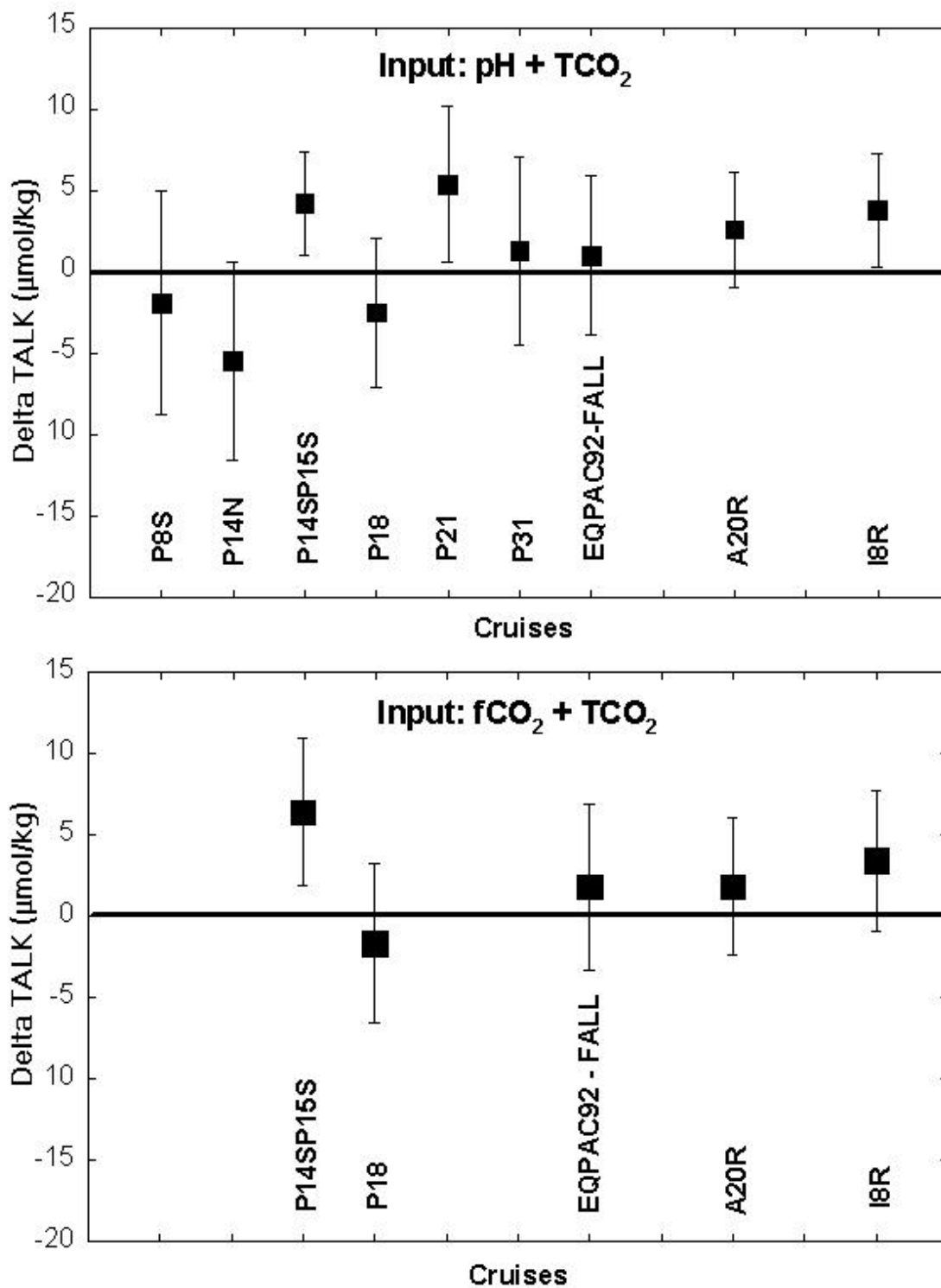


Fig. 20. Summary of internal consistency calculations.

This analysis showed that the measured values of TALK for section P14N are approximately 5  $\mu\text{mol/kg}$  lower than the TALK calculated from  $\text{TCO}_2$  and pH. Sections P21 and P14S15S had measured values that were higher than the calculated values by 5  $\mu\text{mol/kg}$  (based on  $\text{TCO}_2/\text{pH}$  pair) and 4–6  $\mu\text{mol/kg}$  (based on  $\text{TCO}_2/\text{pH}$  and  $\text{TCO}_2/f\text{CO}_2$  pairs), respectively. Note that proposed TALK adjustments implicitly assume that pH,  $f\text{CO}_2$ , and  $\text{TCO}_2$  data are internally consistent from cruise to cruise. All of these results must be considered in concert with the other lines of evidence on the quality of the TALK measurements from the various cruises.

Results of statistical analysis for recommended adjustments of TALK during the Global  $\text{CO}_2$  Survey cruises in the Pacific Ocean are presented in Table 14.

### 2.3.3 Pacific Ocean $f\text{CO}_2$ Crossover Analysis

The purpose of the Pacific Ocean  $f\text{CO}_2$  crossover analysis was to determine if any significant systematic offset existed between the various legs of the WOCE/NOAA/JGOFS Pacific Ocean measurements of  $\text{CO}_2$  fugacity. Three different types of instruments were used to measure discrete  $f\text{CO}_2$  samples. With each system an aliquot of seawater was equilibrated at a constant temperature of either 4° or 20°C with a headspace of known initial  $\text{CO}_2$  content. Subsequently, the  $\text{CO}_2$  concentration in the headspace was determined by a nondispersive infrared analyzer (NDIR) or by quantitatively converting the  $\text{CO}_2$  to  $\text{CH}_4$  and then analyzing the resulting gas composition using a gas chromatograph (GC) with a flame ionization detector. The initial  $f\text{CO}_2$  in the water was determined after correcting for loss or gain of  $\text{CO}_2$  during the equilibration process. This correction can be significant for large initial  $f\text{CO}_2$  differences between headspace and water, and for systems with a large headspace to water volume ratio (Chen et al. 1995).

The system used by Takahashi (Chipman et al. 1993; DOE 1994) involved equilibration of a ~50-mL headspace with a ~500-mL sample at either 4°C (T4 = Takahashi @ 4°C) or 20°C (T20 = Takahashi @ 20°C), depending on ambient surface water temperatures. Note that the Takahashi values, reported as partial pressure of  $\text{CO}_2$  ( $\text{pCO}_2$ ), were converted to  $f\text{CO}_2$  using the correction factor (~0.997) given by Weiss (1974). Wanninkhof and co-workers used two systems during the Pacific Ocean survey cruises. An NDIR-based system (WI20 = Wanninkhof IR @ 20°C) with ~500-mL samples was used for analyses during EQS92 and P18 (Wanninkhof and Thoning 1993). A GC-based system (WG20 = Wanninkhof GC @ 20°C) with samples collected in a closed, septum-sealed bottle having a volume of ~120 mL of seawater and a headspace of ~10 mL was used for P14S15S (Neill et al. 1997).

Detectors were calibrated after every 4 to 12 samples with gas standards traceable to manometrically determined values by C. D. Keeling at SIO. Assessment of  $f\text{CO}_2$  accuracy is difficult to determine because of the lack of aqueous standards. Estimates of precision based on duplicate samples range from 0.1 to 1% depending on  $f\text{CO}_2$  and the measurement procedure, with higher  $f\text{CO}_2$  levels on the WI20 system (>700  $\mu\text{atm}$ ), giving worse reproducibility (Chen et al. 1995).

The stations selected for each crossover were those with carbon data which were close to the crossover point. The number of stations selected was somewhat subjective, but was such to provide sufficient measurements for the analysis without getting too far away from the crossover location. In all cases the stations were within approximately 1° of latitude or longitude of the crossover point. All potential crossovers, including crossovers where measured values could be compared to  $f\text{CO}_2$  values calculated from  $\text{TCO}_2/\text{TALK}$  or  $\text{TCO}_2/\text{pH}$  pairs, were examined. For the crossover comparison all samples run at 4°C were normalized to 20°C by calculating the alkalinity (TALK) from  $f\text{CO}_2$  (4°C) and  $\text{TCO}_2$ , and subsequently calculating  $f\text{CO}_2$  (20°C) from the  $\text{TCO}_2$  and calculated TALK. The carbonate dissociation constants of Mehrbach et al. (1973) as refit by Dickson and Millero (1987) and ancillary constants listed in DOE (1994) are used for these calculations with the program of Lewis and Wallace (1998).

**Table 14. The final results of statistical analysis for recommended TALK adjustments in the Pacific Ocean**

Cruise name	$\Delta$ WDL SQ (Del Poly)	Std. dev.	$\Delta$ WDL SQ (same shape)	Std. dev.	MLR Analyses				Int. cons. (TCO <sub>2</sub> +pH)	Int. cons. (TCO <sub>2</sub> +fCO <sub>2</sub> )	$\Delta$ Isopycnal analysis
					Crossover (residual ave.)	Std. dev.	NP basinwide (residual ave.)	Std. dev.			
P8S	ND <sup>a</sup>	ND	ND	ND	ND	ND	5.6	4.0	1.9	ND	ND
P9	ND	ND	ND	ND	ND	ND	ND	ND	ND	ND	ND
P10	-3.5	2.3	-3.6	2.6	-22.0	3.5	-4.5	6.7	ND	ND	ND
P13	-1.6	1.5	-3.6	1.8	-28.5	5.7	1.9	3.6	ND	ND	ND
P14N	-0.1	1.8	-0.1	2.1	-9.3	2.8	3.0	3.8	5.5	ND	ND
P14S15S	-4.4	1.0	-3.8	1.2	-5.3	1.9	ND	ND	-4.2	-6.4	ND
P15N	0.2	0.9	0.5	0.9	-0.2	2.2	-2.4	6.6	ND	ND	ND
EQS92	-1.5	1.2	1.3	6.0	12.3	ND	ND	ND	ND	ND	ND
P16C	-2.4	1.0	-4.4	0.9	ND	ND	-0.2	4.3	ND	ND	ND
P16N	7.4	1.3	5.0	1.5	20.2	5.3	ND	ND	ND	ND	ND
P16S17S	ND	ND	ND	ND	ND	ND	ND	ND	ND	ND	ND
P16A17A	ND	ND	ND	ND	ND	ND	ND	ND	ND	ND	ND
P17C	-1.0	2.0	-4.0	1.2	ND	ND	-8.7	7.6	ND	ND	-6.0
P17N	-11.0	1.8	-3.6	2.7	-20.2	5.3	-2.6	5.4	ND	ND	-12.2
CGC91	ND	ND	ND	ND	ND	ND	ND	ND	ND	ND	ND
P17E19S	ND	ND	ND	ND	ND	ND	ND	ND	ND	ND	ND
P18	1.6	1.1	3.5	1.0	ND	ND	2.3	7.1	2.5	1.7	ND
P19C	ND	ND	ND	ND	ND	ND	ND	ND	ND	ND	ND
P2	10.4	1.3	8.2	1.5	18.8	1.6	17.1	4.2	ND	ND	14.0
P21	2.2	0.9	1.3	0.9	-1.5	2.3	ND	ND	-5.4	ND	ND
P31	-6.3	1.0	-6.3	1.0	-11.6	2.2	ND	ND	-1.3	ND	-6.0

Table 14 (continued)

					MLR Analyses						
Cruise name	$\Delta$ WDLSQ (Del Poly)	Std. dev.	$\Delta$ WDLSQ (same shape)	Std. dev.	Crossover (residual ave.)	Std. dev.	NP basinwide (residual ave.)	Std. dev.	Int. cons. (TCO <sub>2</sub> +pH)	Int. cons. (TCO <sub>2</sub> +fCO <sub>2</sub> )	$\Delta$ Isopycnal analysis
P6	ND	ND	ND	ND	ND	ND	ND	ND	ND	ND	ND
S4P	2.2	0.9	3.1	1.0	8.6	1.6	ND	ND	ND	ND	ND
SR3S4	0.7	1.1	1.1	1.2	ND	ND	ND	ND	ND	ND	ND

<sup>a</sup>ND — No data

Analysis of the calculated  $f\text{CO}_2$  values revealed that there may be some problems due to uncertainties as to which carbon dissociation constants to use. This is also a problem for the crossovers which required a temperature conversion. For example, the temperature conversion from 4° to 20°C using the Mehrbach constants yield  $f\text{CO}_2$  values for the deep Pacific that are about 50  $\mu\text{atm}$  higher than if the temperature conversion is performed with the Roy constants. Since the discrepancy in dissociation constants has not been fully resolved, the crossover comparison for  $f\text{CO}_2$  data analyzed at different temperatures and for comparisons of measured vs calculated values is problematic.

The crossovers involving calculated values were not considered for the final crossover analysis. Data from deep water (>2000 m) at each of the 15 remaining crossover locations were plotted against the density anomaly referenced to 3000 dbar ( $\sigma\text{-3}$ ) and fit with a second-order polynomial. The difference and standard deviation between the two curves were then calculated from 10 evenly spaced intervals over the density range common to both sets of crossovers. The results of final crossover analysis are given in Table 15.

**Table 15. Results of final crossover analysis for Pacific Ocean  $f\text{CO}_2$**

Crossing no.	Cruise 1 <sup>a</sup>	Cruise 2	Density range <sup>b</sup>	$f\text{CO}_2$ range <sup>c</sup> ( $\mu\text{atm}$ )	Average <sup>d</sup>	Std. dev. <sup>e</sup>	Comments <sup>f</sup>
34	P14S15S (WG20)	S4P (T4)	41.14–41.49	1090–1110	3.4	2.2	concave/convex
40a	P14S15S (WG20)	EQS92 (WI20)	41.46–41.56	1050–1270	22	4.8	EQS92: 5 points
40i	P14S15S (WG20)	EQS92 (WI20)	41.35–41.52	1080–1320	35	3.3	EQS92: 4 points
41b	P14S15S (WG20)	EQS92 (WI20)	41.45–41.59	1030–1180	29.2	2.9	EQS92: 4 points
44	P14S15S-94 (WG20)	P14S15S-93 (WG20)	41.50–41.60	1070–1100	-1	5.4	
45	S4P T(4)	P14S15S (WG20)	41.50–41.67	1095–1130	-12	3.5	
55	P16S17S (T20)	P16A17A T(20)	41.42–41.59	1050–1180	-5.3	0.9	
66b	P16A17A T(20)	P16S17S (T20)	41.40–41.54	1080–1180	1	3.8	
67	P17E19S T(4)	P16A17A T(4)	41.23–41.52	1050–1190	-2.4	4.3	
68	S4P T(4)	P17E19S T(4)	41.46–41.69	1090–1115	-2.5	0.3	
73	P18 (WI20)	EQS92 (WI20)	41.14–41.49	1170–1570	3.4	2.2	EQS92: 6 points
77	P17E19S T(4)	P18 (WI20)	41.26–41.61	1050–1200	21.2	0.4	

Table 15 (continued)

Crossing no.	Cruise 1 <sup>a</sup>	Cruise 2	Density range <sup>b</sup>	<i>f</i> CO <sub>2</sub> range <sup>c</sup> (μatm)	Average <sup>d</sup>	Std. dev. <sup>e</sup>	Comments <sup>f</sup>
78	S4P T(4)	P18 (WI20)	41.48–41.68	1070–1095	7.6	0.5	
82	P19 (T4)	P17E19S T(4)	41.21–41.64	1080–1220	13.6	3.8	
83	S4P T(4)	P17E19S T(4)	41.43–41.67	1080–1130	-15	1.4	

<sup>a</sup> Cruise designation and system used in brackets.

<sup>b</sup> Density range ( $\sigma-3$ ) over which the fit was performed.

<sup>c</sup> *f*CO<sub>2</sub> range over which fit was performed.

<sup>d</sup> Average difference between 2nd-order polynomial fits of data for cruise 1 and cruise 2.

<sup>e</sup> Standard deviation between 2nd-order polynomial fits.

<sup>f</sup> Concave/convex — curve shape for cruise 1 is concave and for cruise 2, convex. The EQS92 cruises had few samples taken within depth range. Other cruises had more than 10 points over appropriate density range.

The standard deviation for the 15 *f*CO<sub>2</sub> crossover comparisons was 16.0 μatm. The average of the absolute value of the differences was 10.3±13.7 μatm. Notable offsets were observed for crossovers 82 and 83, with P19 showing a positive offset and S4P showing a negative offset relative to P17E19S. These two crossovers are both in the southern Pacific Ocean, within 15° of each other. If this offset is systematic throughout the cruises, it would imply that the *f*CO<sub>2</sub> for S4P and P19 differ by about 30 μatm, which is roughly comparable to an offset of ~4–5 μmol/kg in TCO<sub>2</sub> or TALK. The largest offsets (35 μatm) were observed for EQS92. We suspect that the large offset observed on EQS92 is caused by a bias in the analytical system used during this cruise although biases in the other crossovers involving the infrared (IR) system at 20°C (WI20) were less pronounced. Crossover 73 shows excellent agreement where both cruises used the WI20 technique. The large head space-to-water volume of the IR system may be the cause of the error. When *f*CO<sub>2</sub> data obtained using the different types of instruments are compared with the calculated *f*CO<sub>2</sub> values using TALK and TCO<sub>2</sub>, a bias between the IR and small-volume GC systems becomes apparent (Fig 21). The GC-based system (WG20) yielded significantly higher *f*CO<sub>2</sub> values than calculated values using the recommended constants, while the IR-based system did not show a clear trend, but rather increased scatter with increased *f*CO<sub>2</sub> (Fig. 21).

Based on careful laboratory studies, it appears that the IR-based measurements may give low results at *f*CO<sub>2</sub> values >700 μatm. The deep-water data with WI20 are low by about 20–30 μatm in the range of 1000–1100 μatm. This result is in accordance with the recent findings of Lee et al. (2000). As suggested by Lee and co-workers, the trend in the calculated values of *f*CO<sub>2</sub> from TALK and TCO<sub>2</sub> most likely results from a thermodynamic inconsistency with the Merbach et al. (1973) constants. Until this has been resolved, there is insufficient information to warrant further analysis of the *f*CO<sub>2</sub> data.

### 2.3.4 Pacific Ocean pH Crossover Analysis

The purpose of this analysis was to determine if any significant systematic offset existed between the various legs of the WOCE/NOAA/JGOFS Pacific Ocean measurements of pH. Most of the Pacific Ocean pH measurements used a spectrophotometric method (Clayton and Byrne 1993), with m-cresol purple as the indicator and either scanning or diode array spectrophotometers. The pH values obtained on three cruises—P2, P8S, and the eastern section of P21—involved potentiometric measurements with a glass electrode.

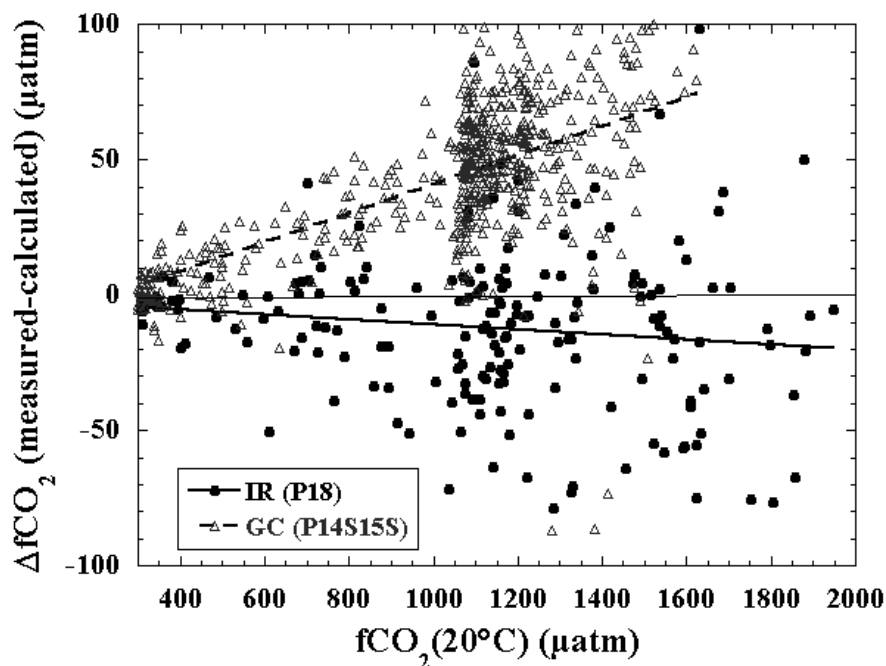


**Fig. 21.  $\Delta f\text{CO}_2$  values (measured – calculated) vs  $f\text{CO}_2$  measurements performed by IR and GC systems.**

Some of the pH values were reported on the total hydrogen scale while others were reported on the seawater scale. The seawater scale considers the interaction of hydrogen ions with bisulfate and fluoride ions in seawater, while the total scale includes only the bisulfate contribution (Dickson and Riley 1979; Dickson and Millero 1987). The two scales are linked by the following equation:

$$\text{pH}_{\text{SWS}} = \text{pH}_{\text{T}} - \log \left\{ \left( 1 + \frac{[\text{SO}_4^{2-}]_{\text{T}}}{K_{\text{HSO}_4}} + \frac{[\text{F}^-]_{\text{T}}}{K_{\text{HF}}} \right) / \left( 1 + \frac{[\text{SO}_4^{2-}]_{\text{T}}}{K_{\text{HSO}_4}} \right) \right\}, \quad (3)$$

where  $\text{pH}_{\text{T}}$  is hydrogen ion concentration on the total hydrogen scale,  $[\text{F}^-]_{\text{T}}$  and  $[\text{SO}_4^{2-}]_{\text{T}}$  are the total concentrations of fluoride and sulphate in seawater, and  $K_{\text{HF}}$  and  $K_{\text{HSO}_4}$  are the dissociation constants of hydrogen fluoride and sulphate in seawater (Dickson and Riley 1979). All pH values on the total hydrogen scale were converted to the seawater scale ( $\text{pH}_{\text{SWS}}$ ) to be consistent with published dissociation constants of carbonic acid.

The stations selected for each crossover were those with carbon data which were close to the crossover point. The number of stations selected was somewhat subjective, but was such that sufficient measurements were present for the analysis without getting too far away from the crossover location. In all cases the stations were within approximately  $1^\circ$  of latitude or longitude of the crossover point. Data from deep water ( $>2000$  m) at each of the crossover locations were plotted against the density anomaly referenced to 3000 dbar ( $\sigma\text{-3}$ ) and fit with a second-order polynomial. The difference and standard deviation between the two curves was then calculated from 10 evenly spaced intervals over the density range common to both sets of crossovers. There were only four crossovers where both cruises measured spectrophotometric pH (Table 16). The average of the absolute value of the differences of pH for those crossover locations was  $-0.0041 \pm 0.0018$ . No crossover examinations were possible with the potentiometric pH measurements.

The limited number of crossovers available for this study suggests that the spectrophotometric pH measurements were very precise and consistent between cruises. DeValls and Dickson (1998) have

suggested, however, that the pH values initially assigned to the tris buffers used to characterize the indicator, m-cresol purple, should be increased by 0.0047. This revision would translate into a comparable increase in the  $pH_T$  values reported for the Pacific Ocean. An upward adjustment in the reported  $pH_T$  values is further supported by internal consistency evaluations by McElligott et al. (1998), Lee et al. (2000), and as a part of this study. Laboratory experiments are still necessary to better constrain the exact magnitude of this adjustment.

The crossover comparisons suggest very good precision, but because of the small number of comparisons available, no further statistical analysis was done with this carbon parameter. No crossover examinations were possible with the potentiometric pH measurements. Given the mounting evidence for the need to adjust the spectrophotometric pH values, we recommend adjusting all spectrophotometric pH values upward by 0.0047 pH units (see Table 5) to be internally consistent with the other carbon parameters.

**Table 16. Pacific Ocean pH crossover information**

Crossover no.	Latitude	Longitude	Cruise 1	Cruise 1 stations	Cruise 2	Cruise 2 stations	$\Delta pH$
40a	0	170° W	P14S15S	174	EQS92	56	-0.0036±0.001
40i	5° S	170° W	P14S15S	169	EQS92	63	-0.0060±0.001
41b	10° S	170° W	P14S15S	157, 159, 161	EQS92	66	-0.0018±0.001
41c	10° S	170° W	P14S15S	157, 159, 161	P31	54, 57, 61	-0.0049±0.001

## 2.4 The Atlantic Ocean Database Synthesis

During the 1990s, measurements of the oceanic inorganic carbon system—which are composed of  $TCO_2$ ,  $fCO_2$ , TALK, and pH—were taken in the Atlantic Ocean on the WOCE Hydrographic Program (WHP) cruises and those of the Ocean-Atmosphere Carbon Exchange Study (OACES) of the National Oceanic and Atmospheric Administration (NOAA) (Fig. 22). These measurements have provided a benchmark of unsurpassed accuracy for the ocean inventory of  $CO_2$  and other properties. The inorganic carbon measurements performed by U.S. investigators were cosponsored by NOAA and DOE as part of the U.S. JGOFS Program. In addition to the U.S. cruises, the Atlantic synthesis included a significant number of cruises sponsored by the science agencies of the foreign nations (Table 17). This section addresses the consistency of oceanic inorganic carbon system parameter measurements taken from 1990 to 1998 in the Atlantic Ocean and lists adjustments to some of the  $TCO_2$  and TALK measurements based on careful analysis of the full data set.

Table 17 gives some details about the individual cruises in Atlantic Ocean which data were compiled for this project. The table is intended to provide information about the database used to generate products for GLODAP. It is not intended to be a primary reference for obtaining original cruise data.

The analysis of the large-scale data quality of inorganic carbon system parameters for the Atlantic syntheses data set is fully described in CDIAC report 140 (Wanninkof et al. 2003). This study followed the procedures outlined in Lamb et al. (2001) and Feely et al. (1999) with the objective of determining the consistency of inorganic carbon data among the different cruise data. The focus was on the  $TCO_2$  and TALK state variables used in the calculation of the anthropogenic  $CO_2$  inventory and for studies of biogeochemical carbon cycling.

In the crossover analyses in Wanninkhof et al. (2003), the four inorganic carbon system parameters ( $\text{TCO}_2$ ,  $f\text{CO}_2$ , TALK, and pH) were compared in density space referenced to 4000 dB ( $\sigma_4$ ) at 53 locations where cruises overlapped throughout the Atlantic Ocean (see Fig. 22 and Table 17). Such comparisons have been made for oceanic carbon parameters in the Indian Ocean (Johnson et al. 1998; Millero et al. 1998; Sabine et al. 1999) and the Pacific Ocean (Lamb et al. 2001).

#### 2.4.1 Atlantic $\text{TCO}_2$ Crossover Analysis

The purpose of this analysis was to determine if any significant systematic offset existed between the various legs of the WOCE/NOAA/JGOFS Atlantic Ocean dissolved inorganic carbon (abbreviated as DIC or  $\text{TCO}_2$ ) measurements. The stations selected for each crossover were those with carbon data that were within roughly 100 km ( $\sim 1^\circ$  latitude) of the crossover point. The number of stations selected was somewhat subjective, but was such that sufficient measurements were present for the analysis without getting too far away from the crossover location. Data from deep water ( $>1500$  m) at each of the crossover locations were plotted against the density anomaly referenced to 4000 dbar ( $\sigma_4$ ) and fit with a second-order polynomial. The difference and standard deviation between the two curves were then calculated from 10 evenly spaced intervals over the density range common to both sets of crossovers. Fig. 23 shows the results in graphical form, where the sequence of values is that of the summary of crossover results in Table 18. The error bars depict the standard deviation of the 10 points over the density range. The horizontal lines are the average (middle line) and standard deviation of the points on the graph, omitting the ones that are excluded from analysis (values in bold in Table 18).

Using the crossover differences estimated from the polynomial fits, the 102 crossover analyses at 53 locations for  $\text{TCO}_2$  had an average and standard deviation of  $-0.4 \pm 3.7 \mu\text{mol/kg}$ . The average of the absolute values of the differences was  $2.7 \pm 2.6 \mu\text{mol/kg}$ .  $\text{TCO}_2$  values from A06, A07, and A23 were deemed of inadequate quality to be included in the basin wide database. More details on the  $\text{TCO}_2$  crossover analysis can be found in Wanninkhof et al. (2003).

# Crossover Locations in the North and South Atlantic

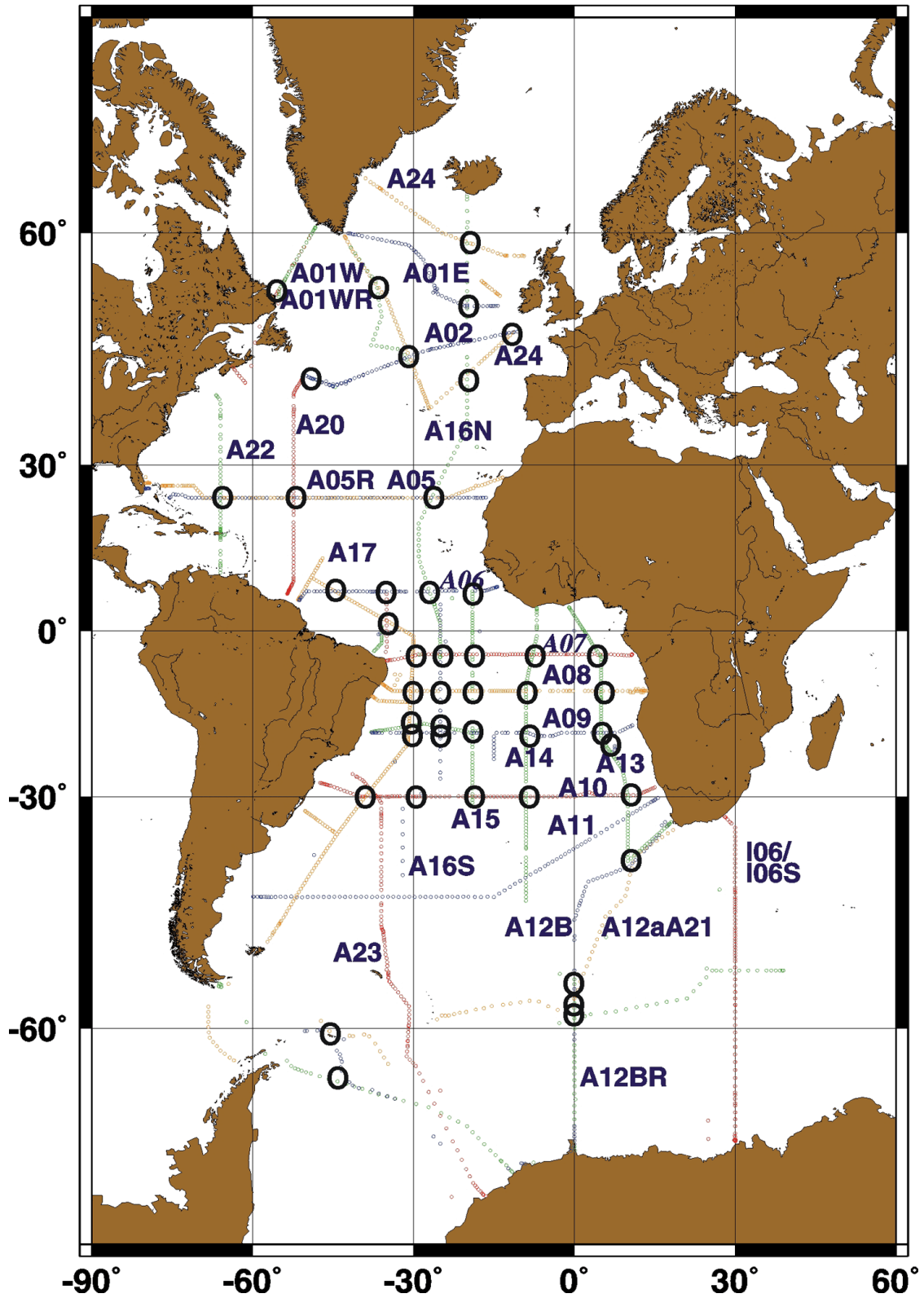


Fig. 22. Atlantic Ocean map of the crossover locations.

**Table 17. Cruises used in the Atlantic Ocean synthesis**

No.	Cruise name	EXPO code <sup>a</sup>	Research vessel	Period	Chief scientist	Carbon-related data contributor	Variables in data set
1	A21/A12	06MT11_5	R/V <i>Meteor</i>	1/23/90-3/8/90	W. Roether/Univ. of Bremen	T. Takahashi/LDEO	Hydrogr., Nutr., DIC, $f\text{CO}_2$ , CFC
2	A09	06MT15_3	R/V <i>Meteor</i>	2/10/91-3/23/91	G. Siedler/Univ. of Kiel	D. Wallace/Univ. of Kiel	Hydrogr., Nutr., DIC, TALK, $f\text{CO}_2$ , CFC
3	A16S	OACES91_1/2	R/V <i>Baldrige</i>	7/11/91-9/2/91	D. K. Atwood/AOML	R. Wanninkhof/AOML	Hydrogr., Nutr., DIC, $f\text{CO}_2$ , TALK, underw. $f\text{CO}_2$
4	A01E	06MT18_1	R/V <i>Meteor</i>	9/2/91-9/26/91	D. Meincke/Univ. of Hamburg	D. Wallace/Univ. of Kiel	Hydrogr., Nutr., DIC, TALK, underw. $f\text{CO}_2$
5	A12B	06AQANTX_4	R/V <i>Polarstern</i>	5/21/92-8/5/92	P. Lemke/Univ. of Kiel	M. Hoppema/Univ. of Bremen	Hydrogr., Nutr., DIC
6	A05	29HE06_1	R/V <i>Hesperides</i>	7/15/92-8/16/92	G. Parrilla/IEO, Spain	A. Ríos/CSIC, Spain	Hydrogr, Nutr., DIC, TALK, pH
7	A10	06MT22_5	R/V <i>Meteor</i>	12/27/92-1/31/93	R. Onken/Univ. of Kiel	D. Wallace/Univ. of Kiel	Hydrogr., Nutr., DIC, TALK, CFC, underw. $f\text{CO}_2$
8	A11	74DI199_1	R/V <i>Discovery</i>	12/22/92-2/1/93	P. Saunders/SOC	N/A	Hydrogr., Nutr., CFC
9	A07	35A3CITHER1_2	R/V <i>L'Atalante</i>	1/2/93-2/10/93	A. Moliere/LODYC	C. Oudot/ORSTOM, Brest, France	Hydrogr., Nutr., DIC, TALK, $f\text{CO}_2$ , pH, CFC
10	A06	35A3CITHER1_2	R/V <i>L'Atalante</i>	2/13/93-3/19/93	A. Moliere/C. Colin, Brest, France	C. Oudot/ORSTOM, Brest, France	Hydrogr., Nutr., DIC, TALK, $f\text{CO}_2$ , pH, CFC

No.	Cruise name	EXPO code <sup>a</sup>	Research vessel	Period	Chief scientist	Carbon-related data contributor	Variables in data set
11	A16N	OACES93	R/V <i>Baldrige</i>	7/4/93-8/30/93	R. Wanninkhof/AOML	R. Wanninkhof/AOML	Hydrogr., Nutr., DIC, TALK, $f\text{CO}_2$ , pH, CFC, underw. $f\text{CO}_2$
12	A17	3230CITHER2 1/2	R/V <i>M Ewing</i>	1/4/94-3/22/94	L. Memery/LODYC	D. Wallace/A. Ríos	Hydrogr., Nutr., DIC, TALK, pH, CFC, underw. $f\text{CO}_2$
13	A15	316N142_3	R/V <i>Knorr</i>	4/3/94-5/21/94	W Smethie/LDEO	C. Goyet/WHOI	Hydrogr., Nutr., DIC, TALK
14	A08	06MT28_1	R/V <i>Meteor</i>	3/29/94-5/11/94	T. Mueller/Univ. of Kiel	D. Wallace/Univ. of Kiel	Hydrogr., Nutr., DIC, $f\text{CO}_2$
15	A14	35A3CITHER3_1	R/V <i>L'Atalante</i>	1/17/95-2/11/95	M. Arhan/LPO	D. Wallace/A. Ríos	Hydrogr., Nutr., DIC, TALK, pH, CFC, underw. $f\text{CO}_2$
16	A13	35A3CITHER3_2	R/V <i>L'Atalante</i>	2/22/95-3/28/95	M. Arhan/LPO	D. Wallace/Univ. of Kiel A. Ríos/CSIC, Spain	Hydrogr., Nutr., DIC, TALK, CFC
17	A23	74JC10_1	RSS <i>JC Ross</i>	3/20/95-5/6/95	B. King/SOC K. Heywood/UEA	Robertson/SOC, England	Hydrogr., Nutr., DIC, $f\text{CO}_2$ , CFC
18	A01W	18HU95011_1	R/V <i>Hudson</i>	6/7/95-7/5/95	J. Lazier/BIO, Canada	P. Jones/BIO, Canada	Hydrogr., Nutr., DIC, TALK, CFC
19	IO6	35MF103_1	R/V <i>M. Dufresne</i>	2/20/96-3/22/96	A. Poisson/Univ. of Paris	A. Poisson/Univ. of Paris	Hydrogr., Nutr., DIC, TALK, CFC
20	A12BR (SR04)	06AQANTXIII_4	R/V <i>Polarstern</i>	3/17/96-5/20/96	E. Fahrbach/AWI	M. Hoppema/Univ. of Bremen	Hydrogr., Nutr., DIC, CFC
21	A02	06MT39_3	R/V <i>Meteor</i>	6/11/97-7/3/97	P. Koltermann/BSH	D. Wallace/Univ. of Kiel	Hydrogr., DIC, TALK

No.	Cruise name	EXPO code <sup>a</sup>	Research vessel	Period	Chief scientist	Carbon-related data contributor	Variables in data set
22	A20	316N151_3	R/V <i>Knorr</i>	7/17/97-8/10/97	R. Pickart/WHOI	F. Millero/RSMAS C. Sabine/PMEL D. Wallace/Univ. of Kiel	Hydrogr., Nutr., DIC, TALK, <i>f</i> CO <sub>2</sub> , pH, CFC
23	A22	316N151_4	R/V <i>Knorr</i>	8/15/97-9/3/97	T. Joyce/WHOI	F. Millero/RSMAS C. Sabine/PMEL D. Wallace/Univ. of Kiel	Hydrogr., Nutr., DIC, TALK, <i>f</i> CO <sub>2</sub> , pH, CFC
24	A24	316N151_2	R/V <i>Knorr</i>	8/15/97-9/3/97	L. Talley/SIO	F. Millero/RSMAS D. Wallace/Univ. of Kiel	Hydrogr., Nutr., DIC, TALK, <i>f</i> CO <sub>2</sub> , pH
25	A05R	OACES98	R/V <i>Brown</i>	1/24/98-2/23/98	K. Lee/AOML	R. Wanninkhof/AOML	Hydrogr., Nutr., DIC, TALK, pH, <i>f</i> CO <sub>2</sub> , CFC
26	A01WR (AR07W)	18HU98023_1	CCGS <i>Hudson</i>	6/22/98-7/8/98	P. Jones/BIO, Canada	P. Jones/BIO, Canada	Hydrogr., Nutr., DIC, TALK, CFC

<sup>a</sup>The official EXPO code for the OACES cruises were unavailable, the ones reported here were created for this report.

*Abbreviations:*

AOML	Atlantic Oceanographic and Meteorological Laboratory
AWI	Alfred-Wegener-Institut für Polar und Meeresforschung
BIO	Bedford Institute of Oceanography
BSH	Bundesamt für Seeschifffahrt und Hydrographie
CFC	chlorofluorocarbon
CSIC	Consejo Superior de Investigaciones Cientificas
IEO	Instituto Español de Oceanografía
LDEO	Lamont-Doherty Earth Observatory
LODYC	Laboratoire d'Océanographie Dynamique et de Climatologie
LPO	Laboratoire de Physique des Océans
ORSTOM	Institut Français de la Recherche Scientifique pour le Développement en Coopération
PMEL	Pacific Marine Environmental Laboratory
RSMAS	Rosenstiel School of Marine and Atmospheric Science
SIO	Scripps Institute of Oceanography
SOC	Southampton Oceanography Centre
UEA	University of East Anglia
WHOI	Woods Hole Oceanographic Institution

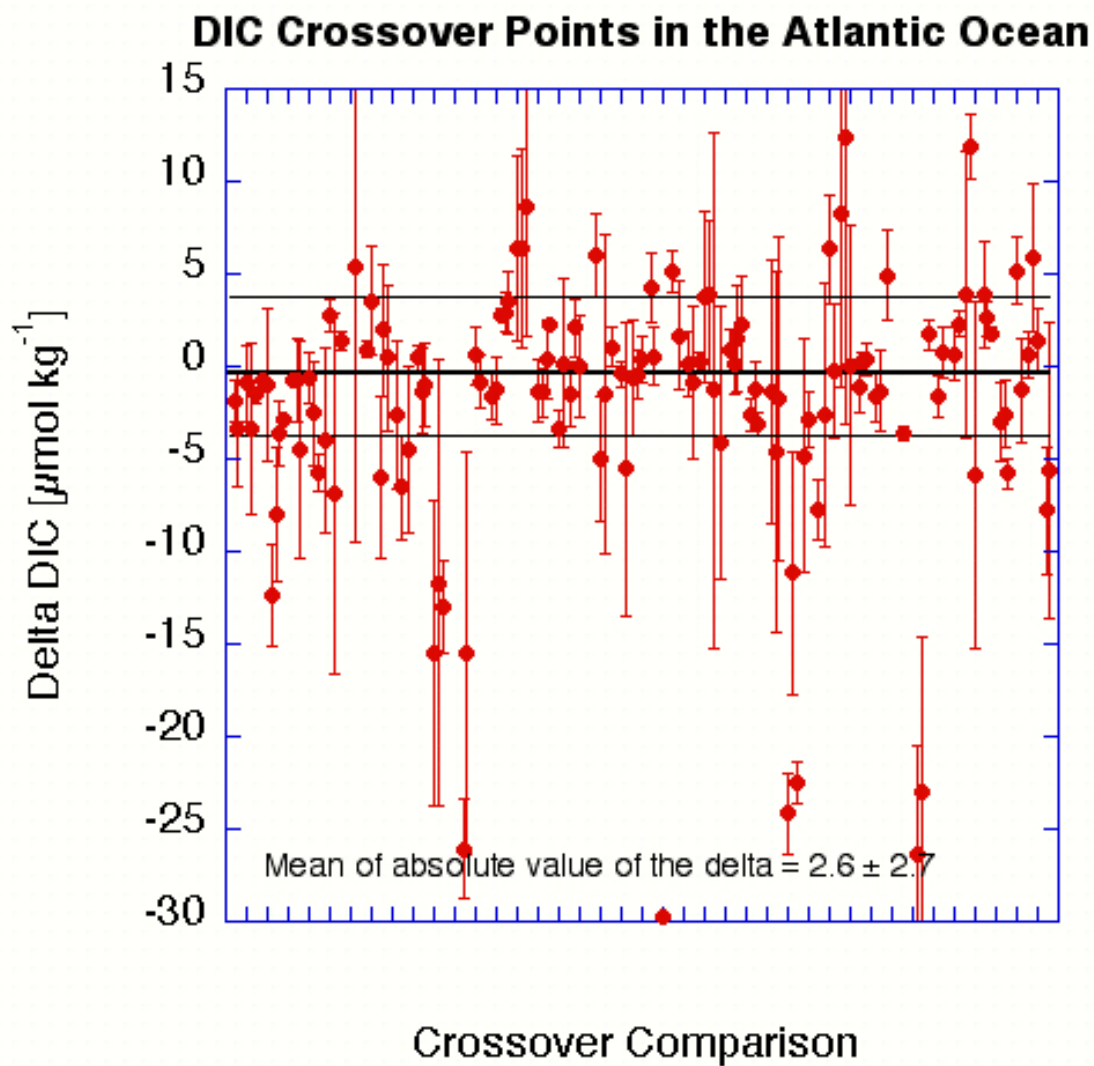


Fig. 23. TCO<sub>2</sub> crossover comparison in the Atlantic Ocean.

**Table 18. Summary of crossover analysis results by location**

Location	Cruise	Station	Total CO <sub>2</sub>			Total alkalinity			pH			fCO <sub>2</sub>		
			Ave.	St. dev.	R <sup>2</sup>	Ave.	St. dev.	R <sup>2</sup>	Ave.	St. dev.	R <sup>2</sup>	Ave.	St. dev.	R <sup>2</sup>
66° W° E 24.2° N	A22	42			0.753			0.767			0.611			
	A22	44	-1.9	1.1	0.804	-1.4	2.4	0.892	-0.0015	0.0031	0.730			
	A05	84	-3.4	3.1	1.000	-2.1	4.7	0.892	0.0383	0.0113	0.364			
66° W° E 24.2° N	A22	42			0.753			0.767			0.611			
	A22	44	-0.9	2.0	0.804	-1.4	2.4	0.892	-0.0016	0.0031	0.730			0.729
	A05R	85	-3.4	4.6	0.714	-0.3	3.0	0.870	0.0119	0.0012	0.625	6.8	3.6	0.280
	A05R	86	-1.5	0.4	0.909	9.0	10.4	1.000	0.0148	0.0022	0.708	7.0	4.0	0.952
55° W° E 53.4° N	A01W	3			0.916			0.922						
	A01W	4	-0.7	0.3	1.000	-1.5	7.9	1.000						
	A01W	5	-1.0	4.1	0.428	-3.3	3.9	0.990						
	A01WR	26	-7.93	2.95	0.961	-29.9	9.9	0.736						
	A01WR	28	-3.15	3.5	0.864	-27.5	7.1	0.770						
	A01WR	30	1.15	2.02	1.000	-19.9	5.2	1.000						
52.3° W° E 24.2° N	A20	47			0.984			0.955			0.915			
	A20	48	-0.7	0.1	0.979	0.5	0.8	0.965	-0.0008	0.0020	0.852			
	A05	62	-0.7	2.3	0.999	-3.5	7.0	1.000	-0.0016	0.0059	0.999			
	A05	64	-4.5	5.9	1.000	-4.4	7.7	1.000	0.0051	0.0371	0.200			
52.3° W° E 24.2° N	A20	47			0.971			0.976			0.908			
	A20	48	-0.7	1.4	0.979	0.6	0.7	0.969	-0.0004	0.0020	0.869			
	A05R	66	-2.5	2.8	0.886	-4.5	1.4	0.975	0.0130	0.0003	0.789			
	A05R	67	-5.7	1.0	0.975	-6.9	3.9	0.992	0.0123	0.0009	0.880			
50° W° E 43.5° N	A20	8			0.903			0.751						
	A20	10	-3.9	5.0	0.287	-10.9	11.2	0.176						
	A02	334	2.7	0.9	0.948	-11.4	13.9	0.827						
	A02	336	-6.9	9.8	0.936									
47.2° W° E 60.2° S	A12	122			0.963									
	A12B	640	1.3	0.5	0.524									
44.5° W° E 7.4° N	<b>A06</b>	<b>140</b>			<b>0.789</b>			<b>0.502</b>			<b>0.970</b>			
	A17	200							-0.0509	0.0487	0.821			
	A17	201	5.4	14.9	0.832	2.2	11.8	0.933	-0.0477	0.0497	0.615			
	A17	202							-0.0512	0.0456	0.848			

Table 18 (continued)

Location	Cruise	Station	Total CO <sub>2</sub>			Total alkalinity			pH			fCO <sub>2</sub>		
			Ave.	St. dev.	R <sup>2</sup>	Ave.	St. dev.	R <sup>2</sup>	Ave.	St. dev.	R <sup>2</sup>	Ave.	St. dev.	R <sup>2</sup>
44° W° E 64° S	A12BR	94			0.933									
	A12B	630	0.9	0.4	0.960									
	A12B	631	3.6	2.9	0.977									
39° W° E 30° S	A17	72			0.715									
	A17	75	-6.0	4.4	0.769	0.0	2.2	0.951						
	A10	11	2.0	3.5	0.872	25.1	2.5	0.784						
	A10	13	0.5	3.9	0.726			0.847						
38° W° E 29° S	<b>A23</b>	<b>115</b>			<b>1.000</b>									
	A17	75	-2.6	4.0	0.963									
	A17	78	-6.5	2.8	0.984									
37° W° E 30° S	<b>A23</b>	<b>115</b>			<b>0.985</b>									
	A10	15	-4.5	4.5	0.918									
36.6° W° E 54° N	A24	115			0.710			0.492						
	A01W	55	0.5	0.7	0.616	15.3	4.9	0.296						
	A01W	57	-1.3	2.3	0.913	-8.6	17.6	0.277						
	A01W	58	-1.0	2.2	0.725	4.0	9.8	0.563						
35° W° E 7.5° N	<b>A06</b>	<b>154</b>			<b>0.603</b>			<b>0.519</b>						
	<b>A06</b>	<b>156</b>	<b>-15.5</b>	<b>8.3</b>	<b>0.894</b>	<b>-15.4</b>	<b>5.2</b>	<b>0.894</b>	<b>0.0042</b>	<b>0.0057</b>	<b>0.995</b>			
	<b>A07</b>	<b>158</b>	<b>-11.7</b>	<b>12.1</b>	<b>0.818</b>	<b>-9.5</b>	<b>10.6</b>	<b>0.882</b>	<b>0.0096</b>	<b>0.0055</b>	<b>0.988</b>			
	<b>A07</b>	<b>119</b>	<b>-13.0</b>	<b>2.5</b>	<b>0.581</b>	<b>-8.7</b>	<b>5.4</b>	<b>0.151</b>	<b>0.0102</b>	<b>0.0063</b>	<b>0.989</b>			
35° W° E 2° N	A17	180									0.873			
	A17	181									0.903			
	A17	182			0.935			0.939	-0.0001	0.0008	0.895			
	A17	183							-0.0106	0.0009	0.962			
	<b>A07</b>	<b>110</b>	<b>-26.1</b>	<b>2.6</b>	<b>0.271</b>	<b>-15.5</b>	<b>6.9</b>	<b>0.021</b>	<b>0.0351</b>	<b>0.0384</b>	<b>0.980</b>			
	<b>A07</b>	<b>112</b>	<b>-15.5</b>	<b>10.9</b>	<b>0.835</b>	<b>-8.5</b>	<b>2.0</b>	<b>0.093</b>	<b>0.0380</b>	<b>0.0343</b>	<b>0.889</b>			
31.6° W° E 45.8° N	A01W	77			0.755			0.201						
	A01W	78	0.6	1.5	0.757	1.2	14.4	0.924						
	A02	307	-0.8	1.4	0.888	-16.0	8.4	0.622						

Table 18 (continued)

Location	Cruise	Station	Total CO <sub>2</sub>			Total alkalinity			pH			fCO <sub>2</sub>		
			Ave.	St. dev.	R <sup>2</sup>	Ave.	St. dev.	R <sup>2</sup>	Ave.	St. dev.	R <sup>2</sup>	Ave.	St. dev.	R <sup>2</sup>
31° W° E 46.2° N	A24	131			0.868			0.898						
	A24	132				5.5	7.9	1.000						
	A24	133	-1.6	1.3	0.857	-1.2	1.4	0.776						
	A24	135	-1.3	1.8	0.927	-1.2	1.4	0.823						
	A01W	76	2.8	0.3	0.878	18.2	16.4	0.539						
	A01W	77	2.9	1.0	0.755	12.9	8.7	0.201						
	A01W	78	3.5	1.7	0.757	11.8	10.6	0.924						
30.4° W° E 11.4° S	A17	145			0.833									
	A17	148	6.4	5.0	0.996									
	A08	186	6.4	5.4	0.655									
	A08	188	8.7	7.0	0.859									
30.8° W° E 46.1° N	A24	131			0.868			0.898						
	A24	132				0.3	0.8	0.879						
	A24	133	-1.3	1.7	0.906	-1.1	1.1	0.776						
	A24	135	-1.4	1.4	0.927	-1.4	1.4	0.823						
	A02	305	0.4	2.1	0.815	-4.5	2.2	0.444						
	A02	307	2.3	0.2	0.888	-1.9	2.3	0.056						
30.8° W° E 18.8° S	A17	102			0.939			0.986						
	A17	105	-3.3	1.0	0.931	3.3	1.4	0.989						
	A09	143	0.2	4.5	0.802	-6.9	3.0	0.945						
30.8° W° E 17.8° S	A17	105			0.945			0.816						
	A17	108	-1.5	1.8	0.921	-1.5	1.3	0.929						
	A15	134	2.1	1.6	0.936	14.4	0.7	0.938						
	A15	136	0.0	2.8	0.962	15.1	0.9	0.994						
30° W° E 5° S	A17	157			0.543			0.970			0.959			
	A17	158							-0.0043	0.0025	0.904			
	A17	159							-0.0030	0.0019	0.899			
	A17	160	6.0	2.2	0.790	0.9	1.1	0.962	-0.0068	0.0048	0.858			
	<b>A07</b>	<b>78</b>	<b>-5.0</b>	<b>3.4</b>	<b>0.353</b>	<b>-5.8</b>	<b>2.8</b>	<b>0.251</b>	<b>0.0253</b>	<b>0.0270</b>	<b>0.995</b>			
	<b>A07</b>	<b>80</b>	<b>-1.5</b>	<b>8.6</b>	<b>0.516</b>	<b>5.2</b>	<b>1.4</b>	<b>0.367</b>	<b>0.0281</b>	<b>0.0292</b>	<b>0.962</b>			
28.5° W° E 29.5° S	A16S	31			0.752			0.456						
	A10	36	1.0	1.0	0.605	2.3	4.6	0.781						



Table 18 (continued)

Location	Cruise	Station	Total CO <sub>2</sub>			Total alkalinity			pH			fCO <sub>2</sub>		
			Ave.	St. dev.	R <sup>2</sup>	Ave.	St. dev.	R <sup>2</sup>	Ave.	St. dev.	R <sup>2</sup>	Ave.	St. dev.	R <sup>2</sup>
19.9° W° E 43.8° N	A24	14			0.990			0.974			0.881			0.606
	A24	16	-2.6	0.9	0.941	0.7	1.1	0.969	0.0115	0.0106	0.833			
	A16N	61	-1.3	1.6	0.987	-5.2	3.1	1.000	-0.0050	0.0111	0.668	0.9	9.8	0.932
	A16N	63	-3.2	0.6	0.966	-4.4	3.3	0.863	-0.0084	0.0129	0.903	7.5	10.7	0.970
19.8° W° E 59.1° N	A24	67			1.000			0.890						0.994
	A24	69				3.1	1.9	0.748			0.877			
	A16N	76	-1.4	7.1	0.963	0.1	2.8	0.985				13.3	3.5	0.998
	A16N	77	-4.6	9.8	0.874	3.3	3.1	0.758	-0.0168	0.0044	0.968	-7.0	22.6	0.746
A16N	78	-1.7	8.7	0.763	3.3	2.0	0.828	-0.0175	0.0032	0.913	3.7	18.0	0.718	
19° W° E 7.5° N	A15	28			0.956			0.983						
	<b>A06</b>	<b>184</b>	<b>-24.2</b>	<b>2.2</b>	<b>0.601</b>	<b>-33.8</b>	<b>5.2</b>	<b>0.437</b>						
	<b>A06</b>	<b>186</b>	<b>-11.2</b>	<b>6.5</b>	<b>0.718</b>	<b>-18.2</b>	<b>4.8</b>	<b>0.838</b>						
	<b>A06</b>	<b>188</b>	<b>-22.5</b>	<b>1.2</b>	<b>0.672</b>	<b>-30.8</b>	<b>5.2</b>	<b>0.716</b>						
19° W° E 30° S	A15	106			0.846			0.613						
	A10	46	-4.8	6.3	0.914									
	A10	48	-2.8	1.5	0.871	-0.6	1.3	0.806						
19° W° E 19° S	A15	82			0.976									
	A09	161	-7.7	1.6	0.785									
19° W° E 11° S	A15	66			0.976									
	A15	68	-2.6	7.1	0.994									
	A08	204	6.4	2.9	0.982									
	A08	206	-0.3	3.7	0.984									
11.2° W° E 49.2° N	A24	32			0.984			0.923						
	A24	33	8.2	9.3	0.999	1.4	0.2	0.878						
	A24	34	12.3	15.5	0.997	0.4	1.2	0.761						
	A02	282	0.1	7.6	0.996	-4.3	2.4	0.934						
9° W° E 11.5° S	A14	37			0.995			0.995						
	A14	40	-1.1	1.4	0.961	0.0	2.0	0.992						
	A08	226	0.2	0.6	0.991	12.1	0.7	0.977						
	A08	228	0.4	0.9	0.994	11.0	1.8	0.984						



**Table 18 (continued)**

Location	Cruise	Station	Total CO <sub>2</sub>			Total alkalinity			pH			fCO <sub>2</sub>		
			Ave.	St. dev.	R <sup>2</sup>	Ave.	St. dev.	R <sup>2</sup>	Ave.	St. dev.	R <sup>2</sup>	Ave.	St. dev.	R <sup>2</sup>
5° E 19° S	A13	179			0.981									
	A13	182	-3.0	2.1	0.995									
	A09	212	-2.6	1.8	0.995									
	A09	214	-5.8	0.8	0.991									
7° E 22.6° S	A13	170			1.000									
	A13	173	5.2	1.8	0.955									
	A09	217	-1.3	2.8	0.978									
10° E 29.8° S	A13	148			0.961									
	A13	151	0.6	1.2	0.962									
	A10	87	5.8	4.0	0.981									
	A10	89	1.4	1.7	0.914									
10° E 40° S	A13	130			0.848									
	A12B	551	-7.8	3.5	0.816									
	A12B	552	-5.6	8.0	0.841									

*Note:* All values are the difference between the first station and the second (or subsequent one). Bold values are from cruises that were not retained in the synthesis.

*Abbreviations:*

Ave. = Average difference of 10 equally spaced points on the two least-squares second-order polynomial lines of property versus  $\sigma-4$  between nominally  $\sigma-4 = 45.5$  and  $45.9$ . The average difference between stations for the same cruise is an indication of the station variability in data.

St. dev. = Standard deviation of 10 equally spaced points on the least-squares second-order polynomial lines of property versus  $\sigma-4$ .

R<sub>2</sub> = Goodness of fit for the line. R<sub>2</sub> = 1 indicates only three points in the selected range, which yields a perfect fit for the second-order polynomial.

## 2.4.2 Atlantic TALK Crossover Analysis

The purpose of this analysis was to determine if any significant systematic offset existed between the various legs of the WOCE/NOAA/JGOFS Atlantic Ocean TALK measurements. The stations selected for each crossover were those with carbon data that were within roughly 100 km ( $\sim 1^\circ$  latitude) of the crossover point. Data from deep water ( $>1500$  m) at each of the crossover locations were plotted against the density anomaly referenced to 4000 dbar ( $\sigma\text{-4}$ ) and fit with a second-order polynomial. The difference and standard deviation between the two curves was then calculated from 10 evenly spaced intervals over the density range common to both sets of crossovers. Fig. 24 shows the results in graphical form, where the sequence of values is that of the summary table of crossover results. The error bars depict the standard deviation of the 10 points over the density range. The horizontal lines are the average (middle line) and standard deviation of the points on the graph (upper and lower lines), omitting the ones that are excluded from analysis (shown as bold values in Table 18).

Using the crossover differences estimated from the polynomial fits, the 63 crossover analyses at 53 locations for TALK had an average and standard deviation of  $0.2 \pm 10.5 \mu\text{mol/kg}$ . The average and the absolute values of the differences was  $5.9 \pm 8.6 \mu\text{mol/kg}$ . TALK values from A06, A07, and A01E were deemed of insufficient quality to be included in the basinwide database. More details on the TALK crossover analysis can be found in Wanninkhof et al. (2003).

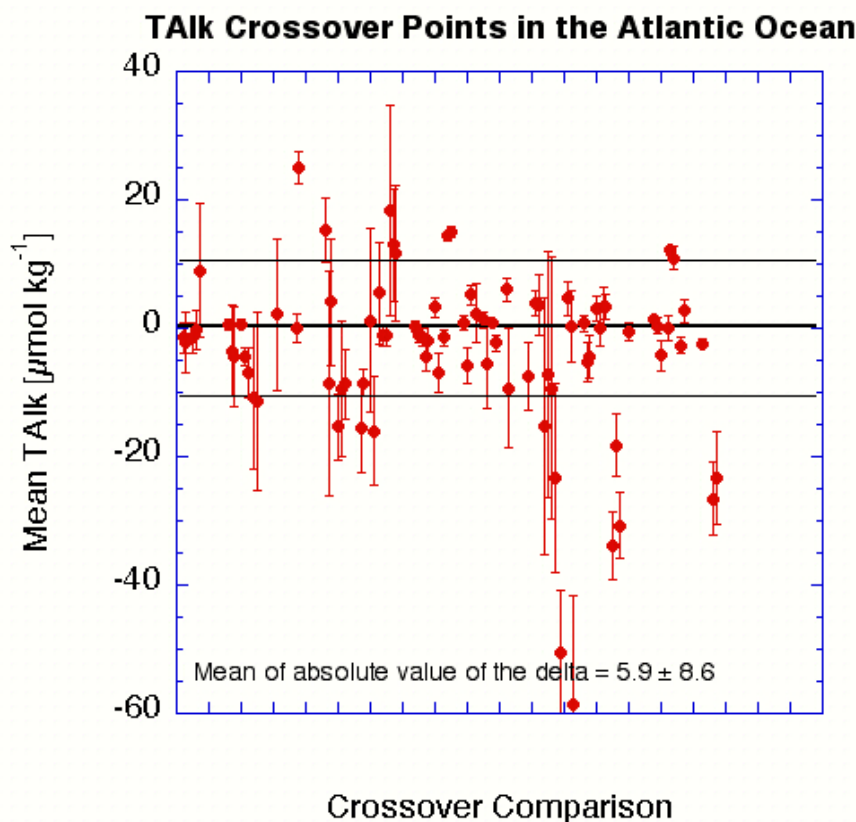


Fig. 24. TALK crossover comparison in the Atlantic Ocean.

### 2.4.3 Atlantic $f\text{CO}_2$ Crossover Analysis

The purpose of this analysis was to determine if any significant systematic offset existed between the various legs of the WOCE/NOAA/JGOFS Atlantic Ocean measurements of  $f\text{CO}_2$ . Three different types of instruments were used to measure discrete  $f\text{CO}_2$  samples. With each an aliquot of seawater was equilibrated at a constant temperature of either 4° or 20°C with a headspace of known initial  $\text{CO}_2$  content. Subsequently, the headspace  $\text{CO}_2$  concentration was determined by NDIR or by quantitatively converting the  $\text{CO}_2$  to  $\text{CH}_4$  and then analyzing it using GC with a flame ionization detector. The initial  $f\text{CO}_2$  in the water was determined after correcting for the loss or gain of  $\text{CO}_2$  during the equilibration process. This correction can be significant for large initial  $f\text{CO}_2$  differences between the headspace and the water, and for systems with a large headspace-to-water volume ratio (Chen et al. 1995).

The system used by Takahashi and co-workers on A21/A12 (Chipman et al. 1993; DOE 1994) involved equilibration of a ~50-mL headspace with a ~500-mL sample at either 4°C or 20°C depending on ambient surface water temperatures. The Takahashi values, reported as  $\text{pCO}_2$ , were converted to  $f\text{CO}_2$  using the correction factor (~ 0.996) given by Weiss (1974). Wanninkhof and co-workers utilized two systems during the Atlantic survey cruises. An NDIR-based system with ~500-mL samples was used for analyses during A16S and A16N (Wanninkhof and Thoning 1993). A GC-based system with samples collected in a closed, septum sealed bottle having a volume of ~120-mL of seawater and a headspace of ~10-mL was used for A05R (Neill et al. 1997). Wallace and co-workers used the setup described in Neill et al. on A08 but with bottles having a volume of ~50-mL of seawater and a headspace of ~5-mL.

Detectors were calibrated after every 4–12 samples with gas standards traceable to manometrically determined values of C. D. Keeling at SIO. An assessment of  $f\text{CO}_2$  accuracy is difficult to determine because of the lack of aqueous standards. Estimates of precision based on duplicate samples range from 0.1 to 1% depending on  $f\text{CO}_2$  and measurement procedure, with higher  $f\text{CO}_2$  levels on the IR-based system (>700  $\mu\text{atm}$ ) giving worse reproducibility (Chen et al. 1995).

The stations selected for each crossover were those with carbon data that were within roughly 100 km (~1° latitude) of the crossover point. Data from deep water (>1500 m) at each of the crossover locations were plotted against the density anomaly referenced to 4000 dbar ( $\sigma\text{-4}$ ) and fit with a second-order polynomial. For the crossover comparison all samples run at 4°C were normalized to 20°C by calculating the TALK from  $f\text{CO}_2$  (4°C) and  $\text{TCO}_2$ , and subsequently calculating  $f\text{CO}_2$  (20°C) from the  $\text{TCO}_2$  and calculated TALK. The carbonate dissociation constants of Mehrbach et al. (1973) as refit by Dickson and Millero (1987) and ancillary constants listed in DOE (1994) are used for these calculations using the program of Lewis and Wallace (1998). Crossover information is given in Table 18.

Upon examination, it became clear that there may be a problem for the crossovers that required a temperature conversion. For example, temperature conversions from 4° to 20°C using the Mehrbach constants yield  $f\text{CO}_2$  values in the deep Pacific that are about 50  $\mu\text{atm}$  higher than those derived from use of Roy constants for the conversion. Since the discrepancy in dissociation constants has not been fully resolved, the crossover comparison for  $f\text{CO}_2$  data analyzed at different temperatures and for comparisons of measured versus calculated values is problematic.

Data from deep water (>1500 m) at each of the 12 crossovers, analyzed at five locations, were plotted against the density anomaly referenced to 4000 dbar ( $\sigma\text{-4}$ ) and fit with a second-order polynomial. The difference and standard deviation between the two curves was then calculated from 10 evenly spaced intervals over the density range common to both sets of crossovers. The standard deviation for the 12  $f\text{CO}_2$  crossover comparisons was 13.4  $\mu\text{atm}$ . The average of the absolute value of the differences was  $9.8 \pm 8.4 \mu\text{atm}$ .

#### 2.4.4 Atlantic pH Crossover Analysis

The purpose of this analysis was to determine if any significant systematic offset existed between the various legs of the WOCE/NOAA/JGOFS Atlantic Ocean measurements of pH. Several different methods of measurement were used, and data were reported on different reference scales. The most precise Atlantic pH measurements used a spectrophotometric method (Clayton and Byrne 1993), with m-cresol purple as the indicator and either scanning or diode array spectrophotometers; these were performed on A16N and A05R. For most cruises (A12B, A07, A06, A17, A14, A20, A22, and A24) pH values were derived from potentiometric measurements with a glass electrode.

Some of the pH values were reported on the total hydrogen scale, while others were reported on the seawater scale. The seawater scale considers the interaction of hydrogen ions with bisulfate and fluoride ions in seawater, while the total scale includes only the bisulfate contribution (Dickson and Riley 1979; Dickson and Millero 1987). The two scales are linked by the following equation:

$$\text{pH}_{\text{SWS}} = \text{pH}_{\text{T}} - \log \left\{ (1 + [\text{SO}_4^{2-}]_{\text{T}} / K_{\text{HSO}_4} + [\text{F}^-]_{\text{T}} / K_{\text{HF}}) / (1 + [\text{SO}_4^{2-}]_{\text{T}} / K_{\text{HSO}_4}) \right\}, \quad (4)$$

where  $\text{pH}_{\text{T}}$  is hydrogen ion concentration on the total hydrogen scale,  $[\text{F}^-]_{\text{T}}$  and  $[\text{SO}_4^{2-}]_{\text{T}}$  are the total concentrations of fluoride and sulfate in seawater, and  $K_{\text{HF}}$  and  $K_{\text{HSO}_4}$  are the dissociation constants of hydrogen fluoride and sulfate in seawater (Dickson and Riley 1979). For the crossover analyses all total hydrogen scale pH values were converted to the seawater scale ( $\text{pH}_{\text{SWS}}$ ).

The stations selected for each crossover were those with carbon data that were within roughly 100 km ( $\sim 1^\circ$  latitude) of the crossover point. Data from deep water ( $>1500$  m) at each of the crossover locations were plotted against the density anomaly referenced to 4000 dbar ( $\sigma-4$ ) and fit with a second-order polynomial. The difference and standard deviation between the two curves was then calculated from 10 evenly spaced intervals over the density range common to both sets of crossovers. The average of the absolute value of the differences of pH for 21 crossovers at 8 locations was  $-0.0092 \pm 0.0086$ . Crossover information is given in Table 18.

The crossover comparisons suggest good precision, but because of the small number of comparisons available, no further statistical analysis was done with this carbon parameter.

#### 2.4.5 Summary of Atlantic Ocean Adjustments

This section summarizes the various lines of evidence to suggest adjustment of parameters. Full discussion is provided in the CDIAC report 140 (Wanninkhof et al. 2003). The recommended adjustments are based on all available evidence, including crossover results, internal consistency checks, regional multilinear regressions, data from overlapping cruises, and calibration information. Based on the overall precision of the measurements on the cruises, we recommend adjustments only if there is clear and consistent evidence for biases greater than  $4 \mu\text{mol/kg}$  for  $\text{TCO}_2$  and  $6 \mu\text{mol/kg}$  for TALK.

In the course of the investigation we determined that data from several cruises were not suitable for further analysis because of significant scatter in the data. These data are not used in the synthesis. The proposed adjustments are recommendations and have been applied only to the GLODAP Atlantic synthesis data files of this NDP, not the original files stored at CDIAC and national data facilities. To adjust the Atlantic data set we omitted the following parameters from the synthesis:

- A06 -  $\text{TCO}_2$  and TALK
- A07 -  $\text{TCO}_2$  and TALK
- A01E - TALK
- A23 -  $\text{TCO}_2$

No adjustments are recommended for  $\text{TCO}_2$ .  $\text{TCO}_2$  data from the cruises are believed to be consistent to  $4 \mu\text{mol/kg}$ . We recommend that all TALK data from the A01W section be adjusted upward

by 14  $\mu\text{mol}/\text{kg}$  and that 7  $\mu\text{mol}/\text{kg}$  be subtracted from TALK data from the A09 section. All other TALK data are believed to be consistent to 6  $\mu\text{mol}/\text{kg}$ .

### 3. DATA SET CONSTRUCTION AND MAPPING PROCEDURE

The GLODAP data set consists of 12,012 oceanographic stations collected on 116 cruises, as summarized in Table 19. GLODAP has produced a calibrated, uniform data set that is the largest compilation of its kind to date. These data were used to produce objectively mapped three-dimensional fields for TCO<sub>2</sub>, TALK, potential alkalinity, calculated anthropogenic CO<sub>2</sub>, CFCs, and <sup>14</sup>C.

For complete details on GLODAP data set construction and mapping procedure refer to Key et al. 2004, reproduced as Appendix C of this NDP.

The GLODAP bottle data files are available for each ocean as flat ASCII files, in Ocean Data View format, and through the CDIAC Live Access Server (LAS); the gridded data files are available as ASCII files and through CDIAC LAS.

**Table 19. Basis of GLODAP data set construction**

<b>Time of data collection</b>	<b>Data collection program</b>	<b>No. of cruises</b>	<b>No. and type of stations</b>
1972–1990	Historical	21	2,393 / hydrographic
1985–1999	WOCE	95	9,618 / oceanographic
Total		116	12,012

#### 4. HOW TO OBTAIN THE DATA AND DOCUMENTATION

This GLODAP database (NDP-083) is available free of charge from CDIAC. The complete data set and documentation can be obtained in one of the following ways:

**From the CDIAC GLODAP web site:**

[http://cdiac.ornl.gov/oceans/glodap/Glodap\\_home.htm](http://cdiac.ornl.gov/oceans/glodap/Glodap_home.htm)

**Through CDIAC's online ordering system:**

[http://cdiac.ornl.gov/pns/how\\_order.html](http://cdiac.ornl.gov/pns/how_order.html)

**By contacting CDIAC directly:**

Carbon Dioxide Information Analysis Center  
Oak Ridge National Laboratory  
P.O. Box 2008  
Oak Ridge, Tennessee 37831-6335  
U.S.A.

Telephone: (865) 574-3645  
Telefax: (865) 574-2232  
E-mail: [cdiac@ornl.gov](mailto:cdiac@ornl.gov)  
Internet: <http://cdiac.ornl.gov>

## 5. REFERENCES

Brewer, P. G., A. L. Bradshaw, R. T. Williams. 1986. Measurements of total carbon dioxide and alkalinity in the North Atlantic Ocean in 1981. In: Trabalka J. R., and D. E. Reichle (eds.), *The Changing Carbon Cycle: A Global Analysis*. Springer, New York, pp. 348–370.

Brewer, P. G., D. M. Glover, C. M. Goyet, and D. K. Schafer. 1995. The pH of the North Atlantic Ocean: Improvements to the global model for sound absorption in sea water. *Journal of Geophysical Research* 100(c5):8761–76.

Clayton, T., and R. H. Byrne. 1993. Spectrophotometric seawater pH measurements: Total hydrogen ion concentration scale calibration of m-cresol purple and at-sea results. *Deep-Sea Research* 40:2115–29.

Chen, H., R. Wanninkhof, R. A. Feely, and D. Greeley. 1995. *Measurement of fugacity of carbon dioxide in sub-surface water: an evaluation of a method based on infrared analysis*. NOAA technical report ERL AOML-85, NOAA/AOML.

Chipman, D. W., J. Marra, and T. Takahashi. 1993. Primary production at 47° N and 20° W in the North Atlantic Ocean: A comparison between the <sup>14</sup>C incubation method and mixed layer carbon budget observations. *Deep-Sea Research II* 40:151–69.

Clayton, T., and R. H. Byrne. 1993. Spectrophotometric seawater pH measurements: Total hydrogen ion concentration scale calibration of m-cresol purple and at-sea results. *Deep-Sea Research* 40:2115–29.

DeValls, T. A., and A. G. Dickson. 1998. The pH of buffers based on 2-amino-2-hydroxymethyl-1, 3-propanediol (“tris”) in synthetic seawater. *Deep-Sea Research* 45:1541–54.

Dickson, A. G., and F. J. Millero. 1987. A comparison of the equilibrium constants for the dissociation of carbonic acid in seawater media. *Deep-Sea Research* 34:1733–43.

Dickson, A. G., and J. P. Riley. 1979. The estimation of acid dissociation constants in seawater media from potentiometric titrations with strong base: I. The ionic product of water-K<sub>w</sub>. *Marine Chemistry* 7:89–99.

DOE (U.S. Department of Energy). 1994. *Handbook of Methods for the Analysis of the Various Parameters of the Carbon Dioxide System in Seawater*. Version 2.0. ORNL/CDIAC-74. A. G. Dickson and C. Goyet (eds.). Carbon Dioxide Information Analysis Center, Oak Ridge National Laboratory, Oak Ridge, Tenn., U.S.A.

Feely, R. A., M. F. Lamb, D. J. Greeley, and R. Wanninkhof. 1999. *Comparison of the carbon system parameters at the Global CO<sub>2</sub> Survey crossover locations in the North and South Pacific Ocean, 1990–1996*. ORNL/CDIAC-115. Carbon Dioxide Information Analysis Center, Oak Ridge National Laboratory, U.S. Department of Energy, Oak Ridge, Tennessee.

Goyet, C., and D. Davis. 1997. Estimation of total CO<sub>2</sub> concentration throughout the water column. *Deep-Sea Research I* 44(5):859–77.

Guenther, P. R., C. D. Keeling, and G. Emanuele. 1994. *Oceanic CO<sub>2</sub> measurements for the WOCE hydrographic survey in the Pacific Ocean, 1990–1991: Shore based analyses*. SIO Reference Series, No. 94-28. Scripps Institution of Oceanography, University of California San Diego, La Jolla, California, U.S.A.

Johnson, K. M., A. E. King, and J. McN. Sieburth. 1985. Coulometric TCO<sub>2</sub> analyses for marine studies: An introduction. *Marine Chemistry* 16:61–82.

Johnson, K. M., P. J. Williams, and L. Brandstroem, and J. McN. Sieburth. 1987. Coulometric TCO<sub>2</sub> analysis for marine studies: Automation and calibration. *Marine Chemistry* 21:117–33.

Johnson, K. M., and D. W. R. Wallace. 1992. *The single-operator multiparameter metabolic analyzer for total carbon dioxide with coulometric detection*. DOE Research Summary No. 19. Carbon Dioxide Information Analysis Center, Oak Ridge National Laboratory, U.S. Department of Energy, Oak Ridge, Tennessee.

Johnson, K. M., K. D. Wills, D. B. Butler, W. K. Johnson, and C. S. Wong. 1993. Coulometric total carbon dioxide analysis for marine studies: Maximizing the performance of an automated gas extraction system and coulometric detector. *Marine Chemistry* 44:167–87.

Johnson, K. M., A. G. Dickson, G. Eiseheid, C. Goyet, P. R. Guenther, R. M. Key, F. J. Millero, D. Purkerson, C. L. Sabine, R. G. Schotle, D. W. R. Wallace, R. J. Wilke, and C. D. Winn. 1998. Coulometric total carbon dioxide analysis for marine studies: Assessment of the quality of total inorganic carbon measurements made during the U.S. Indian Ocean CO<sub>2</sub> Survey 1994–1996. *Marine Chemistry* 63:21–37.

Johnson, K. M., A. G. Dickson, G. Eiseheid, C. Goyet, P. R. Guenther, R. M. Key, K. Lee, E. R. Lewis, F. J. Millero, D. Purkerson, C. L. Sabine, R. G. Schotle, D. W. R. Wallace, R. J. Wilke, and C. D. Winn. 2002. *Carbon Dioxide, Hydrographic and Chemical Data Obtained During the Nine R/V Knorr Cruises Comprising the Indian Ocean CO<sub>2</sub> Survey (WOCE Sections I8SI9S, I9N, I8NI5E, I3, I5WI4, I7N, I1, I10, and I2; December 1, 1994–January 22, 1996)*, A. Kozyr (ed.). ORNL/CDIAC-138, NDP-080. Carbon Dioxide Information Analysis Center, Oak Ridge National Laboratory, U.S. Department of Energy, Oak Ridge, Tennessee.

Key, R. M., A. Kozyr, C.L. Sabine, K. Lee, R. Wanninkhof, J. Bullister, R. A. Feely, F. Millero, C. Mordy, T.-H. Peng. 2004. A global ocean carbon climatology: Results from GLODAP. *Global Biogeochemical Cycles*.

Lamb, M. F., C. L. Sabine, R. A. Feely, R. Wanninkhof, R. M. Key, G. C. Johnson, F. J. Millero, K. Lee, T.-H. Peng, A. Kozyr, J. L. Bullister, D. Greeley, R. H. Byrne, D. W. Chipman, A. G. Dickson, C. Goyet, P. R. Guenther, M. Ishii, K. M. Johnson, C. D. Keeling, T. Ono, K. Shitashima, B. Tilbrook, T. Takahashi, D. W. R. Wallace, Y. Watanabe, C. Winn, and C. S. Wong. 2001. Consistency and synthesis of Pacific Ocean CO<sub>2</sub> survey data. *Deep-Sea Research II* 49:21–58.

Lee, K., F. J. Millero, R. H. Byrne, R. A. Feely, and R. Wanninkhof. 2000. The recommended dissociation constants of carbonic acid in seawater, *Geophysical Research Letters* 27:229–32.

Lewis, E., and D. W. R. Wallace. 1998. *Program developed for CO<sub>2</sub> system calculations*. ORNL/CDIAC-105. Carbon Dioxide Information Analysis Center, Oak Ridge National Laboratory, U.S. Department of Energy, Oak Ridge, Tennessee.

McElligott, S., R. H. Byrne, K. Lee, R. Wanninkhof, F. J. Millero, and R. A. Feely. 1998. Discrete water column measurements of CO<sub>2</sub> fugacity and pH in seawater: A comparison of direct measurements and thermodynamic calculations. *Marine Chemistry* 60:63–73.

- Merbach, C., C. H. Culberson, J. E. Hawley, and R. M. Pytkowicz. 1973. Measurements of the apparent dissociation constants of carbonic acid in seawater at atmospheric pressure. *Limnology and Oceanography* 18:897–907.
- Millero, F. J., J. Z. Zhang, K. Lee, and D. M. Campbell. 1993. Titration alkalinity of seawater. *Marine Chemistry* 44:153–60.
- Millero, F. J. 1995. Thermodynamics of the carbon dioxide system in the oceans. *Geochim. Cosmochim. Acta* 59:661–77.
- Millero, F. J., A. G. Dickson, G. Eiseid, C. Goyet, P. R. Guenther, K. M. Johnson, K. Lee, E. Lewis, D. Purkerson, C. L. Sabine, R. Key, R. G. Schottle, D. R. W. Wallace, and C. D. Winn. 1998. Assessment of the quality of the shipboard measurements of total alkalinity on the WOCE Hydrographic Program Indian Ocean CO<sub>2</sub> survey cruises 1994–1996. *Marine Chemistry* 63:9–20.
- Millero, F. J., D. Pierrot, K. Lee, R. Wanninkhof, R. A. Feely, C. L. Sabine, and R. M. Key. 2002. Dissociation constants for carbonic acid determined from field measurements. *Deep-Sea Research* 49(10):1705–23.
- Neill, C., K. M. Johnson, E. Lewis, and D. W. R. Wallace. 1997. Accurate headspace analysis of *f*CO<sub>2</sub> in discrete water samples using batch equilibration. *Limnology and Oceanography* 42(8):1774–83.
- Perez, F. F., and F. Fraga. 1987. A precise and rapid analytical procedure for alkalinity determination. *Marine Chemistry* 21:169–82.
- Sabine, C. L., R. M. Key, K. M. Johnson, F. J. Millero, J. L. Sarmiento, D. R. W. Wallace, and C. D. Winn. 1999. Anthropogenic CO<sub>2</sub> inventory of the Indian Ocean. *Global Biogeochemical Cycles* 13:179–98.
- Slansky, C. L., R. A. Feely, and R. Wanninkhof. 1997. The stepwise linear regression method for calculating anthropogenic CO<sub>2</sub> invasion into the North Pacific Ocean. In: Tsunogai, S. (ed.), *Biogeochemical Processes in the North Pacific*. Proceedings of the International Marine Science Symposium on Biogeochemical Processes in the North Pacific, 12–14 November 1996, Mutsu, Japan, Japan Marine Science Foundation, pp. 70–79.
- Ono, T., S. Watanabe, K. Okuda, M. Fukasawa. 1998. Distribution of total carbonate and related properties in the North Pacific along 30° N. *Journal of Geophysical Research* 103:30873–83.
- Wallace, D. W. R. 1995. *Monitoring global ocean inventories*, OOSDP Background Rep. 5. Ocean Observatory System Development Panel, Texas A&M University, College Station, Texas, 54 pp.
- Wanninkhof, R., and K. Thoning. 1993. Measurement of fugacity of CO<sub>2</sub> in surface water using continuous and discrete sampling methods. *Marine Chemistry* 44:189–204.
- Wanninkhof, R., T.-H. Peng, B. Huss, C. L. Sabine, K. Lee. 2003. *Comparison of inorganic carbon system parameters measured in the Atlantic Ocean from 1990 to 1998 and recommended adjustments*, A. Kozyr (ed.). ORNL/CDIAC-140. Carbon Dioxide Information Analysis Center, Oak Ridge National Laboratory, U.S. Department of Energy, Oak Ridge, Tennessee.
- Weiss, R. F. 1974. Carbon dioxide in water and seawater: the solubility of a non-ideal gas. *Marine Chemistry* 2:203–15.
- Weiss, R. F., W. S. Broecker, H. Craig, and D. Spencer. 1983. *GEOSECS Indian Ocean Expedition*. Vol. 5, *Hydrographic Data, 1977–1978*, U.S. Government Printing Office, Washington D.C.

Wunsch, C. 1996. *The Ocean Circulation Inverse Problem*. Cambridge University Press, Cambridge, England, p. 442.

## **APPENDIX A:**

### **REPRINT OF PERTINENT LITERATURE**

Lamb, M. F., C. L. Sabine, R. A. Feely, R. Wanninkhof, R. M. Key, G. C. Johnson, F. J. Millero, K. Lee, T.-H. Peng, A. Kozyr, J. L. Bullister, D. Greeley, R. H. Byrne, D. W. Chipman, A. G. Dickson, C. Goyet, P. R. Guenther, M. Ishii, K. M. Johnson, C. D. Keeling, T. Ono, K. Shitashima, B. Tilbrook, T. Takahashi, D. W. R. Wallace, Y. Watanabe, C. Winn, and C. S. Wong. 2001. Consistency and synthesis of Pacific Ocean CO<sub>2</sub> survey data. *Deep-Sea Research II* 49:21–58.



## **APPENDIX B:**

### **REPRINT OF PERTINENT LITERATURE**

Sabine, C. L., R. M. Key, K. M. Johnson, F. J. Millero, J. L. Sarmiento, D. R. W. Wallace, and C. D. Winn. 1999. Anthropogenic CO<sub>2</sub> inventory of the Indian Ocean. *Global Biogeochemical Cycles* 13:179–98.



## **APPENDIX C:**

### **REPRINT OF PERTINENT LITERATURE**

Key, R. M., A. Kozyr, C. L. Sabine, K. Lee, R. Wanninkhof, J. Bullister, R. A. Feely, F. Millero, C. Mordy, and T.-H. Peng. 2004. A global ocean carbon climatology: Results from GLODAP. *Global Biogeochemical Cycles*.